

# **Liquid Crystal Sulfonated Aramids as Proton Exchange Membranes for Fuel Cell Applications**

## **Proefschrift**

ter verkrijging van de graad van doctor  
aan de Technische Universiteit Delft,  
op gezag van de Rector Magnificus prof. ir. K.C.A.M. Luyben;  
voorzitter van het College voor Promoties,  
in het openbaar te verdedigen op  
vrijdag 4 september 2015 om 15:00 uur

Door

**Jianwei GAO**

Master of Science in Chemistry, University of Science and Technology of China,  
Hefei, China  
geboren te Hebei, China

This dissertation has been approved by the

promotor: Prof. dr. T.J. Dingemans

copromotor: Prof. dr. S.J. Picken

Composition of the doctoral committee:

Rector Magnificus

Prof. dr. T.J. Dingemans, promotor

Prof. dr. S.J. Picken, copromotor

Dr. S.J. Garcia Espallargas, LR, TU Delft

Independent members:

Prof. dr. ir. S. van der Zwaag, LR, TU Delft

Prof. dr. F.M. Mulder, TNW, TU Delft

Prof. dr. C.T. Imrie, University of Aberdeen, United Kingdom

Dr. ing. G.J.M. Koper, TNW, TU Delft

Prof. dr. A. Schmidt-Ott, TNW, TU Delft, reservelid

The research presented in this PhD thesis has been financed in part by the China Scholarship Council (CSC), project No. 2010634027.

ISBN: 978-94-6259-824-9

Copyright©2015 Jianwei Gao

Ontwerp omslag door Jianwei Gao

[jianweigao@outlook.com](mailto:jianweigao@outlook.com)

All rights reserved. No part of the material protected by this copyright notice may be reproduced or utilized in any form or by any means, electronic or mechanical, including photocopying, recording or by any information storage and retrieval system, without written permission from the author.

# Table of contents

---

<b>1 Introduction.....</b>	<b>1</b>
1.1 Introduction to fuel cells .....	2
1.1.1 The history of fuel cells .....	2
1.1.2 Working principle of a fuel cell .....	3
1.1.3 Fuel cell types .....	5
1.2 Proton exchange membrane fuel cells .....	8
1.3 Proton exchange membranes .....	9
1.3.1 Perfluorosulfonic acid ionomer membranes .....	10
1.3.2 Polystyrenesulfonic acid based membranes .....	12
1.3.3 Polyimide based membranes .....	13
1.3.4 Poly(arylene ether) based membranes .....	14
1.4 Liquid crystal polymers for proton transport .....	15
1.5 Scope and outline of the thesis .....	17
1.6 References .....	19
<b>2 Water-soluble aramids: sulfonated polymeric model systems</b>	
<b>for proton and ion-transport .....</b>	<b>23</b>
2.1 Introduction .....	24
2.2 Experimental .....	26
2.2.1 Materials .....	26
2.2.2 Interfacial polycondensation procedure .....	27
2.2.3 Membrane preparation .....	28
2.2.4 Characterization .....	28
2.3 Results and discussion .....	29
2.3.1 Chemical structure analysis of Na-PBDT and Na-PBDI .....	29
2.3.2 Molecular weight analysis of Na-PBDT and Na-PBDI .....	31
2.3.3 Thermal properties .....	33
2.3.4 Mechanical properties .....	34
2.3.5 Polarizing optical microscopy .....	36
2.3.6 X-ray diffraction experiments .....	38
2.4 Conclusion .....	42
2.5 References .....	43

### **3 The hydrolytic stability of PBDT and PBDI .....45**

3.1 Introduction.....	46
3.2 Experimental .....	47
3.2.1 Materials .....	47
3.2.2 Ion exchange procedure .....	48
3.2.3 Hydrolysis procedures .....	49
3.2.4 Characterization .....	49
3.3 Results and discussion .....	50
3.3.1 Reduced viscosities of H-PBDT and H-PBDI and their thermal stabilities .....	50
3.3.2 Stability of Na-PBDT under neutral, basic and acidic conditions .....	52
3.3.3 Hydrolysis of Na-PBDI and H-PBDI in hot water: an NMR study .....	53
3.4 Conclusion .....	56
3.5 References.....	57

### **4 Ionic crosslinking of Na-PBDT and Na-PBDI membranes .59**

4.1 Introduction .....	60
4.2 Experimental .....	62
4.2.1 Materials .....	62
4.2.2 Ionic crosslinking procedure .....	62
4.2.3 Characterization .....	63
4.3 Results and discussion .....	64
4.3.1 Ionic crosslinking .....	64
4.3.2 Ionic crosslinking degree and water uptake .....	65
4.3.3 Thermal and mechanical properties of crosslinked Na-PBDT and Na-PBDI .....	69
4.3.4 Polymer morphology (POM) .....	70
4.3.5 Wide-angle X-ray scattering .....	72
4.4 Conclusion .....	75
4.5 References .....	76

### **5 Performance analysis of Na-PBDT as potential proton exchange membrane .....79**

5.1 Introduction.....	80
-----------------------	----

5.2 Experimental .....	82
5.2.1 Materials .....	82
5.2.2 Characterization .....	82
5.3 Results and discussion .....	84
5.3.1 Water diffusion .....	84
5.3.2 Ionic conductivity .....	88
5.3.3 Fuel cell performance .....	90
5.4 Conclusion .....	95
5.5 References .....	96

<b>Summary .....</b>	<b>99</b>
----------------------	-----------

<b>Samenvatting .....</b>	<b>103</b>
---------------------------	------------

<b>Curriculum Vitae .....</b>	<b>107</b>
-------------------------------	------------

<b>Acknowledgements .....</b>	<b>109</b>
-------------------------------	------------



## **Chapter 1**

### **Introduction**

---

In this chapter, various types of fuel cells and their working principle will be reviewed. Special attention will be paid to the role of the proton exchange membrane (PEM) and how the polymer morphology affects proton transport across the membrane. The challenges around the design of all-aromatic PEMs will be discussed and the chapter will be concluded with the aim and outline of the thesis.

## 1.1 Introduction to fuel cells

Nowadays, humanity is faced with several major challenges, of these notably are: a fossil energy crisis and environmental pollution. Different sources of clean energy are currently being explored and wind energy and solar energy are, perhaps somewhat arbitrarily, considered most promising because of their abundance. Another related challenge is energy storage. To achieve this, electric power can either be stored in batteries or used in an electrolysis process to convert water into fuel e.g. by creating oxygen ( $O_2$ ) and hydrogen ( $H_2$ ). This hydrogen gas can be stored and converted back to electric power by means of a fuel cell at a later stage. Hydrogen has a high energy density (triple that of gasoline per mass unit) which makes it a nearly ideal energy carrier. For the hydrogen-to-electricity conversion, hydrogen fuel cells could be the best candidate, because they possess many advantages, such as high efficiency, and quiet and stationary operation. But right now, there are many challenges limiting the application of fuel cells. For example, fuel cells are quite expensive compared to conventional power sources, and their lifetime is relatively short.[1-4]

### 1.1.1 The history of fuel cells

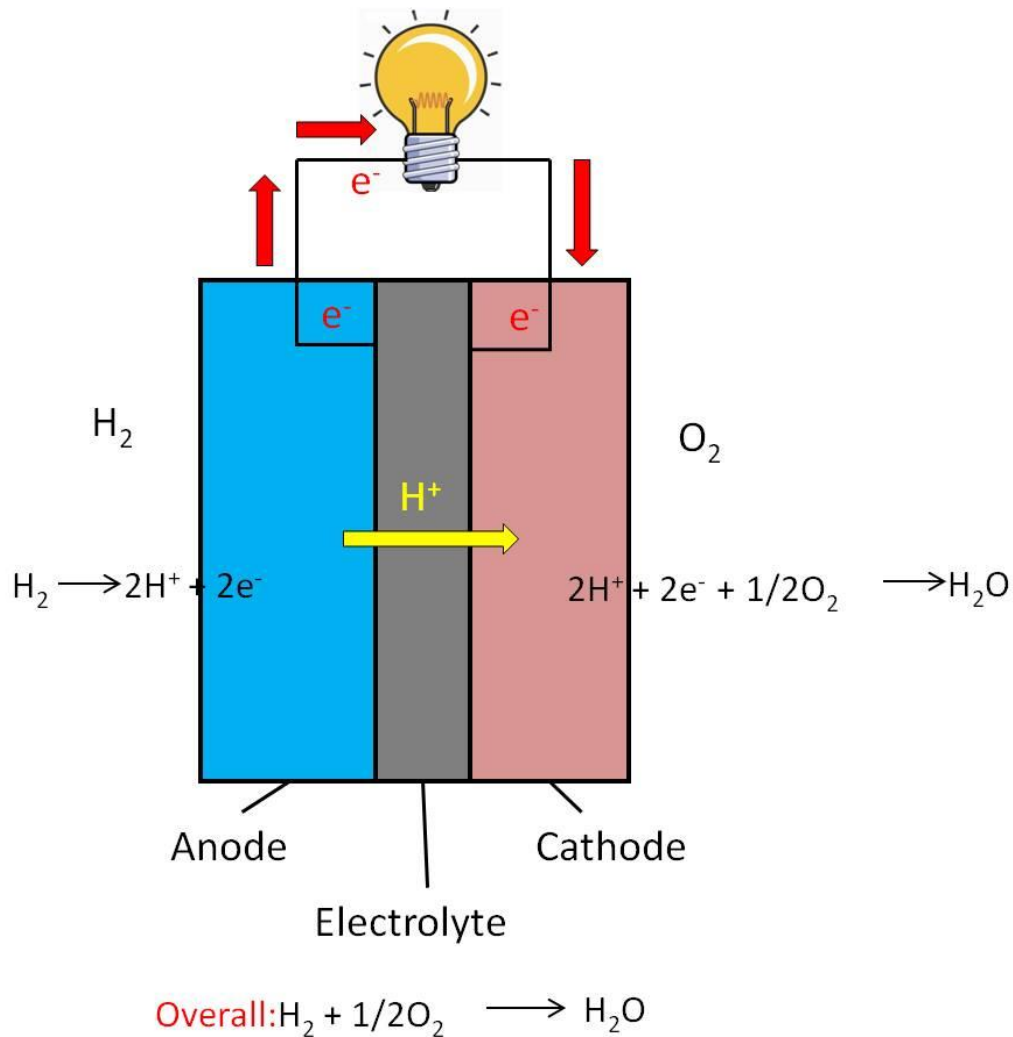
A fuel cell is a device that generates electricity by converting chemical energy from a fuel through a chemical reaction. In 1800, British scientists William Nicholson and Anthony Carlisle discovered that electrical energy can be converted into chemical energy by using electricity to decompose water into hydrogen ( $H_2$ ) and oxygen ( $O_2$ ).[5] Later in 1839, Sir William R. Grove, who is often considered to be the “Father of the Fuel Cell”, took one step further, or more accurately, a reverse step.[6,7] He found that electricity can be produced by reversing the electrolysis of water. Grove did a series of experiments and concluded that an electric current could be produced by connecting a hydrogen anode and an oxygen cathode using platinum as the catalyst. The term “fuel cell” was first coined for this process by Charles Langer and Ludwig Mond in 1889. They created a gas-powered battery by using coal gas as a fuel with electrodes of thin perforated platinum, and generated an output power of  $6.5 \text{ mA/cm}^2$  (electrode area) at 0.73 Volts.[6] In 1932, Francis Bacon, an



engineering professor at the University of Cambridge, modified Mond and Langer's equipment and developed the first successful fuel cell by using hydrogen, oxygen, an alkaline electrolyte and nickel electrodes. By 1959, with the support of Marshall Aerospace Company, Bacon and a co-worker produced a 5 kW fuel cell system with an efficiency of 60%.[7] Also, in the late 1950s and early 1960s, the General Electric Company (GE) developed fuel cell technology for the National Aeronautic and Space Administration (NASA) and McDonell Aircraft during the Gemini program. Two types of fuel cells, alkaline fuel cells (AFCs) and polymer electrolyte membrane fuel cells (PEMFCs) were developed for the Apollo, Gemini and Space Shuttle programs.[6,8] In the 1970s, fuel cells received renewed attention from governments and industry because of environmental problems and the oil crisis. From that time on, the major efforts for fuel cell research and application are generally focused on developing stationary power systems and hydrogen powered vehicles.[9,11] Up till now, there have been more than 2500 stationary power systems installed in hospitals, hotels and schools around the world.[6] At the same time, fuel cell cars and buses have also been manufactured by different car manufacturers, and some of them are now available for consumers.[12]

### **1.1.2 Working principle of a fuel cell**

The general working principle is illustrated in Figure 1.1. Hydrogen enters the anode of a fuel cell and is converted by a catalyst into protons and electrons. The negatively charged electrons travel along the external circuit to the cathode, creating an electric current; meanwhile, the positive protons go through the electrolyte to the cathode. Both electrons and protons react with oxygen at the cathode to produce water.[6]



**Figure 1.1.** The working principle of a fuel cell.[6]

There are various advantages that fuel cells offer over conventional power sources[1,3,5,6], such as internal combustion engines:

1. Since hydrogen is used as the fuel, water is the only side product;
2. The energy efficiency of fuel cells is significantly higher than that of other power sources because chemical energy is converted into electrical energy directly without a combustion process;
3. Fuel cells are very quiet during operation, which allows fuel cells to be installed in residential areas;
4. Fuel cells can be stacked. Individual cells can be connected together to increase the output power. The connected cells can be so arranged to meet specific output needs, like the desired voltage and current.

Although fuel cells are attractive, there are also many challenges to be met[5,7,9,10], for example:

1. Hydrogen is supposed to be the fuel of choice, but the production, transport and proper storage of pure hydrogen has not been completely solved;
2. The durability of fuel cells often is lower than required. At present, the average lifetime is less than 10,000 hours. A fuel cell station is required to operate for at least 60,000 hours in order to be economically viable;[5,9]
3. Fuel cells are quite expensive because of platinum-based catalysts and other costly materials. It is estimated that the cost-per-kW generated by fuel cells needs to decrease by a factor of 10 to compete with conventional power generation solutions, such as internal combustion engines.[5]

### 1.1.3 Fuel cell types

Since hydrogen is considered to be a non-polluting source of fuel, fuel cells have a promising future. Up till now, there are mainly five types of fuel cells: molten carbonate fuel cells, solid oxide fuel cells, phosphoric acid fuel cells, alkaline fuel cells and proton exchange membrane fuel cells. Some technical parameters and application range of these fuel cells are listed in Table 1.1.[1,5,6,13-19]

***Molten carbonate fuel cells (MCFCs)*** MCFCs are operated at a temperature of 650 °C and above. The electrolyte is a mixture of molten carbonate salts, such as lithium carbonate and potassium carbonate. Due to the high operating temperature, precious metals (e.g. Pt) do not need to be used as a catalyst, but some cheaper materials, such as NiO and Ni-Al alloy, are employed, which reduces the overall cost of the fuel cell. The fuel is not limited to hydrogen or natural gas. Cheap coal gas can also be used. Besides the low cost, efficiencies of MCFCs exceeding 60% are also impressive. A lot of heat is generated during fuel cell operation. If this heat can be collected and utilized, the efficiency increases to 85%.[13,14]

***Solid oxide fuel cells (SOFCs)*** Just like MCFCs, SOFCs also operate at high temperatures, typically 600-1000 °C. But different from MCFCs, a solid

oxide material (e.g. CaO or ZrO) is used in SOFCs as the electrolyte to conduct oxide ions ( $O^{2-}$ ) from the cathode to the anode, eliminating the use of liquid electrolytes. Similar to the MCFCs, SOFCs do not require precious metal catalysts, either, and various gases can be used as the fuel, including hydrogen, carbon monoxide and natural gas,. The efficiency is comparable to that of MCFCs.[15,16]

**Phosphoric acid fuel cells (PAFCs)** PAFCs use liquid phosphoric acid as the electrolyte, and the operation temperatures are typically in the 150–200 °C range. Pt is used as the catalyst and hydrogen is the fuel. The efficiency is as high as 80% when considering both the electricity and the heat output. In terms of electrical output the efficiency of this type of fuel cell is 50%. The PAFCs tolerate up to 0.7 vol% of CO in the fuel.[17,52]

**Alkaline fuel cells (AFCs)** AFCs make use of potassium hydroxide (KOH) as the electrolyte and the operating temperature is typically between 65 and 220 °C. AFCs were used in the Apollo missions in the mid-1960s to provide electricity as well as drinking water. Pure hydrogen is necessary for AFCs, which increases the overall operating cost. The catalyst is not limited to Pt, but a lot of other catalysts can be used as well, such as Ni. The efficiency is about 60%. The system is quite sensitive to CO and CO<sub>2</sub> and the lifetime is relatively short.[18]

**Proton exchange membrane (or polymer electrolyte membrane) fuel cells (PEMFCs)** PEMFCs use a solid polymer membrane as the electrolyte to transport protons from the anode to the cathode, and the operating temperature using hydrogen is below 100 °C, typically between 60 to 80 °C. Pt is used as the catalyst. Apart from hydrogen, a variety of other fuels can be used, such as methanol or ethanol, and then the cell is referred to as a direct methanol fuel cell (DMFC) or direct ethanol fuel cell (DEFC) respectively. The efficiency ranges from 50 to 60%. Polymer membranes are used as the electrolyte, so PEMFCs can be made very thin, and also there are no issues with leaking electrolytes, which makes operating PEMFCs quite safe. PEMFCs are currently viewed as the most attractive fuel-cell type.[19]

**Table 1.1** Overview of different fuel cell technologies currently in use.

<b>Fuel Cell type</b>	<b>Catalyst</b>	<b>Electrolyte</b>	<b>Temperature range (°C)</b>	<b>Efficiency (%)</b>	<b>Capacities ( kW )</b>	<b>Application</b>
<b>Molten carbonate (MCFC)</b>	NiO, Ni, Co, Cu, and relative alloys	Molten carbonate salt mixture	>650	45-60	250 -1000	Electric utility
<b>Solid oxide (SOFC)</b>	$\text{La}_{1-x}\text{Sr}_x\text{MnO}_3$ , Ni-Zr cermet	Solid nonporous ceramic materials	600-1000	45-65	300 -3000	Electric utility
<b>Phosphoric acid (PAFC)</b>	Pt and Pt alloys	Concentrated phosphoric acid soaked in a matrix	150-200	37-55	25-250	Distributed power generation
<b>Alkaline (AFC)</b>	Pt, Pd, Ag, Ni and their alloys	Potassium hydroxide solution soaked in a matrix	65-220	50-60	2.2	Spacecraft, Military
<b>Proton exchange membrane (PEMFC)</b>	Pt	Sulfonated polymer membrane	<100	50-60	0.1-250	Transportation, Stationary power, Backup power

## 1.2 Proton exchange membrane fuel cells

As the work described in this thesis will focus on proton exchange membrane fuel cells, a more in-depth review will be provided. PEMFCs were invented at the General Electric Company (GE) in the beginning of the 1960s, with the work of Thomas Grubb and Leonard Niedrach. An initially successful PEMFC was announced by GE in mid-1960s, and applied in the Gemini program of NASA. Despite their success in the space program, fuel cell systems did not reach the commercial phase due to their high installation and operating cost. Until the late 1980s and early 1990s, several pivotal innovations, such as low platinum catalyst loading and thin film electrodes, lowered the cost of fuel cells, making PEMFC systems economically viable.[11]

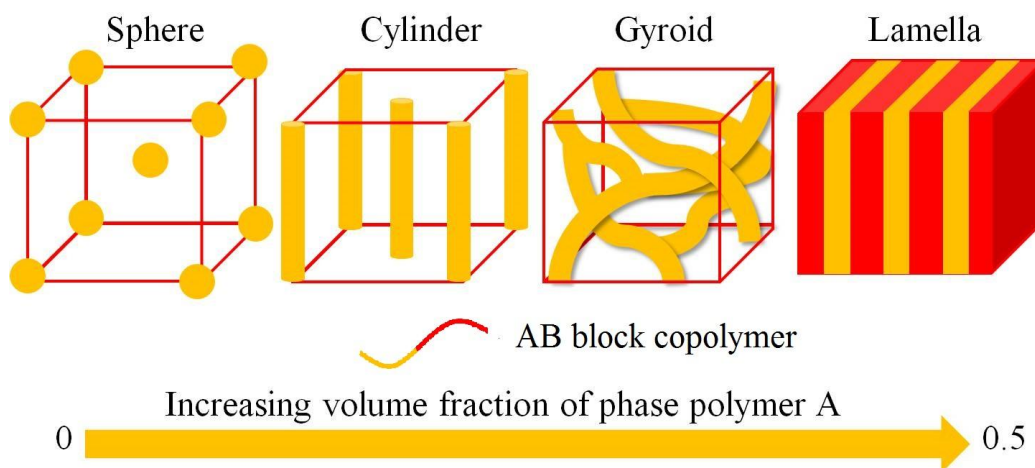
PEMFCs offer several advantages: a solid polymer electrolyte removes the need to handle corrosive acids or bases, which improves safety. The safety is also improved by the low temperature/pressure operating range. PEMFCs are compact, robust and tolerate  $\text{CO}_2$ , which means air can be used instead of pure oxygen. Before using PEMFCs in our daily life, a number of important and rather complex problems must be solved: a. the lifetime and stability of the catalysts and membranes have to be improved; b. the tolerance with respect to CO impurities in  $\text{H}_2$  has to be improved; c. the overall cost of production has to decrease (catalysts without, or containing much less, platinum and cheaper membranes). For the proton exchange membranes (PEMs), the essential functions are simple, including separation of the anode and the cathode gases, and transport of protons from the anode to the cathode, but the operating conditions in a fuel cell are rather demanding. The membranes should have high proton conductivity, should be impermeable to fuel gas (or liquid methanol or ethanol), and exhibit good thermal and mechanical stability, as well as high durability. It is difficult for a membrane to meet all of the above-mentioned requirements, therefore a huge number of polymers have been explored for PEM applications. [19]

### 1.3 Proton exchange membranes

One of the key parameters of a PEM is the proton conductivity. In general, good proton conductivity is easily reached by increasing the ion exchange capacity (IEC) value of a polymer. The ion exchange capacity (IEC) represents the amount of available cations, protons for PEMs, in a material, and is expressed as millimole of ions per gram (mmol/g). A high IEC corresponds to a high degree of sulfonation, which in turn leads to high water uptake. The increased water uptake promotes proton transport as  $H^+$  is typically transported via the hydronium ion (*i.e.*  $H_3O^+$ ). If too much water is absorbed, the membrane will swell and the mechanical strength and chemical stability will be compromised. Therefore a membrane should display high proton conductivity at a relative low IEC.[19]

Besides the IEC, an ordered structure is also very important for a polymer membrane to achieve high proton conductivity. By creating ordered structures in membranes, hydrophilic channels are created to transport protons. For this reason, block copolymers are being developed by many research groups. A block copolymer chain has two or more blocks. Generally two types of blocks are used: hydrophilic blocks and hydrophobic blocks. The hydrophilic blocks usually contain sulfonic groups, which absorb water molecules and aid in proton transfer. The hydrophobic blocks form the matrix and guarantee the mechanical strength of the membrane. By adjusting the degree of sulfonation and the distribution of sulfonic groups in the polymer chains, it is possible to increase the size of the hydrophilic domains and connect them to generate a percolating network of hydrophilic channels. Figure 1.2 shows the morphology of AB diblock copolymers, where A is the hydrophilic block (yellow) and B (red) is the hydrophobic block. For proton exchange membranes, the gyroid structure is an ideal morphology for proton transport due to the well connected hydrophilic channels.[20,21,33]

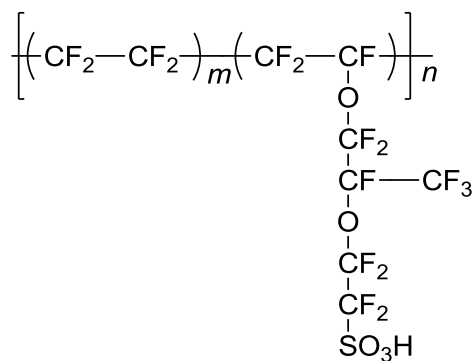
To obtain a membrane with good proton conductivity, numerous polymers have been developed. According to the difference in polymer structures, the membranes are classified into four main types: 1. perfluorosulfonic acid ionomer membranes, 2. polystyrenesulfonic acid based membranes, 3. polyimide based membranes, and 4. poly(arylene ether) based membranes.



**Figure 1.2.** Morphologies of AB diblock copolymer, where A (yellow) is the hydrophilic block and B (red) is the hydrophobic block.

### 1.3.1 Perfluorosulfonic acid ionomer membranes

For this type of membrane, Nafion<sup>®</sup> is probably the most well-known example. Nafion<sup>®</sup> is a copolymer of tetrafluoroethylene (TFE) with perfluorinated vinyl ethers containing sulfonic acid groups, as shown in Figure 1.3.[22,23] This polymer was developed by Walther Grot at the DuPont Company and this material exhibits excellent thermal and mechanical properties, as well as good proton conductivity. At present, Nafion<sup>®</sup> is still the best candidate for PEMFC applications and over the years several series of Nafion<sup>®</sup> membranes were developed by DuPont. Other companies, such as Asahi Glass Company and Dow Chemical Company, also developed various types of sulfonated polyfluoroethylene membranes, which have polymer structures similar to that of Nafion<sup>®</sup>. [24,25]



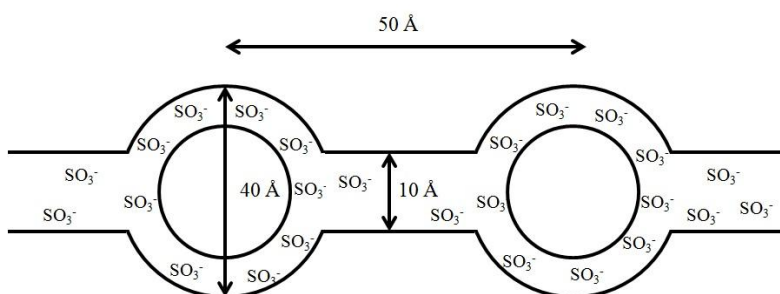
**Figure 1.3.** Polymer structure of perfluorosulfonic acid membranes (Nafion<sup>®</sup>). [22,23]



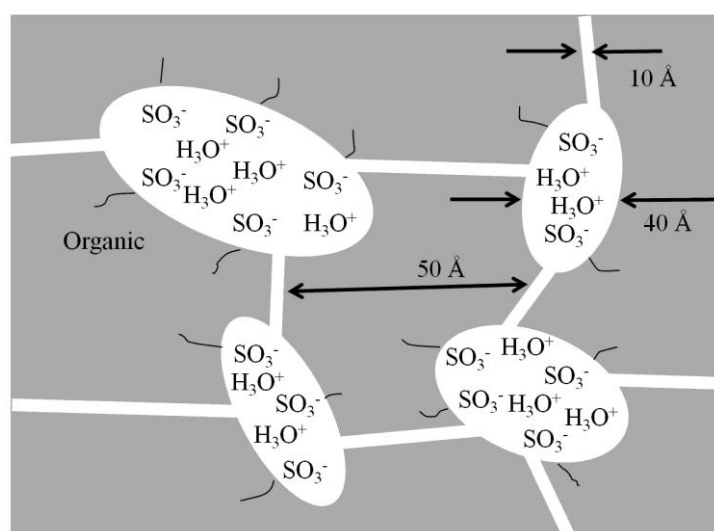
Nafion<sup>®</sup> membranes are chemically stable and have acceptable thermal and mechanical properties. Nafion<sup>®</sup> 115 film for instance displays a proton conductivity as high as 0.1 S/cm, a tensile modulus of 114 MPa, a tensile strength of 34 MPa and an elongation at break of 200%, at room temperature in water. Only alkali metals, particularly sodium, can degrade Nafion<sup>®</sup> under normal operating temperature and pressure conditions.[27]

The high proton conductivity is due to the interconnected hydrophilic clusters in the membrane. Gierke and co-workers described the morphology of Nafion<sup>®</sup> using a cluster network model (Figure 1.4A). Ionic clusters with spherical shape are connected by narrow channels.[23,26,28] Eikerling *et al.* modified this model using a “random network model” (Figure 1.4B). In this model, the side chains terminated with sulfonic groups tend to form clusters within the overall structure of the Nafion<sup>®</sup>, which leads to the formation of hydrated regions.[26,29]

A.



B.

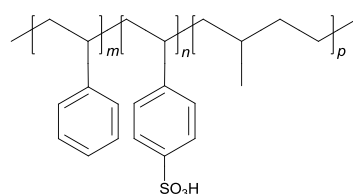


**Figure 1.4.** Models for morphology of Nafion<sup>®</sup>: A) Cluster of network model, and B) random network model.[23,26,28,29]

Despite the excellent properties, Nafion<sup>®</sup> membranes have some drawbacks. Operating at high temperatures ( $> 80\text{ }^{\circ}\text{C}$ ) is harmful for Nafion<sup>®</sup> membranes due to the loss of water and reduction of mechanical strength.[19,26] Besides, the permeability to methanol and ethanol of Nafion<sup>®</sup> is significant, which limits its application for direct methanol/ethanol fuel cells (DMFCs and DEFCs). In addition, Nafion<sup>®</sup> membranes are very expensive due to the high price of the fluorinated monomers used and the complex synthetic procedure of the polymer. Therefore, many other new polymer materials (e.g. partially fluorinated, non-fluoro hydrocarbon polymers) have been developed, which will be briefly introduced in the following sections.

### 1.3.2 Polystyrenesulfonic acid based membranes

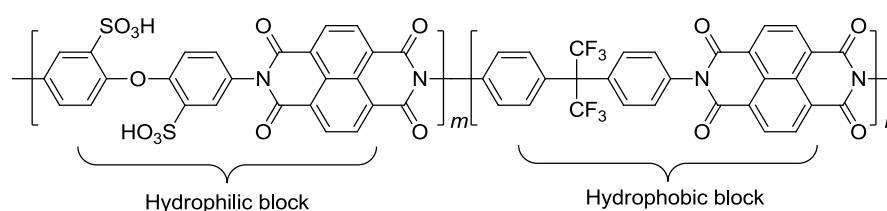
As discussed above, one problem of Nafion<sup>®</sup> and other fluorinated polymers is the cost of the perfluoroalkylether monomers. Therefore, polystyrenesulfonic acid (PSSA) was considered because of the low price. It was even used as an electrolyte membrane in NASA's Gemini flights in the 1960s.[30,31] Park and co-workers synthesized a series of polystyrenesulfonate-*block*-polymethylbutylene (PSS-*b*-PMB) copolymers (Figure 1.5).[32,33] The IEC of the copolymers ranged from 0.887 to 2.692 mmol/g. For a copolymer with an IEC of  $\sim 2$  mmol/g, the proton conductivity was as high as 0.21 S/cm at  $90\text{ }^{\circ}\text{C}$  (RH=98%), which is much higher than that of Nafion<sup>®</sup> 117 (about 0.11 S/cm). According to TEM images, the ideal PEM morphology, a gyroid structure, was obtained in these block copolymers. The downside of PSSA is the oxidative stability of the aliphatic backbone, which is inferior compared to that of the perfluorinated polymers and has significantly hindered its application.[30]



**Figure 1.5.** Polymer structure of PSS-*b*-PMB.[32,33]

### 1.3.3 Polyimide based membranes

Sulfonated polyimides are of interest because they exhibit low gas and liquid permeability and high mechanical strength. Kins and co-workers prepared a series of sulfonated block-copolyimides with the same IEC ( $\sim 1.7$  mmol/g), but different block length (Figure 1.6).[34] The length of the hydrophilic and hydrophobic blocks was determined by the number of repeat units,  $m$  and  $n$ , which ranged from 5 to 50. For each block copolymer,  $m = n$ , i.e. the block length was similar. A random copolyimide with the same IEC was prepared for comparison. The proton conductivity increased with the increase in block length. The proton conductivity of the copolymer with the longest blocks ( $m = n = 50$ ) at 5% RH (50 °C) was  $4.6 \times 10^{-6}$  S/cm, which was more than 12 times higher than that of the random copolyimide, and on increasing the RH to 90%, the proton conductivity was as high as 0.1 S/cm, equal to that of Nafion<sup>®</sup> 117. TEM and AFM experiments revealed that spherical clusters formed and dispersed in the membranes, which indicated a channel-like structure rather than a lamellar structure. Therefore, a cylinder or gyroid morphology was considered to be more favorable than a lamellar morphology. The domain size increased with increasing block length, and the hydrophilic domains eventually formed ionic channels in the longest block copolyimide ( $m = n = 50$ ), resulting in the highest proton conductivity. Similar morphologies for sulfonated copolyimides were also reported by other groups.[35,36]



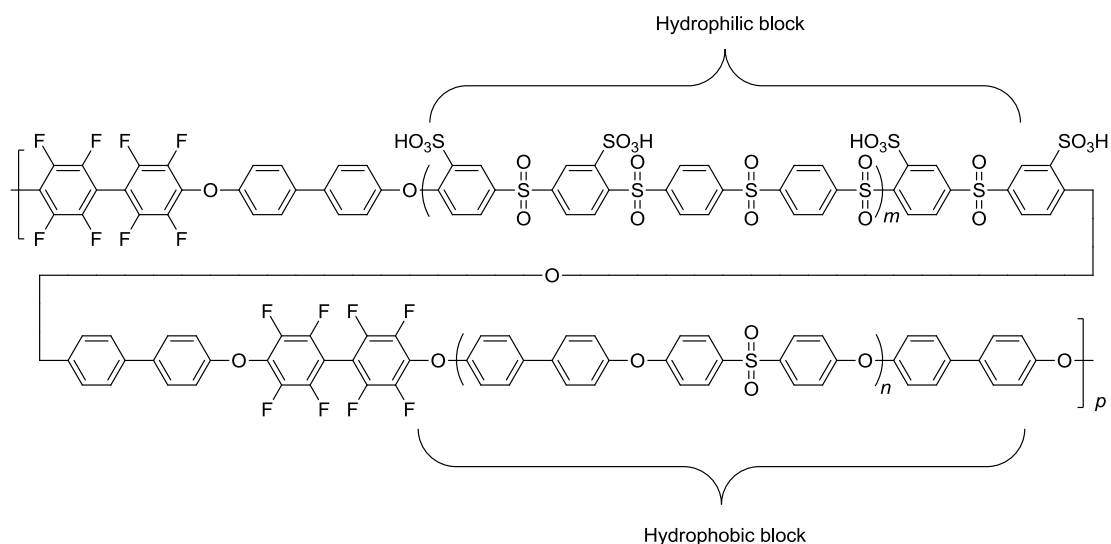
**Figure 1.6.** Polymer structure of sulfonated block copolyimides.[34]

The main disadvantage of sulfonated polyimides is their poor durability.[37,38] Genies *et al.* studied two model compounds of polyimides: five-membered ring and six-membered ring compounds.[38] The results revealed that hydrolysis reactions occurred for both model compounds: the stability of the five-membered ring (phthalic) model compound was less than 1

h at 80 °C in water, whereas the six-membered ring (naphthalenic) model was superior giving up to 100 h under similar conditions. However, it is still far away from the PEMFC durability requirement, at least longer than 5000 h.

#### **1.3.4 Poly(arylene ether) based membranes**

Besides sulfonated polyimides, poly(arylene ether) based membranes have also been investigated because of their excellent thermal, mechanical performance, and chemical stability.[39-42] Jung *et al.* synthesized aromatic multiblock copolymers consisting of sulfonated hydrophilic poly(arylene sulfone) blocks combined with hydrophobic poly(arylene ether sulfone) blocks (Figure 1.7).[42] The sulfonated poly(arylene sulfone) blocks were chosen as the hydrophilic part, which displayed high chain stiffness, strong acidity, and high resistance against desulfonation. The well-defined phase separation between the hydrophilic and hydrophobic domains was observed in all the membranes by AFM. Extremely large well-connected hydrophilic ionic domains (> 20 nm) were observed for the membrane with the longest hydrophilic blocks, indicating a gyroid structure inside of the membranes. At 80 °C and 50% RH, the membranes showed high proton conductivity of 0.028 S/cm, comparable to that of the Nafion<sup>®</sup> 212 membrane, and the durability of this material was higher than 1200 h during an open circuit voltage hold test (80 °C, 10% RH). Other groups developed other series of random and block copolymers based on poly(arylene ether sulfones).[43,44] They also found that for the same sulfonation degree, block copolymers possessed higher conductivities than the random copolymers. Degradation is also a problem for sulfonated poly(arylene ether) polymers. Compared to sulfonated polyimides, poly(arylene ether) based membranes exhibit no hydrolysis but they are sensitive to an oxidative environment.[45]

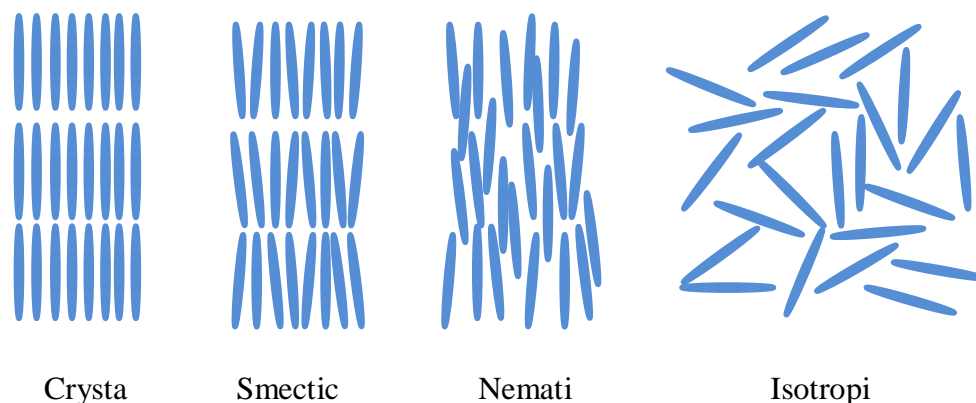


**Figure 1.7.** The multiblock copolymer sPAS-A/Bs.[42]

## 1.4 Liquid crystal polymers for proton transport

From the brief review above, it is clear that the morphology of the PEM has a direct effect on the proton conductivity and this has directed novel polymer chemistries towards a variety of block copolymer designs. Most of them are aromatic polymers because of their unique thermal and mechanical properties and chemical stabilities. Another important class of polymers that have not been explored very extensively are liquid crystal polymers (LCPs).

The liquid crystal (LC) phase is a state of matter between the crystalline (solid) and isotropic (liquid) phase. Correspondingly, liquid crystal polymers (LCPs) are polymers, which possess liquid crystal properties under certain conditions, such as by dissolving in solvents (lyotropic liquid crystal polymers) or by heating above the glass or melt transition (thermotropic liquid crystal polymers). Objects with different shapes (rod-like, disk-like) can produce quite a wide variety of liquid crystal phases. For rod-like objects, some simple liquid crystal organizations are illustrated in Figure 1.8.



**Figure 1.8.** Schematic representation of crystalline (K), smectic A (SmA), nematic (N) and isotropic (I) organizations.

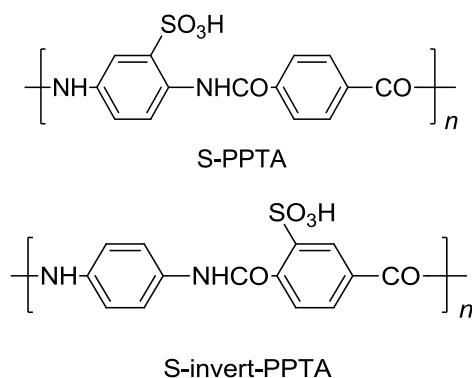
LCPs exhibit unique properties over conventional non-LC polymers, such as high mechanical strength, high chemical resistance and excellent flame retardancy. When the chains are aligned, the polymers possess even higher mechanical strength. Therefore, some of them can be used as high-performance polymers for structural applications.[46] In some recent reports LCPs are found to be unique in forming organized domains that can act as transport channels for ion transport.[47-51]

Chow and co-workers studied the proton transport ability of 4-(octadecyloxy) phenylsulfonic acid under non-humidified conditions.[47] This small molecule forms a smectic A phase in the range of 63–83 °C. A homeotropic aligned sample was obtained by using chlorodimethyloctadecylsilane as an alignment layer. The highest proton conductivity (0.011 S/cm) was observed in the homeotropic smectic A phase, which was better than the solid powder ( $1.5 \times 10^{-7}$  S/cm below 63 °C) and isotropic phase ( $1.2 \times 10^{-4}$  S/cm above 83 °C). By contrast, the proton conductivity in the smectic A phase without alignment was similar to that of a solid state sample at 25 °C. These results confirm that the proton transport is favored in the fluid smectic A phase and it is possible to achieve proton transport under non-humidified conditions.

Tan *et al.* studied a side-chain LCP containing pendant sulfonic acid groups as an proton exchange membrane.[48] The side-chain mesogens were macroscopically aligned using a mechanical shear force in the smectic phase. A lamellar structure was observed in the aligned membrane using SEM.

Enhanced anhydrous proton conductivity was observed at temperatures above 100 °C. The maximum proton conductivity was as high as  $4.7 \times 10^{-3}$  S/cm, while the unaligned polymer displayed a proton conductivity of about  $1.0 \times 10^{-3}$  S/cm.

Every and co-workers studied the proton transport properties of sulfonated poly (*p*-phenylene terephthalamide) (PPTA).[49] Two polymers, S-PPTA and S-invert-PPTA, were studied (structures are shown in Figure 1.9). Both polymers are lyotropic, but the properties are different due to the various positions of the sulfonic acid groups. The in-plane proton conductivity, *i.e.* proton transport within the plane of the membrane, of S-invert-PPTA was higher than that of S-PPTA. At 50 °C, 100% relative humidity, the in-plane proton conductivity of S-invert-PPTA was ~0.17 S/cm, while that of S-PPTA was 0.04 S/cm (Nafion<sup>®</sup> 117 shows 0.12 S/cm under the same conditions in both the in-plane and perpendicular direction). XRD experiments revealed a homeotropic alignment in the S-PPTA membranes, *i.e.* the rigid-rod polymer chains aligned perpendicular to the film surface, while S-invert-PPTA polymer chains were generally aligned parallel to the film surface (a planar alignment).[49,50]

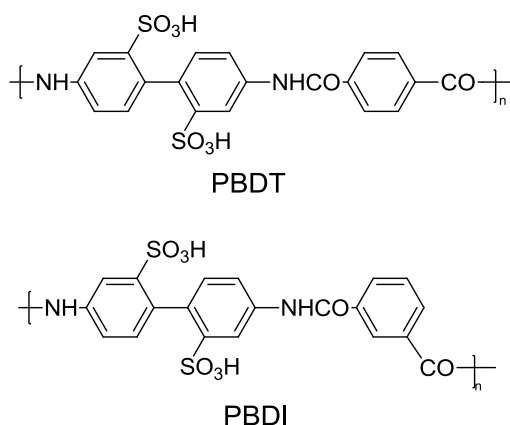


**Figure 1.9.** Structure of sulfonated PPTAs.[49]

## 1.5 Scope and outline of the thesis

The aim of the work presented in this thesis is to better understand the role of liquid crystalline ordering in sulfonated polyamide model compounds and how this affects ion transport and fuel cell performance. Every *et al.* study on LC polyamides, S-PPTA and S-invert-PPTA, indicated that protons prefer to be

transported along the rigid-rod LC polymer chains.[49] However, only limited data was presented on the proton conductivity as the polymers dissolved in water and the low molecular weight of the polymers made it difficult to produce useful membranes that could be handled and investigated. Therefore, we synthesized two sulfonated polyamide model compounds.[51] The two polymers have similar molecular structures (Figure 1.10), but poly(2,2'-disulfonylbenzidine terephthalamide) (PBDT) is a liquid crystalline polymer, which forms a nematic phase in water, while poly(2,2'-disulfonylbenzidine isophthalamide) (PBDI) is a non-liquid crystalline (isotropic) reference polymer. The polymer repeat unit has two sulfonic acid ( $-\text{SO}_3\text{H}$ ) groups, which is anticipated to have a positive effect on the proton transport properties.



**Figure 1.10.** Chemical structures of PBDT and PBDI.[51]

In *Chapter 2*, we discuss the synthesis and characterization of PBDT and PBDI. The molecular weight, phase diagram and polarized optical microscopy images will be presented. The thermal and mechanical stabilities of the polymer films are compared and evaluated and X-ray diffraction is used to investigate the morphology of the PBDT and PBDI films.

In *Chapter 3*, the stability of PBDT and PBDI in the acid-form ( $-\text{SO}_3\text{H}$ ) and sodium-form ( $-\text{SO}_3\text{Na}$ ) will be discussed. Our results show that the stability of the acid-form PBDT and PBDI polyamides is relatively poor. Evidence of amide hydrolysis will be presented.

In *Chapter 4*, different synthetic strategies towards crosslinking PBDT and



PBDI will be discussed. The as synthesized polymers are soluble in water, which makes them unsuitable for fuel cell applications. Therefore the ionic crosslinking method is presented and evaluated. The (thermo)mechanical properties and morphology of the crosslinked PBDT and PBDI films are reported.

In *Chapter 5*, we will present the water diffusion, ion transport properties and fuel cell performance of PBDT and PBDI membranes. The results will be compared to a well-known reference polymer, *i.e.* Nafion<sup>®</sup> 117.

## 1.6 References

- [1] X.G. *Principles of Fuel cells*, New York: Taylor & Francis, **2006**.
- [2] Watt, G.D. *Renew. Energ.* **2014**, 72, 99.
- [3] Pei, P.; Chen, H. *Appl. Energ.* **2014**, 25, 60.
- [4] Lucia, U. *Renew. Sust. Energ. Rev.* **2014**, 30, 164.
- [5] Sharaf, O.Z.; Orhan, M.F. *Renew. Sust. Energ. Rev.* **2014**, 32, 810.
- [6] Andujar J.M.; Segura, F. *Renew. Sust. Energ. Rev.* **2009**, 13, 2309.
- [7] Grimes, P.G. *IEEE AES Systems Magazine* **2000**, 15, 1.
- [8] Choudhury, A.; Chandra, H.; Arora, A. *Renew. Sust. Energ. Rev.* **2013**, 20, 430.
- [9] Bruijn, F. *Green chem.* **2005**, 7, 132.
- [10] Mobius, H.H. *J. Solid State Electr.* **1997**, 1, 2.
- [11] Verspagen, B. *Advs. Complex Syst.* **2007**, 10, 93.
- [12] Eberle, U.; Mueller, B.; von Helmolt, R. *Energ. Environ. Sci.* **2012**, 5, 8780.
- [13] Wee, J.H. *Renew. Sust. Energ. Rev.* **2014**, 32, 178.
- [14] Rady, A.C.; Giddey, S.; Badwal, S.P.S.; Ladewig, B.P.; Bhattacharya, S. *Energ. Fuel.* **2012**, 26, 1471.
- [15] Nesaraj, A.S. *J. Sci. Ind. Res.* **2010**, 69, 169.
- [16] Bishop, S.R. *Acta Mech. Sinica* **2013**, 29, 312.
- [17] Sammes, N.; Bove, R.; Stahl, K. *Curr. Opin. Solid St. M.* **2004**, 8, 372.
- [18] Wang, Y.; Qiao, J.; Baker, R.; Zhang, J. *Chem. Soc. Rev.* **2013**, 42, 5768.
- [19] Higashihara, T.; Matsumoto, K.; Ueda, M. *Polymer* **2009**, 50, 5341.
- [20] Park, H.; Jung, J.; Chang, T. *Macromol. Res.* **2009**, 17, 365.
- [21] Hu, H.; Gopinadhan, M.; Osuji, C.O. *Soft Matter* **2014**, 10, 3867.

- [22] Sondheimer, S.J.; Bunce, N.J.; Fyfe, C.A. *J. Macromol. Sci. R. M. C* **1986**, 26,353.
- [23] Mauritz, K.A.; Moore, R.B. *Chem. Rev.* **2004**, 104, 4535.
- [24] Yaroslavtsev, A.B. *Polym. Sci. Ser. A* **2013**, 55, 674.
- [25] Luo, X.; Holdcroft, S.; Mani, A.; Zhang, Y.; Shi, Z. *Phys. Chem. Chem. Phys.* **2011**, 13, 18055.
- [26] Smitha, B.; Sridhar, S.; Khan, A.A. *J. Membr. Sci.* **2005**, 259, 10.
- [27] DuPont Company, US  
[http://www2.dupont.com/FuelCells/en\\_US/assets/downloads/dfc101.pdf](http://www2.dupont.com/FuelCells/en_US/assets/downloads/dfc101.pdf).
- [28] Hsu, W. Y.; Gierke, T. D. *J. Membr. Sci.* **1983**, 13, 307.
- [29] Eikerling, M.; Kornyshey, A.A.; Stimming, U. *J. Phys. Chem. B* **1997**, 101, 10807.
- [30] Costamagna, P.; Srinivasan, S. *J. Power. Sources* **2001**, 102, 242.
- [31] Kim, J.; Kim, B.; Jung, B. *J. Membr. Sci.* **2002**, 207, 129.
- [32] Park, M. J.; Downing, K. H.; Jackson, A.; Gomez, E. D.; Minor, A. M.; Cookson, D.; Weber, A. Z.; Balsara, N. P. *Nano Lett.* **2007**, 7, 3547.
- [33] Elabd, Y.A.; Hickner, M.A. *Macromolecules* **2011**, 44,1.
- [34] Kins, C.F.; Sengupta, E.; Kaltbeitzel, A.; Wagner, M.; Lieberwirth, I.; Spiess, H.W.; Hansen, M.R. *Macromolecules*, **2014**, 47, 2645.
- [35] Einsla, B. R.; Hong, Y. T.; Kim, Y. S.; Wang, F.; Gunduz, N.; McGrath, J. E. *J. Polym. Sci., Part A: Polym. Chem.* **2004**, 42, 862.
- [36] Chen, K.; Hu, Z.; Endo, N.; Higa, M.; Okamoto, K. *Polymer* **2011**, 52, 2255.
- [37] Miyatake, K.; Furuyaa, H.; Tanakab, M.; Watanabeb, M.K *J. Power Sources* **2012**, 204, 74.
- [38] Genies, C.; Merciera, R.; Silliona, B.; Petiaudb, R.; Cornetc, N.; Gebelc, G.; Pinerid M. *Polymer* **2001**, 42, 5097.
- [39] Gao, Y.; Robertson, G.P.; Guiver, M.D.; Mikhailenko, S.D.; Li, X.; Kaliaguine, S. *Macromolecule* **2005**, 38, 3237.
- [40] Glipa, X.; Haddad, M. E.; Jones, D. J.; Rozie`re, J. *Solid State Ionics* **1997**, 97, 323.
- [41] Xing, P.; Robertson, G.P.; Cuiver, M.D.; Mikhailenko, S.D.; Kaliaguine, S. *Macromolecules* **2004**, 37, 7960.
- [42] Jung, M.S.; Kim, T.H.; Yoon, Y.J.; Kang, C.G.; Yu, D.M.; Lee, J.Y.; Kim,

- H.J.; Hong, Y.T. *J. Memb. Sci.* **2014**, *459*, 72.
- [43] Vogel, C.; Komber, H.; Quetschke, A.; Butwilowski, W.; Potschke, A.; Schlenstedt, K.; Meier-Haack, J. *React. Funct. Polym.* **2011**, *71*, 828.
- [44] Wang, F.; Hickner, M.; Ji, Q.; Harrison, W.; Mecham, J.; Zawodzinski, T. A. McGrath, J. E. *Macromol. Symp.* **2001**, *175*, 387.
- [45] Kim, Y.S.; Hickner, M.A.; Dong, L.; Pivovar, B.S.; McGrath, J.E. *J. Membr. Sci.* **2004**, *243*, 317.
- [46] Hu, X.; Jenkins, S.E.; Min, B.G.; Polk, M.B.; Kumar, S. *Macromol. Mater. Eng.* **2003**, *288*, 823.
- [47] Chow, C.F.; Roy, V.A.L.; Ye, Z.; Lam, M.H.W.; Lee, C.S. Lau, K.C. *J. Mater. Chem.* **2010**, *20*, 6245.
- [48] Tan, S.; Wang, C.H.; Wu, Y. *J. Mater. Chem. A* **2013**, *1*, 1022.
- [49] Every, H.A.; Mendes, E.; Picken, S.J. *J. Phys. Chem. B* **2006**, *110*, 23729.
- [50] Every H.A.; van der Ham, L.; Picken, S.J.; Mendes, E. *Soft Matter* **2009**, *5*, 342.
- [51] Sarkar, N.; Kershner, D. *J. Appl. Polym. Sci.* **1996**, *62*, 393.
- [52] Song, R.H.; Shin, D. R. *Int. J. Hydrogen Energy* **2001**, *26*, 1259.



## Chapter 2

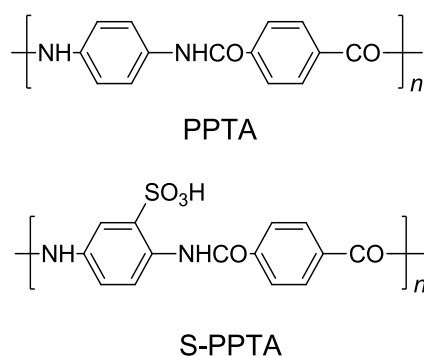
### Water-soluble Aramids: Sulfonated Polymeric Model Systems for Proton and Ion-transport

---

Two sodium-form sulfonated polyamides, poly(2,2'-disulfonylbenzidine terephthalamide) (Na-PBDT) and poly(2,2'-disulfonylbenzidine isophthalamide) (Na-PBDI), have been prepared using interfacial polycondensation. The two polymers were found to have good thermal stabilities. The  $T_d^{5\%}$  is higher than 427 °C. The two polymers show similar storage modulus ( $E'$ ) values. For dry films, the  $E'$  value was as high as 10 GPa, while the films stored in air had a somewhat lower storage modulus of 3-6 GPa at room temperature. Due to the different polymer structures, Na-PBDT shows nematic liquid crystalline behaviour in water while Na-PBDI only forms an isotropic solution. The XRD results reveal that the Na-PBDT films cast from the LC polymer solution possess an alignment along the casting direction ( $\overline{\langle P_2 \rangle} \sim 0.3$ ), whereas the Na-PBDI films do not have such alignment. The difference in membrane morphology make both polymers ideal model systems for studying how protons and ions transport in amorphous and oriented liquid crystal polymer membranes.

## 2.1 Introduction

Poly(*para*-phenylene terephthalamide), or PPTA (Figure 2.1) is an all-aromatic polymer capable of forming a nematic liquid crystal (LC) solution in 100% H<sub>2</sub>SO<sub>4</sub>.<sup>[1]</sup> This unique ability makes it possible to process PPTA into highly aligned fibres and films with unusual optical and mechanical properties. We anticipate that sulfonated PPTA (S-PPTA) (Figure 2.1) may be processed into similar highly aligned fibres and films, which may be beneficial in ion transport membranes for fuel cell applications. In the 1980s, Silver *et al.* synthesized S-PPTA by polymerizing 1,4-bis(trichloromethyl) benzene (1,4-BTMB) with *para*-phenylenediamine sulfate (PPD-S) in SO<sub>3</sub>.<sup>[2]</sup> Both 1,4-BTMB and SO<sub>3</sub> are hazardous chemicals and the degree of sulfonation was difficult to control. An alternative route was explored by Viale and co-workers, who prepared S-PPTA from 2,5-diaminobenzenesulfonic acid and terephthaloyl chloride.<sup>[3]</sup> The 2,5-diamino-benzenesulfonic acid was activated with chlorotrimethylsilane (TMSCl) and immediately polymerized with terephthaloyl chloride in dimethylacetamide (DMAc) at 75 °C for 2 hours. A similar method was used by Taeger *et al.* who prepared sulfonated polyaramides for ion exchange membranes.<sup>[4]</sup> Jo and co-workers synthesized S-PPTA directly using aromatic diamines and sulfonated terephthalic acid in N-methyl-2-pyrrolidone (NMP) at 115 °C for 12 h, and copolymers could be prepared by adding various amounts of terephthalic acid to the reaction system.<sup>[5]</sup> In order to obtain a high molecular weight polymer, one has to carefully control the polymerization reaction conditions, such as monomer purity, the water content of the solvent, the use of an inert atmosphere (argon or nitrogen), and so on. In most literature reports, as discussed above, there is little or no information with respect to polymer molecular weight and polymer mechanical properties. Viale *et al.* are the only authors reporting molecular weight data. In fact, their S-PPTA polymer has a weight-average molecular weight ( $M_w$ ) of 7800 g/mol, which is rather low and processing free-standing films for fuel cell testing proved to be difficult.<sup>[3,11,16]</sup> In addition, S-PPTA, was investigated as a proton transport membrane and displayed a proton conductivity of about 0.1 S/cm, which is comparable to a Nafion<sup>®</sup> membrane.<sup>[9]</sup>

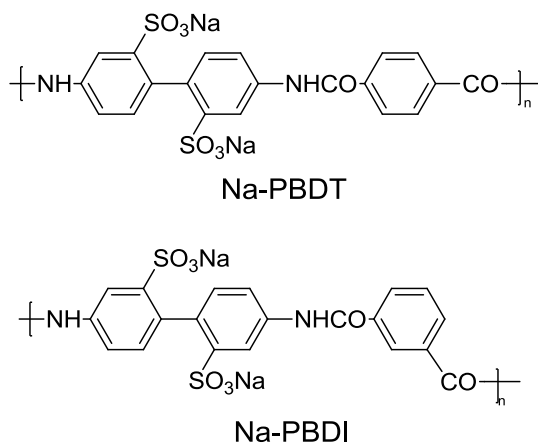


**Figure 2.1.** Polymer structures of PPTA and S-PPTA.

Sarkar and co-workers chose to use an interfacial polycondensation technique to synthesize sodium-form poly(2,2'-disulfonylbenzidine terephthalamide) (Na-PBDT) and sodium-form poly(2,2'-disulfonylbenzidine isophthalamide) (Na-PBDI) (Figure 2.2).[6,17,18] Compared to solution polycondensation, it is much easier to operate the interfacial polycondensation due to the mild conditions, such as 25 °C, no nitrogen or argon protection, no strict requirement for the purity and ratio of diamine and dichloride monomers, and a short reaction time (~30 min).[7,8] The structure of Na-PBDT is similar to that of S-PPTA, and it is also a liquid crystalline polymer, capable of forming a nematic phase in water at concentrations as low as 1.5 wt%. The relative viscosity of the formed Na-PBDT was reported to be as high as 30 (at 0.5 g/dL, 25 °C) and free standing films could be easily prepared.[6,10,17,18] The solution properties of Na-PBDT in water and salt solutions were studied extensively by Sarkar *et al.* They investigated the viscosity of Na-PBDT in water and NaCl solutions and found that Na-PBDT appeared to transform into helical coils, or similar rod-like macromolecular complexes, in the NaCl solution.[6] Gong and co-workers focused on the self-assembled structures of Na-PBDT in aqueous solutions. When increasing the polymer concentration ( $C_p$ ), the self-assembled Na-PBDT structure exhibited a transition from single chains ( $C_p < C^*$ ) to cluster structures ( $C^* < C_p < C_{LC}^*$ ) to LC structures ( $C_p > C_{LC}^*$ ), where  $C^*$  and  $C_{LC}^*$  refers to the overlap concentration and the critical nematic liquid crystal concentration, respectively.[10,19]

Although the solution behaviour of Na-PBDT was studied in detail, some critical basic information for this polymer was not provided, such as thermal

and mechanical properties, and a phase diagram as a function of polymer concentration and temperature. In this chapter, we will report on the polymer thermal and mechanical properties, the phase behaviour and film morphologies.



**Figure 2.2.** Polymer structures of Na-PBDT and Na-PBDI. Na-PBDT is a lyotropic nematic liquid crystalline polymer in water at concentrations >1.5 wt%, whereas Na-PBDI forms an isotropic solution only. Both polymers can be cast into free-standing films from aqueous solution.

## 2.2 Experimental

### 2.2.1 Materials

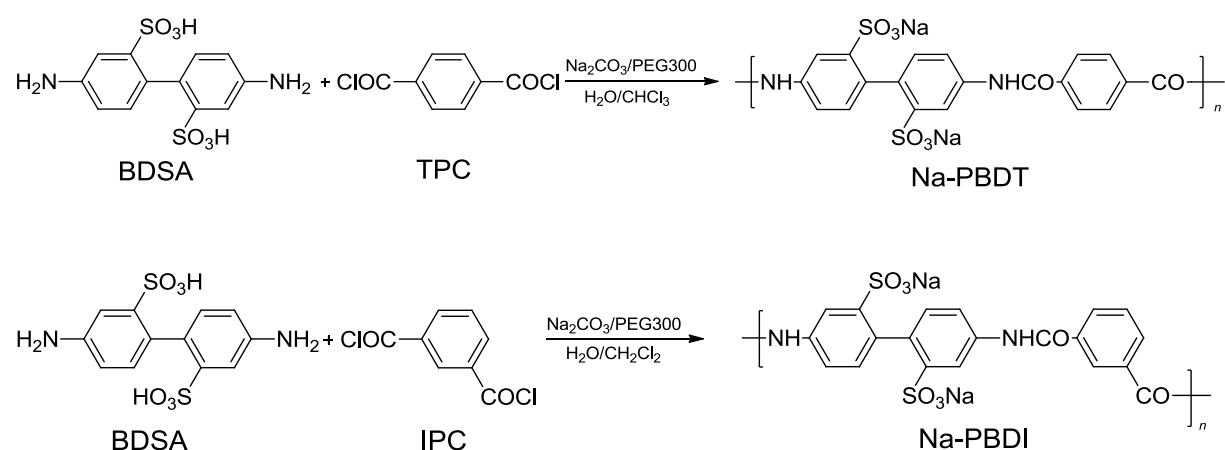
2,2'-Benzidinedisulfonic acid (BDSA) (with 30 wt% water, Alfa-Aesar) was recrystallized using the following procedure: 5.0 g (about 0.01 mol) of BDSA and 0.8 g (0.02 mol) of NaOH were dissolved in 15 mL of deionized water. Ethanol (50 mL) was added to the clear dark-red solution to precipitate the sodium form of BDSA (BDSA-Na). BDSA-Na was collected by filtration and then again dissolved in 25 mL of deionized water. Concentrated HCl (37%, 2 mL) was added to the solution to acidify BDSA-Na after which BDSA crystal precipitated from solution. This procedure was repeated 4 times and resulted in white needle-like crystals with a yield of 95%. Terephthaloyl chloride (TPC, 99%, Sigma-Aldrich) and isophthaloyl chloride (IPC, 99%, Sigma-Aldrich) were purified by vacuum sublimation prior to use. Poly(ethylene glycol) with a molecular weight of 300 (PEG 300, Sigma-Aldrich), chloroform (98%, VWR),



dichloromethane (98%, VWR) and sodium carbonate (99%, Sigma-Aldrich) were used without further purification.

### 2.2.2 Interfacial polycondensation procedure

The synthesis routes of both sulfonated aramids, Na-PBDT (a nematic liquid crystal polymer) and Na-PBDI (isotropic polymer), are shown in Figure 2.3 and are based on a procedure described by Sarkar *et al.*[6]



**Figure 2.3.** Synthetic routes toward Na-PBDT and Na-PBDI.

**Na-PBDT:** A 2 L three-neck round-bottom flask was equipped with a mechanical stirrer and charged with 4.36 g (0.04 mol) sodium carbonate and 480 mL deionized water. While stirring, the diamine monomer BDSA (5.16 g, 0.015 mol) was added to the flask, followed by another 120 mL of deionized water to obtain a clear solution. PEG 300 (4.8 g) surfactant was dissolved in 200 mL of chloroform, and added to the BDSA solution using a stirring rate of ~2000 rpm. After 15 min, TPC (3.045 g, 0.015 mol) in 200 mL of chloroform, was added in one portion to the reaction mixture, and the reaction was allowed to proceed for another 15 min. The mechanical stirring was stopped and the reaction mixture was allowed to stand for another 15 min. The highly viscous reaction mixture was transferred to a round-bottom flask to remove the chloroform under reduced pressure, and then poured into a beaker containing 1000 mL acetone to precipitate the polymer from the aqueous phase. The

polymer was collected by filtration. The polymer product was dissolved in 200 mL water, and precipitated using 400 mL acetone. This purification procedure was repeated at least 5 times until the pH of the polymer solution was close to 7 to make sure that all of the  $\text{Na}_2\text{CO}_3$  and NaCl salts were removed from the polymer. The final polymer was dried at 60 °C for 24 hours to give a 4.7 g white fibrous product with a yield of 60%.

**Na-PBDI:** A similar procedure was used as described for Na-PBDT. Instead of chloroform, dichloromethane was used as it resulted in a higher molecular weight polymer. The yield was about 50%.

Because  $\text{Na}_2\text{CO}_3$  was used during the synthetic procedure all polymers are of the sodium-salt form (Na-PBDT and Na-PBDI) in the following discussion.

### 2.2.3 Membrane preparation

The Na-PBDT- and Na-PBDI-based membranes were prepared using the same method: 6 wt% of an aqueous Na-PBDT solution (deionized water) was cast onto a clean glass plate using a doctor blade (film applicator). The film was dried at 60 °C for 3 h, after which the dry membrane could be removed from the glass plates by soaking in acetone. The thickness of the membranes was around 80  $\mu\text{m}$ .

### 2.2.4 Characterization

A PerkinElmer Spectrum 100 FT-IR Spectrometer was used to collect IR spectra.

$^1\text{H}$ -NMR spectra were collected on a Bruker Avance-400 NMR spectrometer. The spectra were recorded at 400 MHz with 128 scans at 25 °C.

The molecular weight, and molecular weight distribution of the samples was determined by size exclusion chromatography (SEC, measured at the Teijin Company) using Twaron 1010, as a reference. Concentrated sulfuric acid was used as the solvent and mobile phase. As the stationary phase, a Zorbax GPC column (250  $\times$  6.2 mm) was used.

The liquid crystalline properties of the polymers were studied using a polarizing optical microscope (Leica, DM/LP).

Wide-angle X-ray diffraction (XRD, Bruker D8 Discover) was used to

investigate the morphology of the polymer membranes. The wavelength of the X-ray beam was 1.54 Å (Cu-K $\alpha$ ) and the distance between sample and detector was 6 cm.

Thermal gravimetric analysis (TGA) was carried out using a Perkin-Elmer Pyris Diamond TG/DTA. Generally, the samples were first heated to 150 °C for 30 min under a nitrogen atmosphere to remove most of the remaining water, followed by cooling the sample down to ~30 °C. At this point the samples were analyzed from 30 to 590 °C at a scanning rate of 10 °C/min under a nitrogen atmosphere.

The thermal properties of Na-PBDT and Na-PBDI were investigated using differential scanning calorimetry (Perkin-Elmer, Pyris Diamond DSC). The polymer samples were scanned at a rate of 10 °C/min under a nitrogen atmosphere.

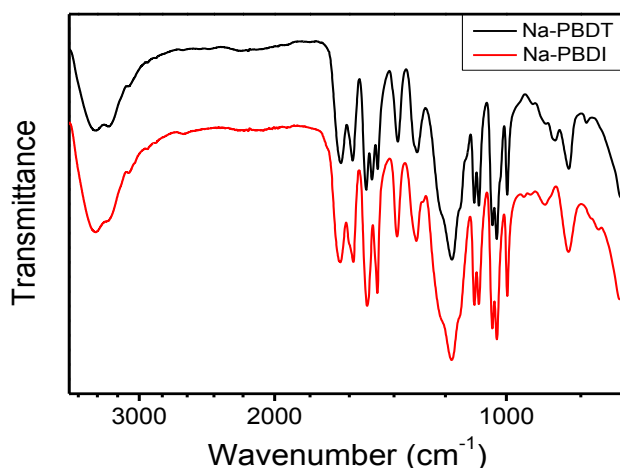
Dynamic mechanical analysis (PerkinElmer, Pyris Diamond DMA) was used to measure the storage modulus ( $E'$ ) of the free-standing films. The samples were measured at a scanning rate of 2 °C /min in a nitrogen atmosphere at 0.1, 1 and 10 Hz.

## 2.3 Results and discussion

### 2.3.1 Chemical structure analysis of Na-PBDT and Na-PBDI

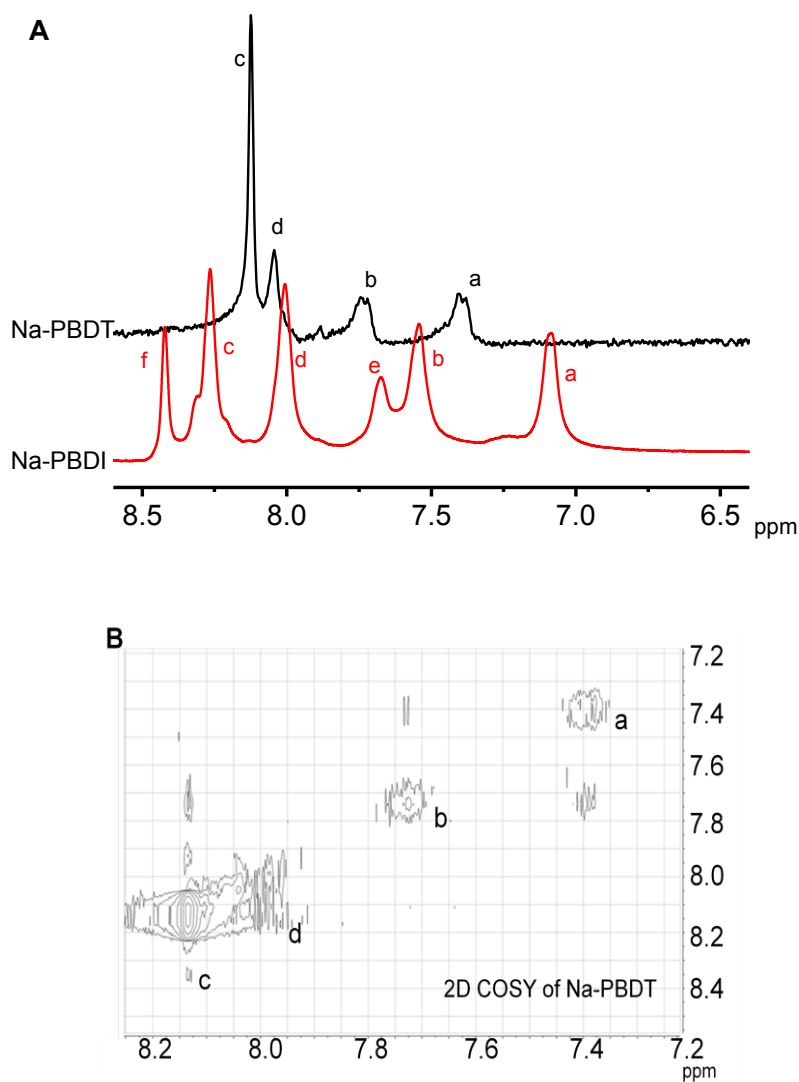
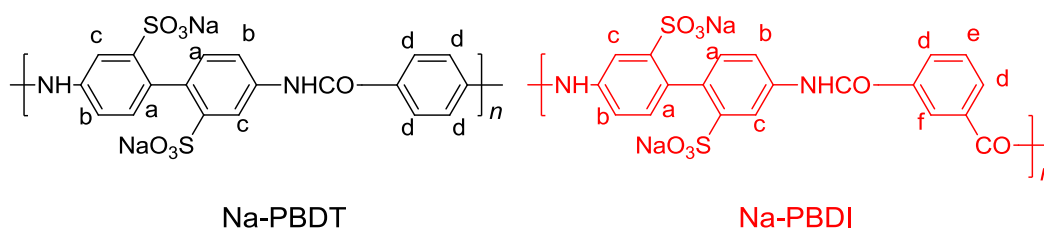
The two polymers, Na-PBDT and Na-PBDI, were analyzed using FT-IR and  $^1\text{H}$ -NMR in order to confirm the final polymers structures.

Figure 2.4 shows the FT-IR spectra of Na-PBDT and Na-PBDI. Due to the similar chemical structures of the two polymers, their FT-IR spectra are quite similar to each other. Some typical characteristic bands can be observed in the two spectra, such as  $\nu_{\text{N-H}}$  (~ 3370  $\text{cm}^{-1}$ ),  $\nu_{\text{C=O}}$  (~ 1640  $\text{cm}^{-1}$ ),  $\delta_{\text{N-H}}$  (~ 1580  $\text{cm}^{-1}$ ),  $\nu_{\text{C=O}}$  (~ 1520  $\text{cm}^{-1}$ ), and  $\nu_{\text{S=O}}$  (~ 1098  $\text{cm}^{-1}$ ).



**Figure 2.4.** FT-IR spectra of Na-PBDT and Na-PBDI.

The  $^1\text{H}$ -NMR results are given in Figure 2.5.  $\text{D}_2\text{O}$  was selected as the main solvent for the experiment due to the good solubility of the two polymers in water. The prepared Na-PBDI solution was  $\sim 3$  wt% in  $\text{D}_2\text{O}$ . The peaks in the  $^1\text{H}$ -NMR spectrum are assigned in Figure 2.5 according to the chemical shifts and integrated areas. With respect to Na-PBDT, the polymer was dissolved in 50 wt%  $\text{D}_2\text{O}$  and 50 wt%  $\text{CD}_3\text{CN}$ . The final polymer concentration obtained was  $\sim 0.5$  wt%. As Na-PBDT is a liquid crystalline polymer in solution (see Section 2.3.5), the aim of adding  $\text{CD}_3\text{CN}$  and lowering the polymer concentration is to avoid the formation of a liquid crystalline solution as this would result in significant peak broadening and complicating the peak assignment. The proton peaks were assigned, as shown in Figure 2.5, based on the chemical shifts and a 2D COSY experiment.



**Figure 2.5.** NMR spectra: A)  $^1\text{H}$ -NMR of Na-PBDT and Na-PBDI; B) 2D COSY of Na-PBDT.

### 2.3.2 Molecular weight analysis of Na-PBDT and Na-PBDI

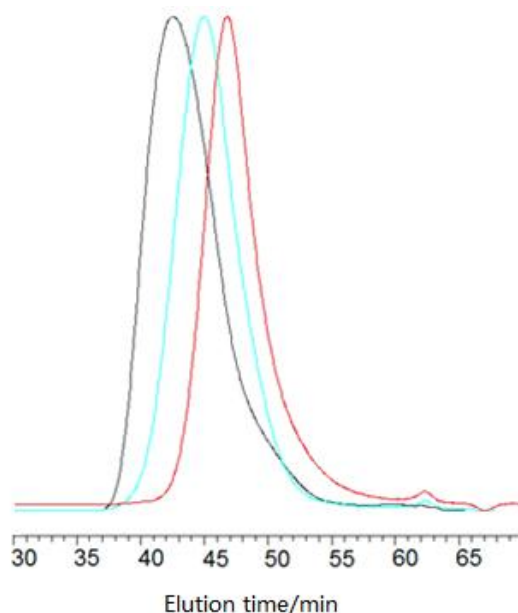
The obtained sulfonated polyamides, Na-PBDT and Na-PBDI, have good solubility in water because of the sulfonic functionalities in the polymer backbone. Solution viscosities of the two polymers were measured using an

Ubbelohde capillary viscometer at 25 °C and a polymer concentration of 0.5 g/dL in water. The elapsed time ( $t_e$ ) of the solution was recorded. The reduced viscosity was calculated using the following equation:

$$\eta_{\text{red}} = \left[ \frac{t_e}{t_s} - 1 \right] / C \quad (1)$$

where  $t_s$  = elapsed time for the pure solvent,  $C$  = concentration of polymer (0.5 g/dL). The reduced viscosity of Na-PBDT was found to be 30.2 dL/g, and that of Na-PBDI was 4.3 dL/g.

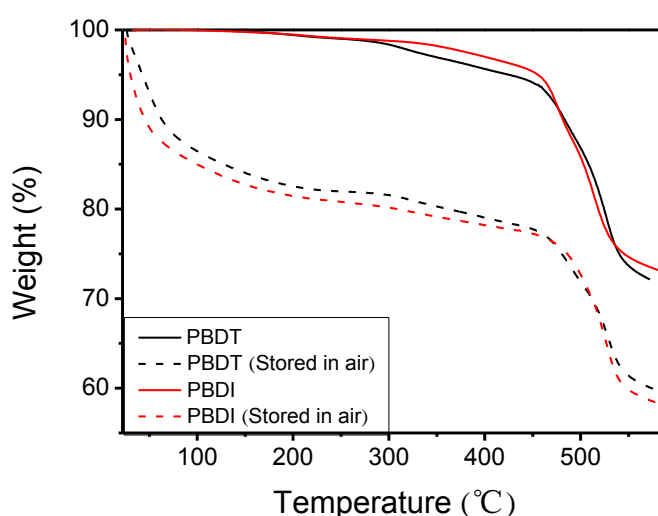
The molecular weight distribution and polydispersity of both polymers was measured using the SEC equipment at Teijin Aramid (Arnhem, The Netherlands). Samples were dissolved in concentrated  $\text{H}_2\text{SO}_4$  (1 mg/ml) for the measurement. The SEC curves are shown in Figure 2.6 and show a unimodal molecular weight distribution. For Na-PBDT, the number-average molecular weight ( $M_n$ ), weight-average molecular weight ( $M_w$ ), and polydispersity index ( $\text{PDI} = M_w/M_n$ ) were 7900 g/mol, 17300 g/mol, and 2.2, respectively; and for Na-PBDI, the  $M_n$ ,  $M_w$  and PDI were 3900 g/mol, 8200 g/mol and 2.1, respectively.



**Figure 2.6.** SEC results of Na-PBDT (blue curve) and Na-PBDI (red curve). Twaron 1010 ( $M_n$  = 10300 g/mol,  $M_w$  = 31400 g/mol,  $\text{PDI}$  = 3.0) was used as a reference (black curve).

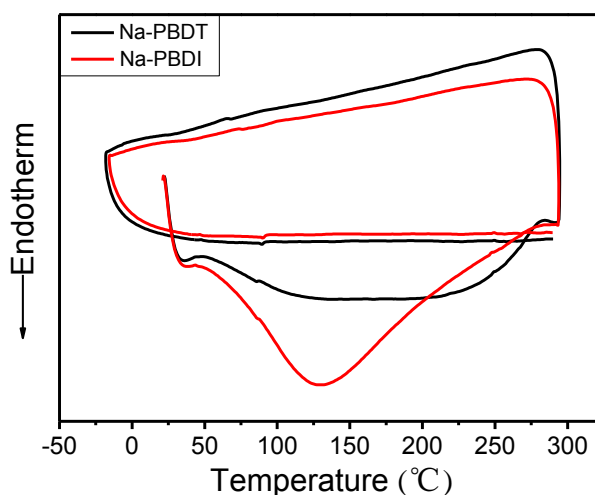
### 2.3.3 Thermal properties

The thermal stability of Na-PBDT and Na-PBDI was investigated using thermogravimetric analysis (TGA). As shown in Figure 2.7, a Na-PBDT membrane stored under ambient conditions (in air at room temperature) absorbs about 17 wt% water. A similar water uptake (~18 wt%) was observed for Na-PBDI membranes. In order to evaluate the thermal stability of our membranes, Na-PBDT and Na-PBDI were first pre-heated at 150 °C for 30 min to remove as much of the physisorbed water as possible. After this drying procedure the samples were cooled to 30 °C and the TGA run was started. The results are shown in Figure 2.7. The TGA scans show that both polymers are stable, *i.e.* little weight loss is found up to 200 °C. Above this temperature both polymers start to lose weight slightly, which is probably due to outgassing of water and decomposition of the sulfonic acid groups.[15] The stability of sulfonic sodium groups is much better than that of sulfonic acid groups, so the 5% mass loss temperatures  $T_d^{5\%}$  for these membranes are high, about 427 °C for Na-PBDT and 454 °C for Na-PBDI respectively. The degradation of the Na-PBDT and Na-PBDI polymer backbone starts around 480 °C. In summary, according to the TGA results, Na-PBDT and Na-PBDI are quite stable below 200 °C, which is acceptable for most fuel cell membrane applications.



**Figure 2.7.** TGA results of Na-PBDT and Na-PBDI polymers. Recorded under a nitrogen atmosphere and a heating rate of 10 °C /min.

Differential scanning calorimetry (DSC) curves of Na-PBDT and Na-PBDI samples are shown in Figure 2.8. The measurements were conducted from 25 °C to 300 °C (heat 1), cooled down to -20 °C, and heating again to 300 °C (heat 2). The two polymers displayed similar thermal behaviour. During the first heating a broad endothermic peak can be observed, which is absent during the successive cooling and second heating. The broad endotherm is the result of water evaporating from the sample. The subsequent heating trace shows a flat baseline only, indicating that most water has been removed during the first heating cycle. No  $T_g$  is observed for both Na-PBDT and Na-PBDI polymers, which is typical for all-aromatic (rigid-rod) amide-based polymers.



**Figure 2.8.** DSC curves for Na-PBDT and Na-PBDI polymers, recorded under a nitrogen atmosphere and a scanning rate of 10 °C /min.

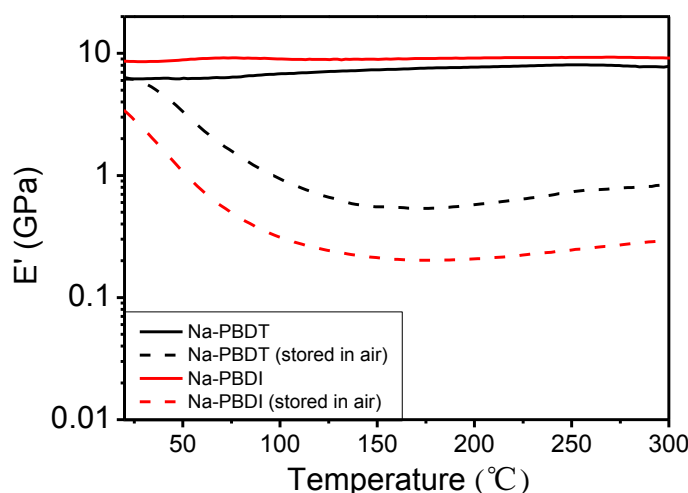
### 2.3.4 Mechanical properties

Good mechanical properties are required for PEMs, because they can influence the manufacturing conditions of membrane electrode assemblies (MEAs) and affect durability of fuel cell operations. DMTA measurements were employed to analyse the mechanical properties of Na-PBDT and Na-PBDI membranes. The storage modulus  $E'$  results of the samples as a function of temperature are shown in Figure 2.9. Similar to the TGA experiments, two samples of the same polymer were measured; one dry polymer film and one film stored in air.



For the two samples stored in air, the storage modulus showed a similar trend with increasing temperature. The storage modulus first decreases, and then remains at a relatively constant value above about 150 °C. The  $E'$  of Na-PBDT was around 6 GPa at 25 °C, and dropped to ~0.6 GPa at 150 °C and higher. For Na-PBDI, the  $E'$  values at 25 °C and 150 °C were 3 GPa and ~0.2 GPa, respectively.

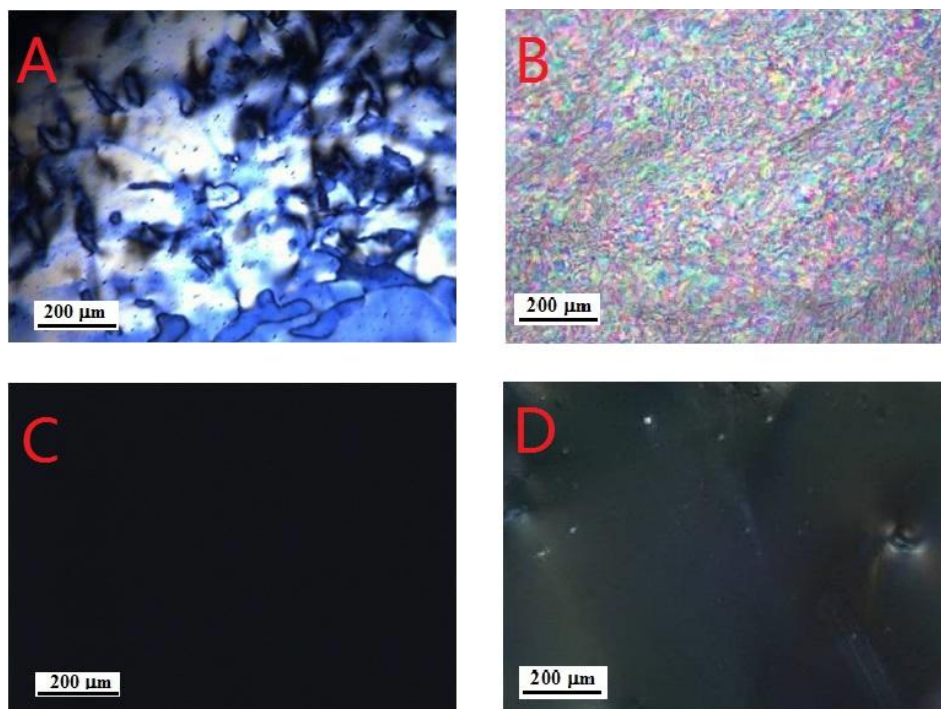
To study the influence of water uptake on the storage modulus of the membrane, dry films were prepared for DMTA measurements. The film was first placed in the DMTA oven. The oven temperature was set to increase to 150 °C and held at this temperature for 30 min. After this procedure, the sample was cooled to room temperature and the actual measurement was started. As shown in Figure 2.9, the dry films showed a much higher storage modulus. At room temperature, the  $E'$  of Na-PBDT was about 6 GPa, which is close to the Na-PBDT sample stored in air. When increasing the temperature, the storage modulus was maintained at around 6 GPa. A similar result was obtained for the dry Na-PBDI samples. The storage modulus was even higher than that of Na-PBDT, around 9 GPa, and this value could also be maintained up to 300 °C. The decrease in  $E'$  of samples stored in air is most likely due to the water absorbed by the samples. The water molecules act as plasticizer, allowing the polymer chains to slide past one another, resulting in a decrease in storage modulus. When increasing the temperature, water evaporates and the polymer chains in the dry film can no longer slide, resulting in a constant and high  $E'$ . For commercial PEMs, the  $E'$  value is typically below 5 GPa.[12-14] Both Na-PBDT and Na-PBDI have higher storage moduli. This is the result of strong inter-chain interactions, which is direct consequence of the high concentration of ionic groups ( $-\text{SO}_3\text{Na}$ ) and the ability to form hydrogen bonds (amide functionalities).



**Figure 2.9.** Storage modulus of Na-PBDT and Na-PBDI polymers as a function of temperature. Data were collected using a heating rate of 2 °C /min and a nitrogen atmosphere.

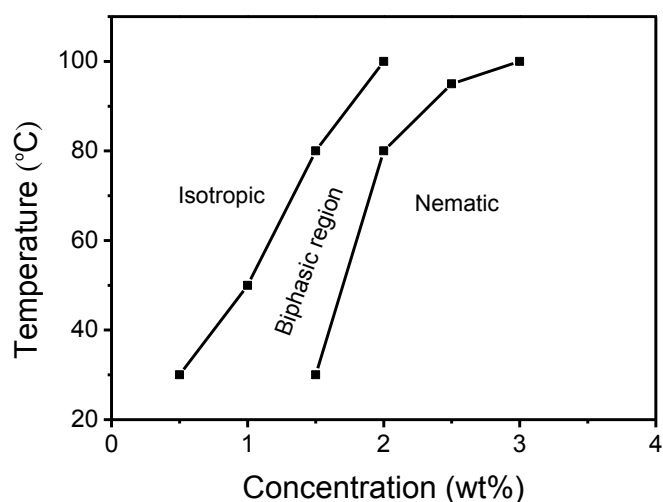
### 2.3.5 Polarizing optical microscopy

Although Na-PBDT and Na-PBDI are both all-aromatic polymers, their different ring substitution patterns results in quite different morphologies. The all *para*-substituted Na-PBDT forms a liquid crystal solution in water whereas the kinked backbone, induced by isophthalic acid, in Na-PBDI yields an isotropic polymer solution only.[9, 16] Figure 2.10 shows the textures of both polymers in water. A 10% Na-PBDT solution in water displays a typical nematic schlieren texture (Figure 2.10A), whereas a 10% Na-PBDI solution in water, and all concentrations above 10% for that matter, shows an isotropic phase only (Figure 2.10C). Free-standing Na-PBDT and Na-PBDI films were cast from 6 wt% solution in water using a film applicator (doctor blade) and dried at 60 °C for 3 hours. The nematic morphology was preserved for Na-PBDT in the solid film (Figure 2.10B) and isotropic films were obtained for Na-PBDI (Figure 2.10D).

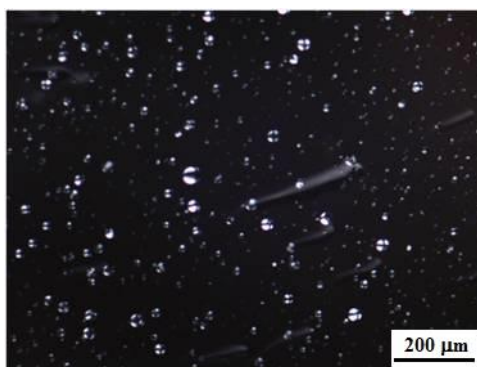


**Figure 2.10.** Optical microscopy (crossed polars) of Na-PBDT and Na-PBDI: A) Na-PBDT solution in water (10%); B) Na-PBDT film; C) Na-PBDI solution in water (10%); and D) Na-PBDI film.

Yang and co-workers studied the solution behaviour of Na-PBDT in aqueous salt solutions at room temperature, and they constructed a phase diagram as a function of polymer concentration and salt concentration.[10] We studied the phase diagram of Na-PBDT in water as a function of polymer concentration and temperature. The phase diagram was determined using polarized optical microscopy, and the result is shown in Figure 2.11. The polymer solution was sandwiched between two cover slips, and placed on the hotplate of a microscope. The heating rate was controlled at 10 °C /min, from 25 °C to 100 °C. At 25 °C, the isotropic phase is observed at low concentration (< 0.5 wt%), while the nematic phase appears at higher concentration (> 1.5 wt%). Between 0.5 wt% and 1.5 wt%, a biphasic region can be observed, where the isotropic phase (I) and nematic phase (N) coexist (Figure 2.12). This result is in agreement with the data at 25 °C reported by Yang and co-worker.[10] The observed phase behaviour of Na-PBDT moreover is very similar to what has been reported for S-PPTA.[9]



**Figure 2.11.** Phase diagram of Na-PBDT in water.



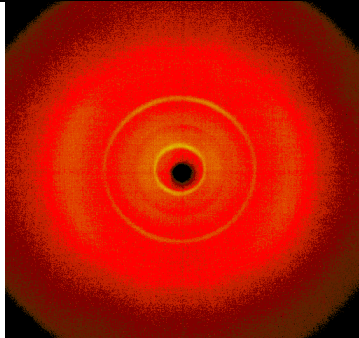
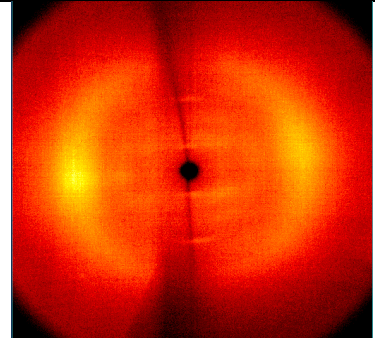
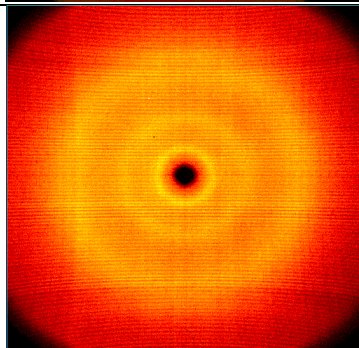
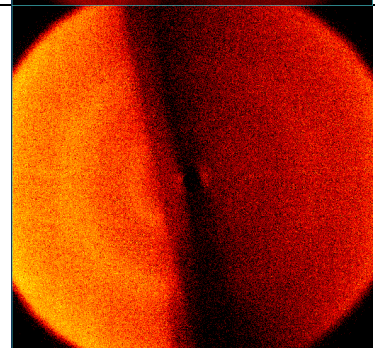
**Figure 2.12.** Biphasic behavior of Na-PBDT in water (1.0 wt%) at 25 °C.

### 2.3.6 X-ray diffraction experiments

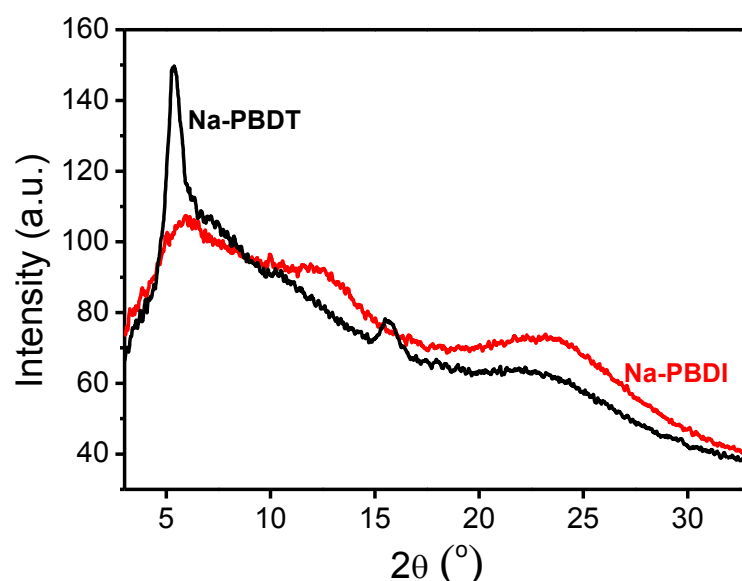
The main focus of our research is to understand whether aligned liquid crystal polymers can be used as ion transport membranes. Since the presence of an ordered structure is very important for ion transport, it is necessary to understand to what degree our films become oriented during the film casting process. Therefore, we used XRD to study the structure of the Na-PBDT and Na-PBDI films. The films were placed either perpendicular ( $\perp$ ) or parallel ( $\parallel$ ) to the X-ray beam, and the scattering images are shown in Table 2.1. The scattering images of Na-PBDT and Na-PBDI confirm that there is a small degree of alignment in the Na-PBDT film whereas Na-PBDI is a fully isotropic

membrane.

**Table 2.1.** XRD scattering images of the Na-PBDT and Na-PBDI membranes.

	X-ray beam $\perp$ film surface	X-ray beam $\parallel$ film surface
Na-PBDT		
Na-PBDI		

The scattering intensities as a function of the scattering angle  $2\theta$  are shown in Figure 2.13. These results refer to the measurement in which the films were placed perpendicular to the incident X-ray beam. For Na-PBDT, there are three main peaks: two sharp peaks at  $2\theta = 5.2^\circ$  and  $15.6^\circ$ , and a broad peak at  $22.8^\circ$ . According to Bragg's law ( $n\lambda = 2d\sin\theta$ ), the  $d$ -spacing results for these peaks are  $16.8 \text{ \AA}$  ( $5.2^\circ$ ),  $5.7 \text{ \AA}$  ( $15.6^\circ$ ), and  $3.9 \text{ \AA}$  ( $22.8^\circ$ ). For Na-PBDI, there are also three peaks, one sharp peak at  $5.9^\circ$  and two broad peaks at  $12.9^\circ$  and  $23.6^\circ$ . The corresponding  $d$ -spacings of the three peaks are  $14.9 \text{ \AA}$ ,  $6.8 \text{ \AA}$  and  $3.7 \text{ \AA}$ , respectively.



**Figure 2.13.** XRD results of Na-PBDT and Na-PBDI free standing film.

The polymer structures of Na-PBDT and Na-PBDI are similar to that of S-PPTA, so it is worth comparing these results with the S-PPTA XRD results. The  $2\theta$  values and related  $d$ -spacings of Na-PBDT, Na-PBDI, and S-PPTA are listed in Table 2.2. For S-PPTA, the peak at  $19.5^\circ$  refers to the interchain spacing, and another peak at  $8.8^\circ$  is indicative of the number of polymer repeat units. The latter peak is a sharp one, and related to the strong diffraction of the sulfonic groups.[11] For both Na-PBDT and Na-PBDI samples, the peaks around  $23^\circ$  are related to the intermolecular spacing between chains. The broad peaks indicate the distance is not well defined. The peaks at  $5.2^\circ$  for Na-PBDT and  $5.9^\circ$  for Na-PBDI correspond to the length of the repeat units of Na-PBDT and Na-PBDI.

The calculated  $d$ -spacing of Na-PBDT ( $16.8 \text{ \AA}$ ) is larger than that of Na-PBDI ( $14.9 \text{ \AA}$ ), which agrees with the fact that the para-structure of Na-PBDT is longer than the meta-structure of Na-PBDI repeat unit.

**Table 2.2.** X-ray diffraction peaks and  $d$ -spacing for Na-PBDT and Na-PBDI. The diffraction peaks and  $d$ -spacings for S-PPTA are added for reference purposes.[16]

Sample	$2\theta$ (°)	$d$ -spacing (Å)	
Na-PBDT	5.2	16.8	Repeat unit
	15.6	5.7	Intermonomer sulfonate distance
	22.8	3.9	Interchain spacing
Na-PBDI	5.9	14.9	Repeat unit
	12.9	6.8	Intramonomer sulfonate distance
	23.6	3.7	Interchain spacing
S-PPTA	8.8	10.1	Repeat unit
	19.5	4.6	Interchain spacing

The orientational ordered parameter of Na-PBDT film was calculated by fitting the intensity data of the broad reflections as a function of azimuthal angle  $\chi$ , with a Maier-Saupe type function.

$$I = I_0 + A \exp\{\alpha \cos^2(\chi - \chi_0)\} \quad (2)$$

In equation 2,  $I$  is the scattering intensity,  $I_0$  is the baseline scattering intensity,  $A$  is the amplitude of scattering intensity, and  $\alpha$  is a parameter that determines the width of the distribution function. The distribution function of  $\beta$  (the angle of the director) is determined by substituting  $\alpha$  into equation 3, which is then used to obtain the average degree of alignment,  $\overline{\langle P_2 \rangle}$  (equation 4). [10]

$$f(\beta) = \exp(\alpha \cos^2 \beta) \quad (3)$$

$$\overline{\langle P_2 \rangle} = \frac{\int_{-1}^1 f(\beta) P_2(\cos \beta) d\cos \beta}{\int_{-1}^1 f(\beta) d\cos \beta} \quad (4)$$

When the Na-PBDT membrane was placed perpendicular to the X-ray beam, an orientation along the casting direction was observed. The calculated  $\overline{\langle P_2 \rangle}$  was about 0.3, which is not particularly high. As mentioned in section 2.2.3, a Na-PBDT aqueous solution of 6 wt% was used to cast the membranes. The orientation was introduced during the casting procedure, which is not really strong enough to align the polymer chains into a highly ordered structure. Therefore a low degree of orientation was obtained. When the membrane was placed parallel to the X-ray beam, the orientation direction was found to be along the membrane surface, indicating that the polymer chains were aligned parallel to the membrane surface. The calculated  $\overline{\langle P_2 \rangle}$  was about 0.6, indicating that the polymer chains are much better aligned parallel to the membrane surface compared to along the casting direction. When drying the film, the polymer aggregates might prefer to deposit parallel to the surface due to the counter-ion mediation and the surface tension of the solution.[20-22] Moreover, there may be an effect resulting from shrinkage during drying, which is mainly in the film thickness direction and leads to an enhanced level of director alignment.[23]

In contrast to the diffraction pattern of Na-PBDT, the Na-PBDI membrane shows symmetric diffraction rings only, indicating that the cast membrane is completely amorphous.

## 2.4 Conclusion

Two highly sulfonated polyaramids, poly(2,2'-disulfonylbenzidine terephthalamide) (PBDT) and poly(2,2'-disulfonylbenzidine isophthalamide) (PBDI), were synthesized via an interfacial polycondensation technique. Sodium-form polymers (Na-PBDT and Na-PBDI) were obtained due to  $\text{Na}_2\text{CO}_3$  being used during the synthetic procedure. Terephthaloyl chloride was used to react with 2,2'-benzidinedisulfonic acid to synthesize the Na-PBDT polymer, and the polymer solution showed nematic liquid crystalline (LC) behaviour when the polymer concentration was higher than 1.5 wt% in water. For Na-PBDI, isophthaloyl chloride was used for the synthesis, which resulted in an isotropic polymer solution. The rigid polymer structures exhibit good thermal stabilities, with  $T_d^{5\%} > 427\text{ }^\circ\text{C}$ . In addition, cast membranes showed excellent



storage moduli. The storage modulus could be as high as 10 GPa for dry membranes, and 3 to 6 GPa for membranes stored in air. The nematic order was maintained in the Na-PBDT membrane after casting from 6 wt% water solution, and the XRD results revealed an alignment along the casting direction, with an orientation degree of about 0.3. When the Na-PBDT membrane was placed parallel to the X-ray beam, an orientation degree of about 0.6 was found, indicating that the polymer chains are aligned quite well parallel to the membrane surface. In contrast, membranes cast from an aqueous Na-PBDI solution were shown to be fully isotropic.

## 2.5 References:

- [1] Marchildon, K. *Macromol. React. Eng.* **2011**, *5*, 22.
- [2] Silver F.M. *J. Polym. Sci. Polym. Chem. Ed.* **1980**, *18*, 1787.
- [3] Viale, S.; Jager, W.F.; Picken, S.J. *Polymer* **2003**, *44*, 7843.
- [4] Taeger, A.; Vogel, C.; Lehmann, D.; Jehnichen, D.; Komber, H.; Meier-Haack, J.; Ochoa, N.A.; Nunes, S.P.; Peinemann, K.V. *React. Funct. Polym.* **2003**, *57*, 77.
- [5] Jo, T.S.; Ozawa, C.H.; Eagar, B.R.; Brownell, L.V.; Han D.; Bae, C. *J. Polym. Sci., Part A: Polym. Chem.* **2009**, *47*, 485.
- [6] Sarkar, N.; Kershner, D. *J. Appl. Polym. Sci.* **1996**, *62*, 393.
- [7] Frunze, T.M.; Kurashev, V.V.; Kozlov, L.V. *Russ. Chem. Rev.* **1961**, *30*, 252.
- [8] Wittbecker, E.L.; Morgan, P.W. *J. Polym. Sci.* **1959**, *40*, 289.
- [9] Every, H.A.; Mendes, E.; Picken, S.J. *J. Phys. Chem. B* **2006**, *110*, 23729.
- [10] Yang, W.; Furukawa, H.; Shigekura, Y.; Shikinaka, K.; Osada, Y.; Gong, J. *Macromolecules* **2008**, *41*, 1791.
- [11] Every, H.A.; Janssen, G.J.M.; Sitters, E.F.; Mendes, E.; Picken, S.J. *J. Power Sources* **2006**, *162*, 380.
- [12] Sgreccia, E.; Chailan, J.F.; Khadhraoui, M.; Di Vona, M.L.; Knauth, P. *J. Power Sources* **2010**, *195*, 7770.
- [13] Bai, Z.W.; Houtz, M.D.; Mirau, P.A.; Dang, T.D. *Polymer* **2007**, *48*, 6598.

- [14] Wen, S.; Gong, C.L.; Tsen, W.C.; Shu, Y.C.; Tsai, F.C. *Int. J. Hydrogen Energ.* **2009**, *34*, 8982.
- [15] Mabrouk, W.; Ogier, L.; Vidal, S.; Sollogoub, C.; Matoussi, F.; Fauvarque, J.F. *J. Membr. Sci.* **2014**, *452*, 263.
- [16] Viale, S.M.J. Liquid crystalline behavior of water-soluble sulfonated polyaramids, *PhD thesis*, Delft University of Technology, 2005.
- [17] Kershner, L.D.; Rieneke, C.E.; Sarkar, N.; Wilson, L. U.S. Pat. 4,824,916 (**1989**).
- [18] Kershner, L.D.; Rieneke, C.E.; Sarkar, N.; Wilson, L. U.S. Pat. 4,895,660 (**1990**).
- [19] Yang, W.; Furukawa, H.; Gong, J. *Adv. Mater.* **2008**, *20*, 4499.
- [20] Sisbandini, C.; Every, H.A.; Viale, S.; Mendes, E.; Picken, S.J. *J. Polym. Sci. Pol. Phys.* **2007**, *45*, 666.
- [21] Ha, B.Y.; Liu, A. *J. Phys. Rev. Lett.* **1997**, *79*, 1289.
- [22] Narayanan, J.; Mendes, E.; Manohar, C. *J. Phys. Chem.* **1996**, *100*, 18524.
- [23] Zlopasa, J.; Norder, B.; Koenders, E.A.B.; Picken, S.J. *Macromolecules* **2015**, *48*, 1204.

## Chapter 3

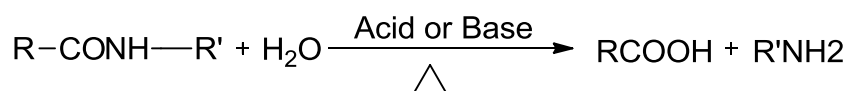
### The Hydrolytic Stability of PBDT and PBDI

---

In this chapter the hydrolytic stability of sulfonated PBDT and PBDI will be discussed. PBDT and PBDI were prepared in the sodium-form (Na-PBDT and Na-PBDI with  $-\text{SO}_3\text{Na}$  groups on the polymer chains) and acid-form (H-PBDT and H-PBDI with  $-\text{SO}_3\text{H}$  groups on the polymer chains). The reduced viscosity of the Na-PBDT and Na-PBDI in water is relatively stable, but the reduced viscosity of the acid-form decreased from 25.0 dL/g to 0.6 dL/g (H-PBDT), and from 4.3 dL/g to 0.2 dL/g (H-PBDI), respectively.  $^1\text{H}$ -NMR experiments confirmed almost complete hydrolysis of H-PBDI when heated at 80 °C for 6 days. The sodium-form of PBDI (Na-PBDI) appeared to be stable under these conditions.

### 3.1 Introduction

Amide groups can be hydrolyzed in strong acid or base at high temperature (Figure 3.1). In the case of polyamides this will lead to random chain scission, a decrease in the molecular weight and lower mechanical and thermal stabilities of the polyamides.[1-6,19] Sulfonated aramids contain both amide and sulfonic groups. When using these polymers as proton exchange membranes (PEMs), the working environment for the membrane is acidic since protons are transported through the membrane during the operation of the fuel cell. The acidic working environment might lead to hydrolysis of amide groups and hence reduced durability. Therefore it is necessary to investigate the stability of PBDT and PBDI.



**Figure 3.1.** Acid- or base-catalysed hydrolysis of amide groups.

As reported in the literature, aliphatic polyamides tend to be hydrolyzed in strong acidic or basic conditions (Figure 3.1).[7,8] For example, Nylon 66 can be completely hydrolyzed in hot HCl solution or KOH solution. The stability of aramids is higher than aliphatic polyamides, but it is still not good enough. Morgan and co-workers studied the hydrolytic degradation mechanism of Kevlar<sup>®</sup> fibres.[9] Kevlar<sup>®</sup>, *i.e.* poly(*para*-phenylene terephthalamide) (PPTA), is one of the strongest commercial fibres. Dissolving this polymer in 100% H<sub>2</sub>SO<sub>4</sub>, a dark-golden highly viscous solution is formed. The polymer solution can be maintained for three months. However, exposing the prepared solution to 125-150 °C in air for only 10 minutes, the solution yields an insoluble (crystalline) precipitate. The crystals were confirmed to be one of the monomers, namely terephthalic acid according to the FTIR results, which meant that the polymer was hydrolysed at high temperature in concentrated H<sub>2</sub>SO<sub>4</sub>. Lin and co-workers treated Kevlar<sup>®</sup> fibres in a concentrated aqueous solution of sulfuric acid (5 M) and a sodium hydroxide water solution (10 M) at 100 °C for more than 5 h.[10] The fibres were not dissolved but the tensile

strength decreased significantly, which was ascribed to the hydrolysis of amide groups on the surface of the fibres. Since Kevlar<sup>®</sup> fibres become unstable under strong acidic and basic conditions, the stability of sulfonated polyamides might be questionable as well. Genies and co-workers studied the stability of a series of sulfonated amides, which were heated in water under dilute acidic conditions at 135 °C.[11] For sulfonated amides, desulfonation could not be detected, but the inherent viscosities significantly decreased after heating to 135 °C, which was ascribed to the cleavage of amide bonds. Vogel and co-workers studied a series of low molecular weight sulfonated aramids.[12] These materials were heated in water at temperatures ranging from 130–200 °C. Hydrolytic cleavage of amide linkages was concluded from <sup>1</sup>H-NMR experiments.

According to these papers, aramids and sulfonated aramids are unstable at temperatures in excess of 130 °C or under harsh conditions (such as concentrated H<sub>2</sub>SO<sub>4</sub>). In contrast, sulfonated polyamides, poly(amide imide)s and poly(ether amide)s were reported as proton exchange membranes for fuel cell application in several papers.[13-16,20] However, our experimental results indicate poor chemical stability of the two sulfonated aramids, PBDT and PBDI, when we synthesized these polymers in the acid-form (-SO<sub>3</sub>H). Hydrolytic cleavage occurred even at room temperature without the addition of strong bases or acids. No free-standing film could be prepared from the acid-form aramids. For fuel cell applications, the acid-form (-SO<sub>3</sub>H) polymer obviously is preferred, as this will result in the best possible proton conductivity. Therefore, we have investigated the stability of our two sulfonated polyamides, PBDT and PBDI, in the sodium-form and acid-form in order to get a better understanding of their hydrolytic stability.

## 3.2 Experimental

### 3.2.1 Materials

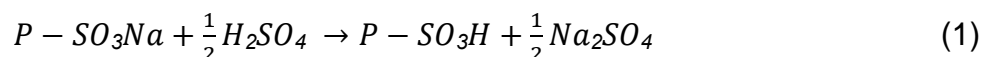
The two aramids in their sodium-form, poly(2,2'-disulfonylbenzidine terephthalamide) (Na-PBDT) and poly(2,2'-disulfonylbenzidine isophthalamide) (Na-PBDI) were prepared using the same method as described in Chapter 2.

The compound 2,2'-benzidinedisulfonic acid (BDSA) (with 30 wt% of water) was purchased from Alfa-Aesar and recrystallized 4 times using the procedure described in Chapter 2. Isophthalic acid (IPA) was purchased from Sigma-Aldrich and used as received. A Dowex<sup>®</sup> ion exchange resin in the hydrogen form was purchased from Sigma-Aldrich.

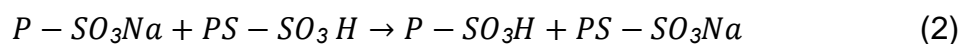
### 3.2.2 Ion exchange procedure

As discussed in Chapter 2, the sulfonic groups ( $-\text{SO}_3\text{H}$ ) on the polymer chain were neutralized to  $-\text{SO}_3\text{Na}$  by  $\text{Na}_2\text{CO}_3$  during the polymerization. In a PEM,  $-\text{SO}_3\text{H}$  groups are preferred to get optimal proton conductivity, because the mobility of protons is much faster than that of 'heavy' sodium ions ( $\text{Na}^+$ ).

A common method of converting  $-\text{SO}_3\text{Na}$  to  $-\text{SO}_3\text{H}$  in sulfonated polymer membranes is soaking the membrane in a 1 M  $\text{H}_2\text{SO}_4$  solution for 24 h, and washing the membrane using deionized water to remove the  $\text{Na}_2\text{SO}_4$  salt and excess  $\text{H}_2\text{SO}_4$  from the membrane. The reaction for this is shown below:



$P - \text{SO}_3\text{Na}$  and  $P - \text{SO}_3\text{H}$  refer to the polymer membranes in the sodium-form and acid-form, respectively. Both  $P - \text{SO}_3\text{Na}$  and  $P - \text{SO}_3\text{H}$  are insoluble in sulfuric acid. However, this method is not suitable for our polymers, because both PBDT and PBDI are soluble in water and sulfuric acid. Therefore we used an ion-exchange column instead of the reaction with sulphuric acid. The sodium-form polymers were dissolved in water at a concentration of 0.5 wt%. The clear solution was passed over a strong acid ion-exchange column. The equation is similar to equation (1), but now the free sulphuric acid is replaced with polystyrene sulfonic acid:



Where  $\text{PS} - \text{SO}_3\text{M}$  ( $M$ :  $\text{H}$  or  $\text{Na}$ ) refers to polystyrene sulfonic acid, while  $P - \text{SO}_3\text{M}$  ( $M$ :  $\text{H}$  or  $\text{Na}$ ) refers to PBDT or PBDI. Upon adding the polymer solution onto the ion-exchange column, the equilibrium of equation 2 shifts to the right, and sulfonated PBDT or PBDI in the acid form is obtained.

A hydrogen-form ion-exchange column was used to convert the sodium-form polymers to their acid form. The ion-exchange resin (100 g) was regenerated using diluted  $\text{H}_2\text{SO}_4$  solution (5 wt%) before use.

The sodium-form PBDT and PBDI are labelled as Na-PBDT and Na-PBDI, while H-PBDT and H-PBDT are used to refer to the acid-form polymers.

The Na-PBDT or Na-PBDI (~0.5 g) was dissolved in 100 mL of deionized water. The solution was slowly passed over the ion-exchange column in 30 min to exchange the sodium ions for protons. Water was removed from the acidified polymer solution under reduced pressure at 60 °C, and the obtained polymer was dried under vacuum at 60 °C for 24 h. A similar method, using an ion-exchange column in the sodium form, was used to convert the acid-form polymers back to their sodium-forms.

### 3.2.3 Hydrolysis procedures

Two hydrolysis procedures were considered for this study:

**1-** Na-PBDT was stored for 28 days at 25 °C under different conditions: **A-** in deionized water (pH=7), **B-** in an acidic environment (HCl, pH = 2) and **C-** in a basic environment (NaOH, pH = 12). The polymer concentration of these solutions was 0.5 wt%. Hydrolysis was followed in terms of a reduction in reduced viscosity versus time.

**2-** Na-PBDI (reduced viscosity = 4.3 dL/g) and H-PBDI (reduced viscosity = 0.2 dL/g) was dissolved in deionized water and hydrolysed at 80 °C for 6 days. The changes in composition were followed using  $^1\text{H}$ -NMR. For the NMR study, we did not consider the NMR spectra of Na-PBDT and H-PBDT. The liquid crystalline PBDT forms liquid crystal aggregates in solution, resulting in broad, and hence difficult to interpret,  $^1\text{H}$ -NMR spectra.

### 3.2.4 Characterization

$^1\text{H}$ -NMR spectra were collected on a Bruker Avance-400 NMR spectrometer using  $\text{D}_2\text{O}$  as a solvent. The spectra were recorded at 400 MHz with 128 scans at 25 °C.

Solution viscosities of the sulfonated polyamides, PBDT and PBDI, were measured at 0.5 g/dL using an Ubbelohde capillary viscometer at 25 °C. Deionized water was used as the solvent unless stated otherwise.

Thermal gravimetric analysis (TGA) was carried out using a thermogravimetric analyzer (Perkin-Elmer, Pyris Diamond TG/DTA). In general, the samples were heated from 30 to 590 °C at a scanning rate of 10 °C/min under a nitrogen atmosphere.

### 3.3 Results and discussion

#### 3.3.1 Reduced viscosities of H-PBDT and H-PBDI and their thermal stabilities

The sodium-form polymer solutions were passed over the ion-exchange column to get the acid-form polymers in solution. The obtained solutions were evaporated under reduced pressure at 60 °C for around 2 h to remove the water solvent, and the polymer was dried at 60 °C under vacuum for 24 h. Both PBDT- and PBDI-membranes in the sodium form display excellent mechanical properties, because of the rigid-rod polymer chains, as reported in Chapter 2. However, the cast acid-form polymer membranes were very brittle after drying. No free-standing membranes could be prepared from the acid-form polymers.

The reduced viscosities of the two polymers were measured before and after acidification, and also when the acidified polymers were converted back to the sodium form. The results are listed in Table 3.1. The reduced viscosities decreased substantially after acidification and this effect proved to be irreversible after converting the polymers back to their sodium form.

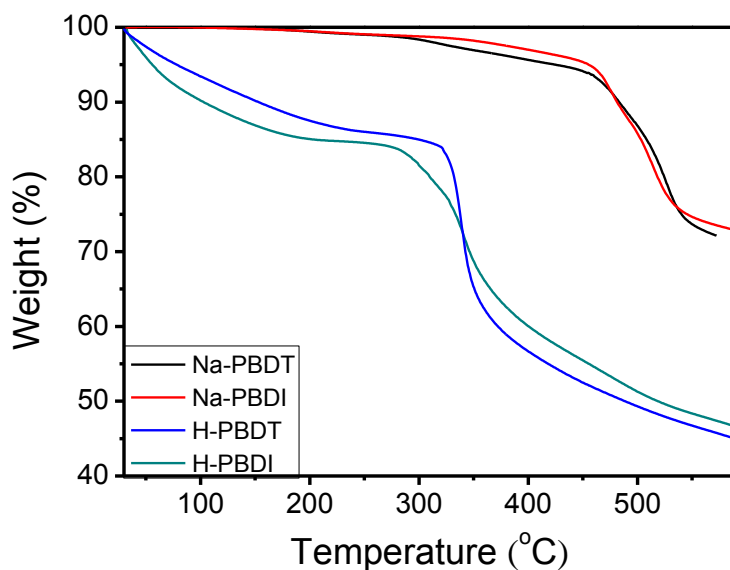
**Table 3.1** Reduced viscosities of polymers in the sodium- and acid-form (25 °C, 0.5 g/dL).

	Na (dL/g)	Na→H (dL/g)	H→Na (dL/g)
<b>PBDT</b>	25.0	0.6	0.6
<b>PBDI</b>	4.3	0.2	0.2



The decrease in viscosities of the two polymers indicates that the molecular weights of the two polymers decreased dramatically after acidification. However, as reviewed in the introduction, the hydrolysis temperature of sulfonated polyamides was generally above 130 °C.[7-10] It is striking that the stability of the acid form sulfonated aramids used in this study is so poor.

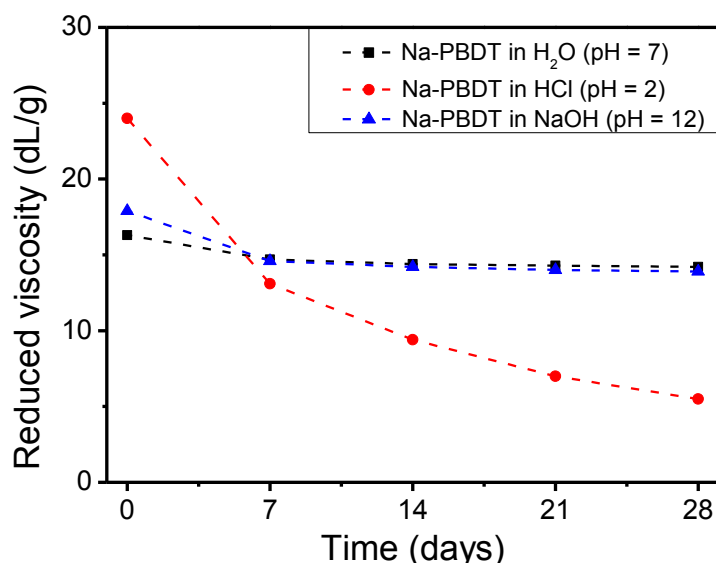
TGA was employed to investigate and compare the thermal stabilities of PBDT and PBDI in their acidic and sodium forms. The results are shown in Figure 3.2. In contrast to the sodium-form polymers, the two polymers in the acid form were not pre-heated at 150 °C for 0.5 h, to avoid damaging the samples. As a consequence, the large weight loss at low temperatures is due to water evaporation. The weight decreased abruptly around 320 °C for H-PBDT and 300 °C for H-PBDI, respectively. For H-PBDT the weight loss was about 27% from 320 to 400 °C, which is close to the weight percentage of  $-\text{SO}_3\text{H}$  groups in the polymer, and H-PBDI had similar weight loss from 300 to 400 °C. This could be due to the desulfonation of the polymer. On the other hand, the TGA curves of Na-PBDT and Na-PBDI show only minimal weight loss going from 300 to 450 °C, and the desulfonation started from around 450 °C. This confirms that the sulfonic groups in polymers are more stable in the sodium form than the acid form.



**Figure 3.2.** TGA results of PBDT and PBDI polymers.

### 3.3.2 Stability of Na-PBDT under neutral, basic and acidic conditions

We compared the reduced viscosity of the Na-PBDT polymer (concentration of 0.5 g/dL) in deionized water (pH=7), dilute HCl solution (pH=2) and dilute NaOH solution (pH=12). The polymer solutions were prepared and stored at room temperature ( $\sim 25^\circ\text{C}$ ). The reduced viscosity was followed in time and measured at  $25^\circ\text{C}$ . The results are shown in Figure 3.3.



**Figure 3.3.** Change of viscosity of the Na-PBDT polymer in water, HCl solution (pH=2) and NaOH solution (pH=12).

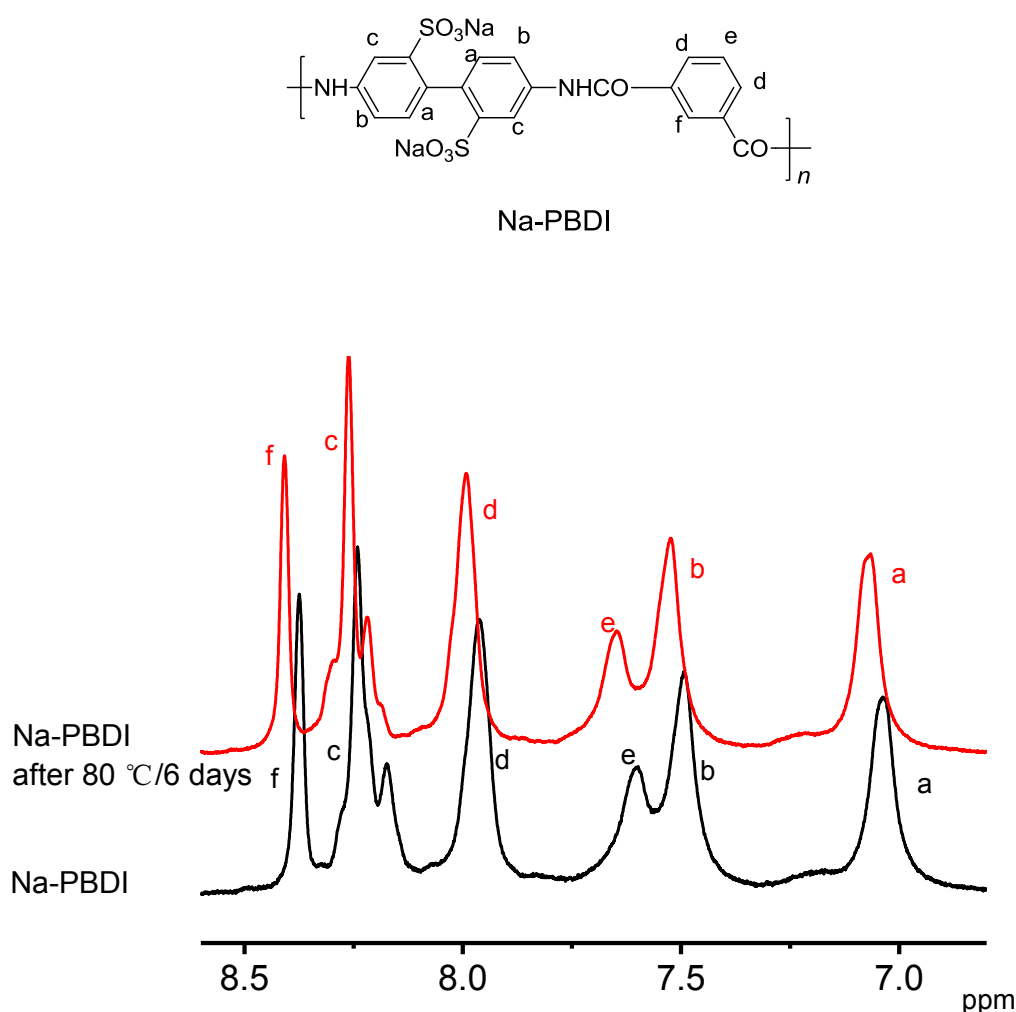
The reduced viscosity of Na-PBDT polymer in deionized water solution decreased by about 10% after 7 days (from 16.3 dL/g to 14.7 dL/g). The decrease in viscosity is caused by the relatively long time for the polyelectrolyte chains to reach equilibrium in solution. After the initial viscosity reduction, the viscosity stabilized (14.2 dL/g on the 28<sup>th</sup> day, with a decrease of  $\sim 3\%$  comparing with 14.7 dL/g on the 7<sup>th</sup> day). Similar behaviour was observed for Na-PBDT in aqueous NaOH: the viscosity value decreased from 17.9 dL/g to 14.6 dL/g after one week, and then to 13.9 dL/g (the 28<sup>th</sup> day). As reported by Meyer and co-workers, high molecular weight PA-11 ( $M_w \sim 78,000$  g/mol) hydrolyzed in deionized water at  $90\text{--}135^\circ\text{C}$ . [17] Sarkar and co-workers reported the viscosity of a Na-PBDT solution was still decreasing even after half a year [18]. Therefore, the slight decrease of viscosity of Na-PBDT in neutral water is probably only due to slow hydrolysis of amide groups. The

viscosity decrease in NaOH solution follows most likely the same mechanism. In contrast, the reduced viscosity of PBDT in HCl solution drastically decreased during the test, from 24.0 dL/g at the start of the experiment to 13.1 dL/g (the 7<sup>th</sup> day), and to 5.5 dL/g (the 28<sup>th</sup> day), which indicates that the amide groups are much more susceptible to hydrolysis in an acidic environment compared to a neutral or basic environment.

### **3.3.3 Hydrolysis of Na-PBDI and H-PBDI in hot water: an NMR study**

According to the viscosity and TGA results, both molecular weight and thermal stability clearly decrease after exchanging the sodium atoms for protons in the sulfonated polyamides. As discussed in the introduction, the reason for the decrease in viscosity of the two polymers could be due to the hydrolysis of the amide groups in an acidic environment. Some sulfonated aramids, such as sulfonated PPTA, have been used for PEM application, but no stability problems were reported.[13-16] Some more direct evidence is needed to confirm that hydrolysis is indeed taking place. Therefore the hydrolysis study of Na-PBDI and H-PBDI was followed using the <sup>1</sup>H-NMR spectroscopy.

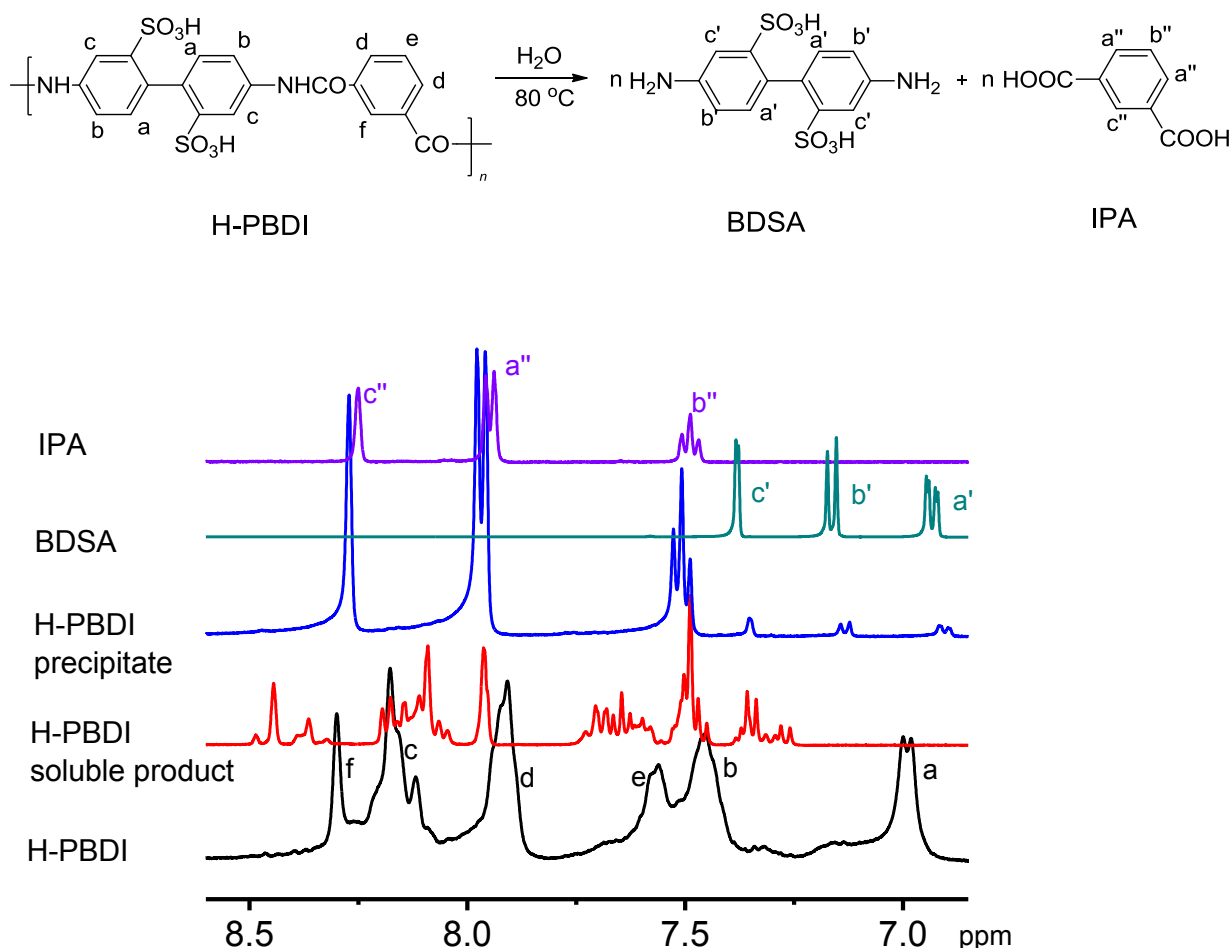
Na-PBDI (0.5 g, reduced viscosity = 4.3 dL/g) and H-PBDI (0.5 g, reduced viscosity = 0.2 dL/g) were dissolved in 10 mL of deionized water. The two polymer solutions were heated at 80 °C for 6 days. It was observed that the Na-PBDI solution was clear throughout the whole experiment. The <sup>1</sup>H-NMR spectra of Na-PBDI before and after the experiment were compared. As shown in Figure 3.4, the two spectra are almost the same.



**Figure 3.4.**  $^1\text{H}$ -NMR spectra of Na-PBDI before and after 6 days at 80 °C.  $^1\text{H}$ -NMR experiments were performed in  $\text{D}_2\text{O}$ .

In contrast, the H-PBDI solution behaved completely differently over time. An insoluble white precipitate appeared in the H-PBDI solution after 1 day, and the amount of precipitate increased gradually during the experiment. After 6 days, the precipitate in the H-PBDI solution (labelled “H-PBDI precipitate”) was collected by filtration, and dried under vacuum at 60 °C for 24 h. The filtrated solution was also collected. The solvent was removed under reduced pressure at 60 °C, and the obtained white product was dried under vacuum at 60 °C for 24 h (labelled “H-PBDI soluble product”). The  $^1\text{H}$ -NMR analysis of these products, “H-PBDI precipitate” and “H-PBDI soluble” are shown in Figure 3.5, together with the spectra of H-PBDI (before exposure to 80 °C hot water for 6

days), the diamine monomer (BDSA) and the diacid monomer (IPA) for reference purposes.



**Figure 3.5.**  $^1\text{H}$ -NMR spectra of H-PBDI and hydrolysis products after 6 days at 80 °C.  $^1\text{H}$ -NMR experiments were performed in  $\text{D}_2\text{O}$ .

As shown in Figure 3.4, the spectrum of Na-PBDI after six days in hot water is similar to the spectrum of Na-PBDI starting material, indicating no hydrolysis has taken place. In contrast, the “H-PBDI soluble product” spectrum is totally different from the H-PBDI spectrum at the start of the experiment. Many peaks are observed in the H-PBDI soluble product spectrum and it is difficult to assign all the peaks. On the other hand, the “H-PBDI precipitate” spectrum is very clear: three large peaks in the range of 8.4 – 7.4 ppm and three small

peaks in the range of 7.4 – 6.9 ppm. By comparing this with the spectra of the monomer starting material, the three large peaks can be attributed to isophthalic acid (IPA), while the three small peaks are in agreement with 2,2'-benzidinedisulfonic acid (BDSA). BDSA has a better solubility in water, compared to IPA, because of the two sulfonic groups. Therefore, the content of IPA in the insoluble precipitate was higher than that of BDSA, resulting in stronger signals in the  $^1\text{H}$ -NMR spectrum. This is direct evidence for the degradation mechanism of the sulfonated polymers occurring through hydrolysis of the amide bond in the presence of sufficient water molecules.

The poor stability of the acid-form PBDT and PBDI is problematic for future applications. Even when the materials are not heated, the molecular weight already starts to decrease at room temperature. Sulfonated PPTA, however, could be used for fuel cell membranes for more than 500 h.[15] One possible reason for the inferior stability of H-PBDI and H-PBDT is the high sulfonic concentration. In both polymers, two sulfonic groups per repeat unit are present, while for sulfonated PPTA, there is one sulfonic group per repeat unit.

### 3.4 Conclusion

The chemical stability of protonated sulfonated polyamides and their sodium counterparts were investigated. Sulfonated PBDT and PBDI proved to be unstable in their acid-form ( $-\text{SO}_3\text{H}$ ). The reduced viscosity of Na-PBDI was 4.3 dL/g, but when exchanging the sodium ions for protons, the viscosity dropped to 0.2 dL/g, indicating a drastic reduction in molecular weight. A  $^1\text{H}$ -NMR hydrolysis study confirmed that after heating the H-PBDI polymer solution at 80 °C for 6 days, monomers precipitated from solution, which indicated the hydrolysis reaction occurs in water. From these results it is clear that sulfonated polyamides in the acid-form are probably not suitable for long-term fuel cell applications. In the following chapters, we will therefore focus on the performance of sulfonated polyamide membranes in the sodium-form.

### 3.5 References

- [1] Hocker, S.; Rhudy, A.K.; Ginsburg, G.; Kranbuehl, D.E. *Polymer*, **2014**, 55, 5057.
- [2] Chaupart, N.; Serpe, G.; Verdu, J. *Polymer*, **1998**, 39, 1375.
- [3] Hoshino, K.; Watanabe, M. *J. Am. Chem. Soc.*, **1951**, 73, 4816.
- [4] Marchildon, K. *Macromol. React. Eng.* **2011**, 5, 22.
- [5] Heikens, D. *J. Polym. Sci.* **1956**, 22, 65.
- [6] Owen, W.S. *Mikrochim. Acta.* **1965**, 53, 88.
- [7] Haslam, J.; Swift, S.D. *Analyst*, **1954**, 79, 82.
- [8] Berkowitz, W.F. *J. Chem. Educ.*, **1970**, 47, 536.
- [9] Morgan, R.J.; Butler, N.L. *Polym. Bull.* **1992**, 27, 689.
- [10] Lin, J.S.; Chiu H.T. *Polym. Polym. Compos.* **2001**, 9, 239.
- [11] Genies, C.; Mercier, R.; Sillion, B.; Petiaud, R.; Cornet, N.; Gebel, G.; Pineri, M. *Polym.* **2001**, 42, 5097.
- [12] Vogel, C.; Meier-Haack, J.; Taeger, A.; Lehmann, D. *Fuel Cells*, **2004**, 4, 4.
- [13] Every, H.A.; Mendes, E.; Picken, S.J. *J. Phys. Chem. B* **2006**, 110, 23729.
- [14] Chen, G.; Zhang, X.; Wang, J.; Zhang, S. *J. App. Polym. Sci.* **2007**, 106, 3179.
- [15] Every, H.A.; Janssen, G.J.M.; Sitters, E.F.; Mendes, E.; Picken, S.J. *J. Power Sources* **2006**, 162, 380.
- [16] Taeger, A.; Vogel, C.; Lehmann, D.; Jehnichen, D.; Komer, H.; Meier-Haack, J.; Ochoa, N.A.; Nunes, S.P.; Peinemann, K.-V. *React. Funct. Polym.* **2003**, 57, 77.
- [17] Meyer, A.; Jones, N.; Lin, Y.; Kranbuehl, D. *Macromolecules*, **2002**, 35, 2784.
- [18] Sarkar, N.; Kershner, D. *J. Appl. Polym. Sci.* **1996**, 62, 393.
- [19] Cohen, T.; Lipowitz, J. *J. Am. Chem. Soc.*, **1964**, 86, 5611.
- [20] Chang, Y.; Lee, Y.-B.; Bae, C. *Polymers* **2011**, 3, 222.





## Chapter 4

### Ionic Crosslinking of Na-PBDT and Na-PBDI Membranes

---

The two sulfonated aramids, Na-PBDT and Na-PBDI, were crosslinked via ionic crosslinking using barium ions. Membranes with various crosslinking degrees, 40%, 60%, 80%, and 100%, were prepared. The water uptake of the membranes decreased linearly as a function of the crosslink density. The thermal stability was better than the neat polymers after crosslinking, with  $T_d^{5\%} > 427\text{ }^{\circ}\text{C}$ , whereas the storage modulus increased from about 4 GPa to about 10 GPa. The excellent thermal and mechanical performance indicates that the membranes should be able to survive the harsh conditions in a fuel cell. Polarized optical microscopy and XRD results revealed that the liquid crystalline order ( $\sim 0.3$ ) of the Na-PBDT membrane was maintained after crosslinking, whereas crosslinked Na-PBDI membranes remained isotropic.

## 4.1 Introduction

Once installed in a proton exchange membrane fuel cell (PEMFC), the proton exchange membrane (PEM) will experience harsh conditions, such as low pH, high humidity, oxidation by oxygen at the cathode. With the increase in operating temperature of a PEMFC, the durability of the membrane will decrease. Therefore the membrane needs to meet several prerequisites, such as good proton conductivity, and high chemical and thermal stability.[1-4] In general, a membrane with high proton conductivity usually has a relative high ion exchange capacity (IEC), which in turn results in high water uptake of the membrane. It is undesirable for a membrane to absorb too much water as this will result in excessive swelling and a reduction in thermal and mechanical properties.[1] It is a challenge to find the right balance between good proton conductivity and good mechanical stability, and we sometimes need to give up proton conductivity to ensure membrane integrity. The two sulfonated aramids in our research, Na-PBDT and Na-PBDI, have good solubility in water. This is not suitable for fuel cell operation, because the membrane will dissolve rapidly under the high humidity operating conditions. To overcome this problem, crosslinking of the membranes has been considered.[5] In general, there are two ways to crosslink sulfonated hydrocarbon polymers: covalent crosslinking and ionic crosslinking.

For covalent crosslinking, there are several chemical approaches:

**A.** Esterification of sulfonic groups using polyhydroxy compounds, such as glycol or polyvinylalcohol, which act as crosslinking agents[6,7];

**B.** Formation of sulfone bridges ( $-\text{SO}_2$ ) by a dehydration reaction between adjacent sulfonic acid groups either by thermal treatment or by exposing the sulfonic acid groups to hot polyphosphoric acid (PPA)[8];

**C.** Friedel-Crafts reaction between carboxylic acid groups and electrophilic aromatic rings to form new carbon-carbon covalent crosslinking points

[9-11];

**D.** Addition reactions between polymer chains containing carbon-carbon double or triple bonds [12].

For the first two methods (**A** and **B**), sulfonic acid groups are required. As discussed in Chapter 3, the sulfonated polyamides are not stable in the acid-form, so we cannot use these two methods. The Friedel-Crafts reaction, method **C**, is an electrophilic substitution reaction, so electrophilic aromatic rings are required. However, there are no electrophilic aromatic rings available in our Na-PBDT and Na-PBDI polymer systems. All the rings on the polymer chains are nucleophilic rings, since they are all connected with electron withdrawing groups – sulfonic and carbonyl groups. The addition reaction, method **D**, has no such critical requirements. However, suitable end-groups are not commercially available and therefore have to be synthesized. Also, crosslinking via carbon-carbon double bonds might compromise the nematic nature of Na-PBDT, which is not desirable.

In another inexpensive and fast crosslinking method, known as ionic crosslinking, polyvalent cations are used to crosslink sulfonated polymers. These cations can form ionic bridges between sulfonic groups acting as the crosslinking points.[13,14] When using cations for crosslinking, the water solubility of the sulfate salts of the cations should be considered to ensure that the solubility of the polymers decreases after crosslinking. Some cation's (such as  $\text{Ca}^{2+}$ ,  $\text{Sr}^{2+}$ ,  $\text{Ba}^{2+}$ , *etc.*) sulfate salts have low solubility in water at room temperature. For example, the solubilities of  $\text{CaSO}_4$ ,  $\text{SrSO}_4$ , and  $\text{BaSO}_4$  in water at 20 °C are 0.255 g/100 mL,  $1.32 \times 10^{-2}$  g/100 mL, and  $2.448 \times 10^{-4}$  g/100 mL respectively.[16] Other sulfates that have solubilities in water that are too high are not suitable for crosslinking (*e.g.*, 35.1 g/100 mL for  $\text{MgSO}_4$  at 20 °C).

In this chapter, the ionic crosslinking method will be discussed for sulfonated polyamides Na-PBDT and Na-PBDI, as this appears to be the most

convenient and effective route towards producing crosslinked membranes, without compromising the nematic nature of Na-PBDT.

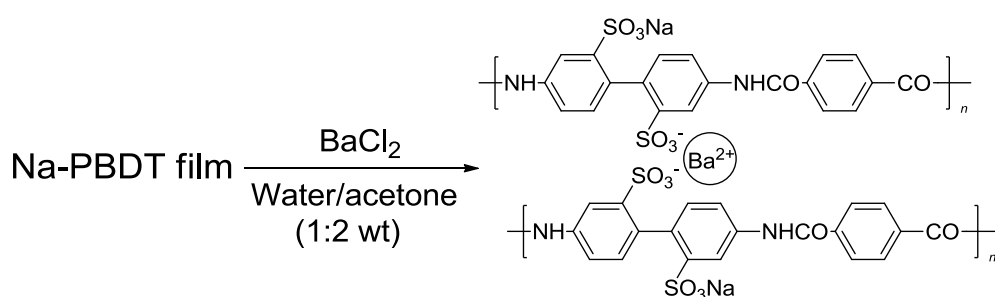
## 4.2 Experimental

### 4.2.1 Materials

Barium chloride dihydrate ( $\text{BaCl}_2 \cdot 2\text{H}_2\text{O}$ , 99%) was purchased from Sigma-Aldrich and used as received. 2,2'-Benzidinedisulfonic acid (BDSA, 70 wt%, Alfa-Aesar) and isophthaloyl chloride (IPC, 99%, Sigma-Aldrich) were purified using the same method described in Chapter 2.

### 4.2.2 Ionic crosslinking procedure

$\text{BaCl}_2 \cdot 2\text{H}_2\text{O}$  was used to crosslink the polymer membranes. The degree of crosslinking is defined by the percentage of sulfonic groups ( $-\text{SO}_3^-$ ) coordinated to  $\text{Ba}^{2+}$  ions. This was controlled by adding a pre-calculated amount of  $\text{BaCl}_2 \cdot 2\text{H}_2\text{O}$  solution (0.5 wt%), see Figure 4.1.



**Figure 4.1.** Barium-crosslinking reaction for Na-PBDT films.

The dry polymer was weighed first and the mole amount of sulfonic groups was calculated. The barium chloride solution was then mixed with acetone with a weight ratio of 1:2. The acetone was used to avoid the membrane dissolving during the crosslinking procedure. The polymer membrane was immersed in the mixture for 24 h. After crosslinking, the membrane was washed with

acetone to remove the trace barium chloride, and formed a free-standing insoluble membrane. The membrane was dried under vacuum at 60 °C for 24 h. The remaining solution containing barium sulfate was analysed using atomic emission spectroscopy (AES) to determine the barium ion concentration after crosslinking, which was used to calculate the degree of crosslinking of the membrane. The targeted degree of crosslinking was 40%, 60%, 80% and 100%. The percentage refers to the molar ratio of sulfonic groups reacted with barium ions.

#### **4.2.3 Characterization**

The liquid crystalline properties of the polymers were studied using an optical microscope, equipped with crossed polarizers (Leica, DM/LP).

Wide-angle X-ray diffraction (XRD, Bruker D8 Discover) was also employed to examine the crystalline structure of the polymer membranes. The wavelength of X-ray beam was 1.54 Å (Cu-K $\alpha$ ) and the distance between sample and detector was 6 cm.

Thermal gravimetric analysis (TGA) was carried out by using a thermogravimetric analyzer (PerkinElmer, Pyris Diamond TG/DTA). The samples were isothermally held at 150 °C for half an hour under a nitrogen atmosphere to remove water, then cooled to 30 °C, and scanned from 30 to 590 °C at a scanning rate of 10 °C /min.

Differential mechanical analysis (DMA, PerkinElmer, Pyris Diamond DMA) was used to measure the storage modulus ( $E'$ ). The samples were stored in a chamber with a relative humidity (RH) of 60% for 2 days before the test. During the test, the samples were heated from 30 to 300 °C at a scanning rate of 2 °C/min under a nitrogen atmosphere at frequencies of 0.1, 1 and 10 Hz.

The water uptake was determined by the change in the weight between the dry and wet state. The films were placed in a chamber with a relative humidity

of 97%. After 48 h, the films were weighed, then put in a vacuum oven at 60 °C for 24 h, and 150 °C for 1 h, and weighed again. The water uptake was calculated by the following equation:

$$\text{Water uptake (\%)} = (W_{\text{wet}} - W_{\text{dry}}) / W_{\text{dry}} \times 100\% \quad (1)$$

## 4.3 Results and discussion

### 4.3.1 Ionic crosslinking

As discussed in the introduction, sulfate salts with a low solubility in water could be selected for ionic crosslinking. Calcium chloride was tried first to crosslink Na-PBDT. The polymer membrane was soaked in a 2 wt% calcium chloride solution, and dried after crosslinking. When soaked in deionized water again, the membrane swelled and partially dissolved in water. The same method was used for barium chloride to crosslink Na-PBDT, and the membrane became insoluble in water. Since the solubility of BaSO<sub>4</sub> in water is much worse than that of CaSO<sub>4</sub>, it is reasonable that the membranes crosslinked using barium ions had a lower solubility than the membranes crosslinked by calcium ions. Therefore, barium ions were selected for the crosslinking.

The two sulfonated polymers Na-PBDT and Na-PBDI could be crosslinked very easily using BaCl<sub>2</sub>, but when 20% of sulfonic groups were crosslinked by barium ions (IEC of about 3 mmol/g), the crosslinked membrane swelled too much in water and broke into pieces. On the other hand, membranes with 40% crosslinking degree or more proved to be insoluble in water. For this reason, only higher crosslinking degrees ( $\geq 40\%$ ) were used in our study. The crosslinking degree was controlled by using different amounts of BaCl<sub>2</sub> solution. The crosslinked polymers were labelled as polymer name + crosslinking degree. For example, “Na-PBDT 40%” means 40% of sulfonic groups in the

Na-PBDT membrane are crosslinked. We studied the properties of crosslinked Na-PBDT and Na-PBDI with crosslinking degree of 40%, 60%, 80% and 100%.

#### **4.3.2 Ionic crosslinking degree and water uptake**

As shown in Table 4.1, the experimental crosslinking degrees (determined by AES) were generally lower than theoretically predicted, especially for the 100% crosslinking degree. The main reason is that with the increase of crosslinking degree, the concentration of free sulfonic groups in the membranes decreases dramatically. It becomes difficult for barium ions to find, and bind, with two adjacent sulfonic groups.

The IEC was calculated based on the degree of crosslinking. The experimental degree of crosslinking was used in the calculation. For example, the IEC of a neat Na-PBDT membrane is 3.9 mmol/g, so the IEC of 40% crosslinked Na-PBDT membrane is  $3.9 \times (100\% - 40\%) = 2.3$  mmol/g. For reference purposes, the IEC of Nafion<sup>®</sup> 117 is ~0.9 mmol/g. The value is close to the 80% crosslinked Na-PBDT and Na-PBDI membrane. Similar to Nafion<sup>®</sup> 117, the 80% and 100% Ba<sup>2+</sup> crosslinked membranes did not swell significantly in water, but the thickness of 40% and 60% crosslinked membranes increased more than 5 times when soaked in water.

The water uptake is dramatically affected by the degree of crosslinking. The water uptake of Na-PBDT and Na-PBDI membranes in 97% relative humidity environment was measured, and the results are shown in Table 4.1. With the increase in the degree of crosslinking, the water uptake decreased for both Na-PBDT and Na-PBDI membranes, because a fraction of the sulfonic groups is coordinated to the barium ions. The free sulfonic groups are very hydrophilic, but the crosslinked sulfonic groups are not so hydrophilic, and they are not able to absorb too much water. In addition, the polymer chains were locked in place after crosslinking, which lowered the mobility of the chains and reduces

the ability of polymer chains to swell in water. Therefore the water absorption capacity was reduced. Na-PBDT and Na-PBDI membranes did not show a significant difference in water uptake, especially at high crosslinking degree (80% and 100%).

When plotting the water uptake as a function of experimental degree of crosslinking, a linear relationship was found. We fitted the data for Na-PBDT, as shown in Figure 4.2. The fitting formula is:

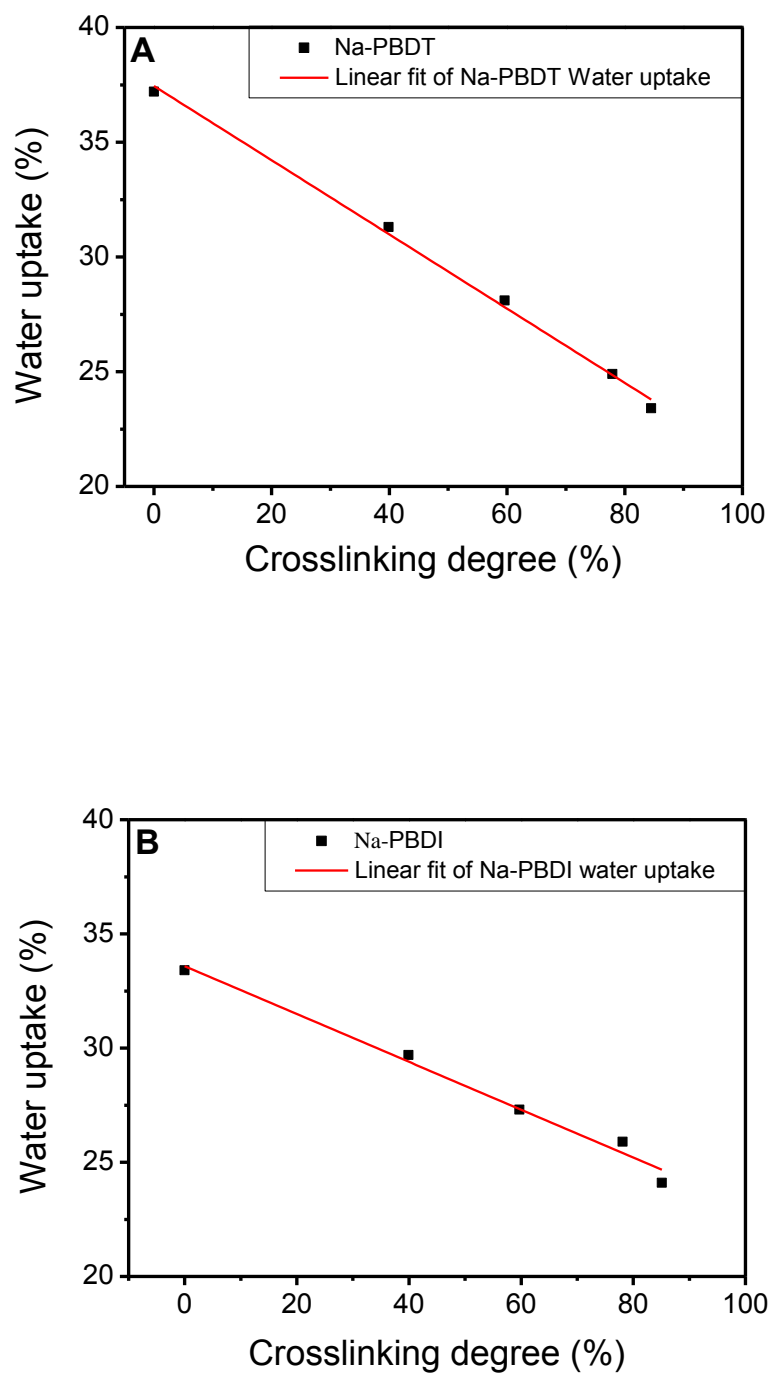
$$y = -0.162x + 37.4 \quad (2)$$

where  $y$  is the water uptake (%) and  $x$  is the experimental crosslinking degree (%). The adjusted coefficient of determination ( $\text{adj. } R^2$ ) is 0.996, indicating this model fits the data very well. Based on this formula, we calculated the water uptake of a 100% crosslinked Na-PBDT to be 21%, which is close to the experimental value of 23% (Table 4.1). A similar method was used for the Na-PBDI water uptake data, and the fitting formula is:

$$y = -0.105x + 33.6 \quad (3)$$

The  $\text{adj. } R^2$  is 0.982, indicating a good fit. Based on the fit, the Na-PBDI membrane with a crosslinking degree of 100%, would take up 23% of water (experimental value = 24%, Table 4.1). The results indicate that even if the sulfonated aramids are fully crosslinked by barium ions, they still allow some water uptake. This information is very important for understanding the water diffusion and ion conductivity in the crosslinked membranes (Chapter 5).





**Figure 4.2.** Water uptake results as a function of the experimental degree of crosslinking and relative fitting lines: A) Na-PBDT membranes, and B) Na-PBDI membranes.

**Table 4.1.** Water uptake and thermo(mechanical) results of the neat polymers and crosslinked polymers.

Sample	XLink degree (Theoretical) (%)	XLink degree (Experimental) (%)	IEC (mmol/g)	Water uptake (wt%) <sup>1</sup>	T <sub>d</sub> <sup>5%</sup> (°C) <sup>2</sup>	Char yield at 590 °C (%) <sup>2</sup>	E' at 25 °C (GPa) <sup>3</sup>
Na-PBDT Neat	-	-	3.9	37	427	72	3.4
Na-PBDT 40%	40	40	2.3	31	453	76	6.0
Na-PBDT 60%	60	60	1.6	28	454	78	6.7
Na-PBDT 80%	80	78	0.9	25	456	78	8.3
Na-PBDT 100%	100	85	0.6	23	474	81	15.1
Na-PBDI Neat	-	-	3.9	33	454	73	4.8
Na-PBDI 40%	40	40	2.3	30	448	77	4.0
Na-PBDI 60%	60	60	1.6	27	445	78	6.8
Na-PBDI 80%	80	78	0.9	26	445	79	7.0
Na-PBDI 100%	100	85	0.6	24	463	80	9.4

1- Water uptake at 97% relative humidity;

2- Determined by TGA from 30 to 590 °C using a heating rate of 10 °C/min under a nitrogen atmosphere;

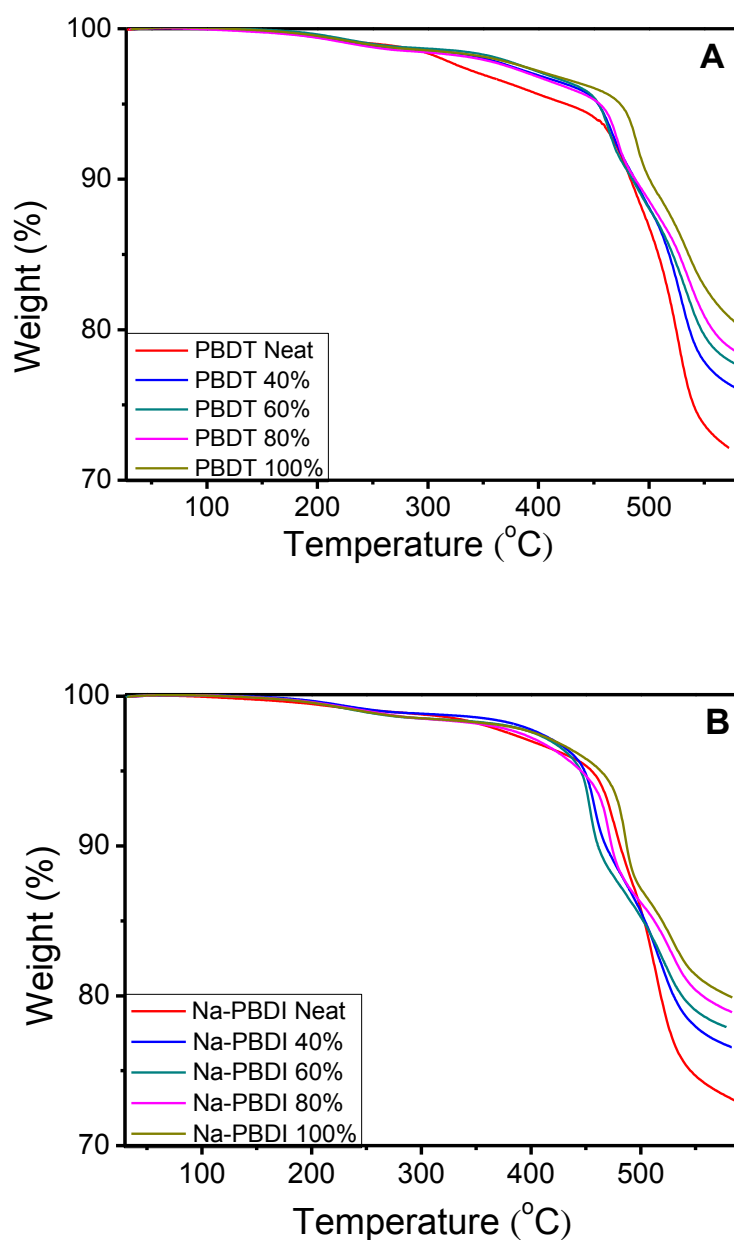
3- Determined by DMTA (1Hz) using a heating rate of 2 °C/min under a nitrogen atmosphere.

### 4.3.3 Thermal and mechanical properties of crosslinked Na-PBDT and Na-PBDI

The thermal stability of neat and crosslinked Na-PBDT and Na-PBDI has been investigated by TGA measurements. All samples absorbed moisture from the air, so they were first pre-heated at 150 °C under nitrogen to remove the absorbed water, and then cooled down to 30 °C followed by starting the test. In general, the thermal stability of crosslinked polymers increased, as can be seen in Figure 4.3. In the case of Na-PBDT, the  $T_d^{5\%}$  increased from 427 °C (Na-PBDT neat) to 474 °C (Na-PBDT 100%), and for PBDI, it increased from 454 °C (Na-PBDI neat) to 463 °C (Na-PBDI 100%). The residual weight of crosslinked polymers (char yield Table 4.1) was higher than the neat polymers, and increased with the increase in degree of crosslinking because of the amount of barium ions present.

The storage modulus ( $E'$ ) of the samples was measured with DMTA and the  $E'$  at 25 °C are shown in Table 4.1. The  $E'$  increased for both of Na-PBDT and Na-PBDI membranes with increasing degree of crosslinking. The storage modulus of the PBDI 100% membrane was about 100% higher than that of the neat membrane. And the storage modulus of the Na-PBDT 100% membrane increased 3 times with respect to the neat polymer membrane. This is because the sulfonic groups were crosslinked by barium ions, which decreased the mobility of polymer chains, resulting in higher storage modulus.

Comparing with other PEMs, the thermal and mechanical properties of the crosslinked membranes are sufficient to test the membranes in a fuel cell.[17-20]



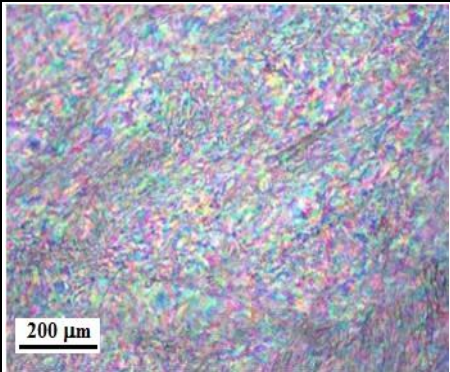
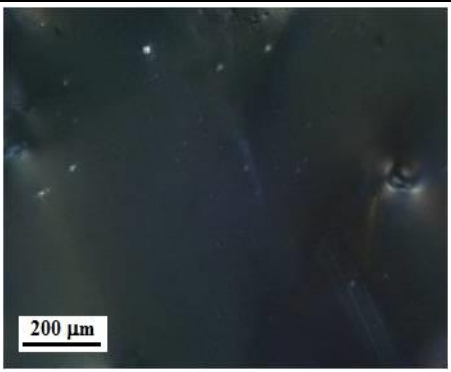
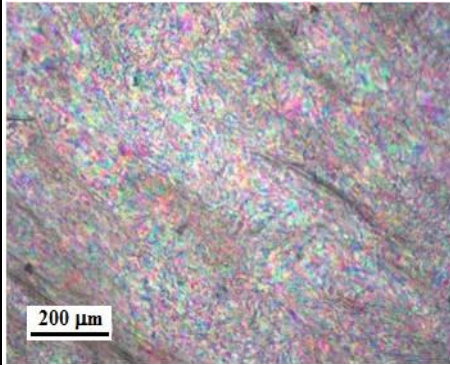
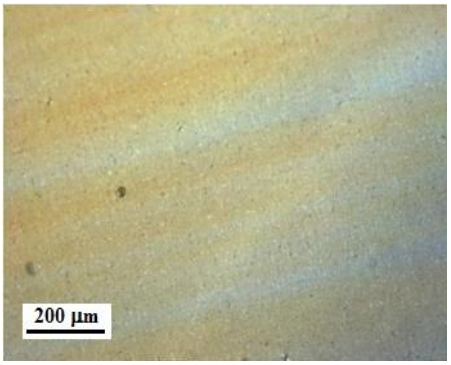
**Figure 4.3.** TGA results of neat and barium-crosslinked membranes: A) Na-PBDT, and B) Na-PBDI membranes.

#### 4.3.4 Polymer morphology (POM)

The POM images of neat polymer solution and films had already been discussed in Chapter 2. The liquid crystalline structure was maintained in the dry membranes of Na-PBDT, as well as in the crosslinked membranes, while

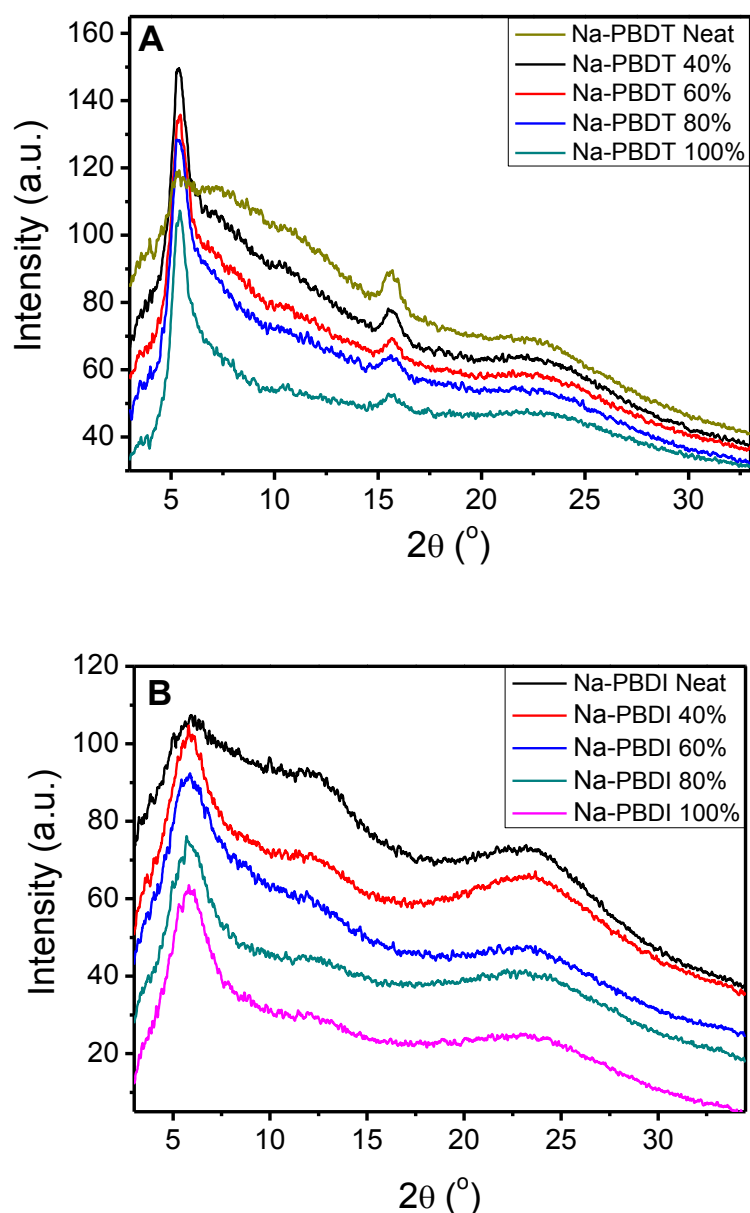
Na-PBDI and the crosslinked membranes were still isotropic (Table 4.2). This indicates that during the crosslinking procedure, the liquid crystalline order was not destroyed. Therefore we are sure that we are still comparing the ion transport properties between LC and non-LC membranes when performing the conductivity measurements and fuel cell testing.

**Table 4.2.** POM images of Na-PBDT and Na-PBDI membranes.

Polymer	Na-PBDT	Na-PBDI
Structure	$\left[ \text{NH} - \text{C}_6\text{H}_3(\text{SO}_3\text{Na})_2 - \text{NHCO} - \text{C}_6\text{H}_4 - \text{CO} \right]_n$	$\left[ \text{NH} - \text{C}_6\text{H}_3(\text{SO}_3\text{Na})_2 - \text{NHCO} - \text{C}_6\text{H}_3(\text{CO})_2 \right]_n$
Neat membrane		
Membrane with crosslinking degree of 60%		

### 4.3.5 Wide-angle X-ray scattering

The scattering intensities of the Na-PBDT and Na-PBDI membranes, as a function of scattering angle  $2\theta$ , are displayed in Figure 4.4.

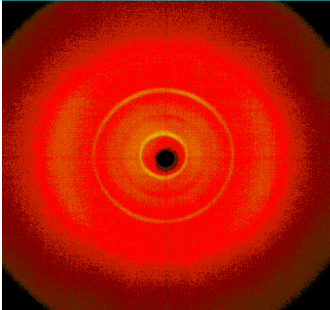
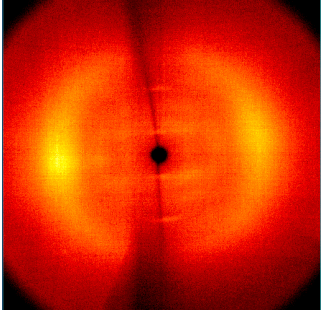

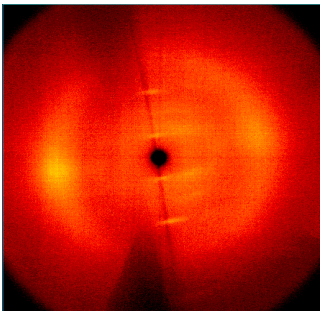
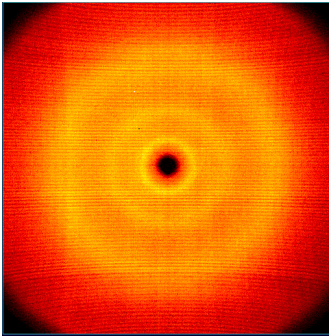
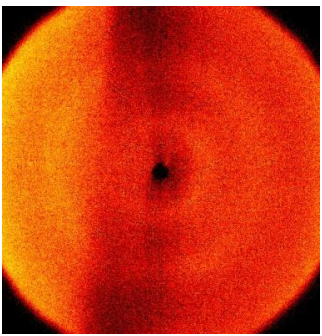
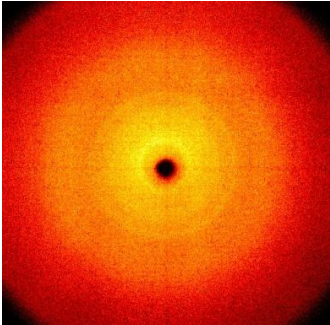
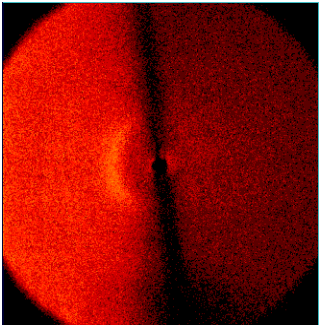


**Figure 4.4.** XRD results of neat and barium-crosslinked free-standing films: A) Na-PBDT, and B) Na-PBDI.

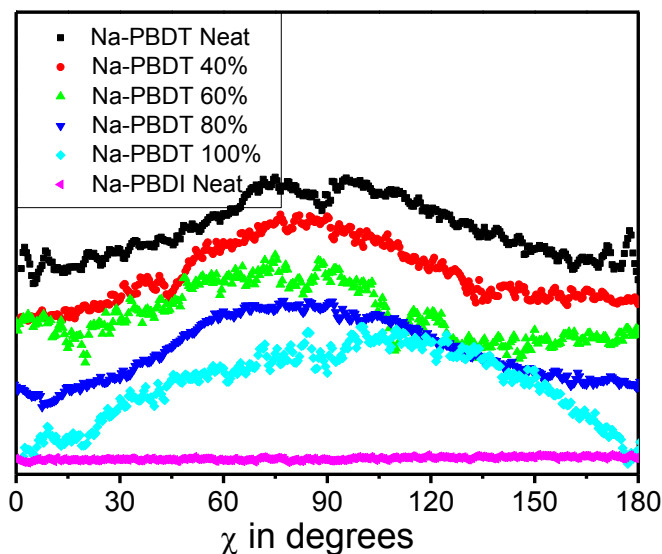
The XRD results of neat Na-PBDT and Na-PBDI membranes have been discussed in Chapter 2. For Na-PBDT, the peak at  $5.2^\circ$  refers to the repeat unit

length ( $d$ -spacing, 16.8 Å), and the peak at 22.8° refers to the average intermolecular distance between the polymer chains ( $d$ -spacing, 3.9 Å). Similarly for Na-PBDI, two peaks at 5.9° and 23.6° refer to the repeat unit length (14.9 Å) and intermolecular distance (3.7 Å), respectively. For the crosslinked membranes, the diffraction peaks become somewhat sharper when compared to the neat Na-PBDT and Na-PBDI membranes, indicating that the crystallinity increased. One possible reason for the increase in crystallinity is that the sodium ions in the polymer chains were partially replaced by barium ions. The intensity of the diffraction peak is proportional to the square of atomic number. In general, a heavier element has more electrons. When scattering X-rays, the heavier element results in stronger peak intensity.[21] The barium atom has an atomic number of 56, which is much higher than Na (11), C (6), N (7), O (8) and S (16), so after decorating with barium ions, the intensity of the peaks increased, and the peaks are sharper than for the neat membrane. In addition, ionic crosslinking resulted in a more ordered chain structure due to the strong interaction of barium ions between polymer chains, reducing the amorphous fraction. Therefore an increase in crystallinity was observed. The scattering images of Na-PBDT and Na-PBDI membranes are shown in Table 4.3. For Na-PBDT, an azimuthal scan at low angles (around 5.2°) was performed to obtain the orientation degree of the neat and crosslinked films, with neat Na-PBDI membranes as a reference. As shown in Table 4.3, the anisotropic behaviour of Na-PBDT membrane was maintained after crosslinking, and the Na-PBDI membranes remain isotropic. The orientation degree  $\overline{\langle P_2 \rangle}$  of the crosslinked membranes were calculated from the data of Figure 4.5 using the same method as for the Na-PBDT neat membranes and S-PPTA membranes.[15] The results show that the orientation degree was also preserved ( $\overline{\langle P_2 \rangle} \sim 0.3$ ). These results confirm that the morphologies of the Na-PBDT and Na-PBDI membranes were maintained after the ionic crosslinking procedure.

**Table 4.3.** XRD scattering images of Na-PBDT and Na-PBDI neat and crosslinked membranes.

	X-ray beam $\perp$ film surface	X-ray beam $\parallel$ film surface
Na-PBDT Neat		
Na-PBDT 60%		
Na-PBDI Neat		
Na-PBDI 60%		





**Figure 4.5.** Azimuthal scan of neat and crosslinked Na-PBDT membranes, with Na-PBDI neat membrane as a reference.

## 4.4 Conclusion

We developed a successful route towards crosslinking Na-PBDT and Na-PBDI membranes while maintaining the LC order for Na-PBDT. Barium ions were used for crosslinking, and membranes could be prepared with degrees of crosslinking of 40%, 60%, 80% and 100%. The water uptake of the crosslinked polymers decreased linearly on increasing the degree of crosslinking, because the sulfonic groups were locked by barium ions. The  $T_d^{5\%}$  of the membranes was higher than 427 °C, and the storage modulus ( $E'$ ) of Na-PBDT, increased from 3.4 GPa (Na-PBDT neat) to 15.1 GPa (Na-PBDT 100%), and for Na-PBDI, from 4.8 GPa (Na-PBDI neat) to 9.6 GPa (Na-PBDI 100%). The POM and XRD scattering images showed that the liquid crystalline structure of Na-PBDT was maintained in the crosslinked Na-PBDT membranes, while the crosslinked Na-PBDI remains isotropic. The orientation degree of crosslinked Na-PBDT membranes was  $\sim 0.3$ , close to that of the Na-PBDT

neat membrane.

## 4.5 References

- [1] Shao. Y.; Yin, G.; Wang, Z.; Gao, Y. *J. Power Sources* **2007**, *167*, 235.
- [2] Liu Y.; Yi, B.; Shao, Z.; Xing, D.; Zhang, H. *Electrochem. Solid State Lett.* **2006**, *9*, A356.
- [3] Healy, J.; Hayden, C.; Xie, T.; Olson, K.; Waldo, R.; Brundage, A.; Gasteiger, H.; Abbott, J. *Fuel Cells*, **2005**, *5*, 302.
- [4] Knights, S.D.; Colbow, K.M.; St-Pierre, J.; Wilkinson, D.P. *J. Power Sources* **2004**, *127*, 127.
- [5] Hou, H.; Di Vona, M.L.; Knauth, P. *J. Membr. Sci.* **2012**, *423*, 113.
- [6] Gu, S.; He, G.; Wu, X.; Guo, Y.; Liu, H.; Peng, L.; Xiao, G. *J. Membr. Sci.* **2008**, *312*, 48.
- [7] Mikhailenko, S.D.; Wang, K.; Kaliaguine, S.; Xing, P.; Robertson, G.P.; Guiver, M.D. *J. Membr. Sci.* **2004**, *233*, 93.
- [8] Di Vona, M.L.; Sgreccia, E.; Licoccia, S.; Alberti, G.; Tortet, L.; Knauth, P. *J. Phys. Chem. B* **2009**, *113*, 7505.
- [9] Zhang, Y.; Wan, Y.; Zhang, G.; Shao, K.; Zhao, C.; Li, H.; Na, H. *J. Membr. Sci.* **2010**, *348*, 353.
- [10] Rhoden, S.L.N.H.; Linkous, C.A.; Mohajeri, N.; Diaz, D.J.; Brooker, P.; Slattery, D.K.; Fenton, J.M. *J. Membr. Sci.* **2011**, *376*, 290.
- [11] Grassie, N.; Gilks, J. *J. Polym. Sci. Polym. Chem. Ed.* **1973**, *11*, 1985.
- [12] Yang, S.J.; Jang, W.; Lee, C.; Shul, Y.G.; Han, H. *J. Polym. Sci. Pol. Phys.* **2005**, *43*, 1455.
- [13] Gasa, J.V.; Weiss, R.A.; Shaw, M.T. *J. Membr. Sci.* **2007**, *304*, 173.
- [14] Luu, D.X.; Kim, D. *Solid State Ionics* **2011**, *192*, 627.
- [15] Every, H.A.; Mendes, E.; Picken, S.J. *J. Phys. Chem. B* **2006**, *110*, 23729.
- [16] [http://en.wikipedia.org/wiki/Solubility\\_table](http://en.wikipedia.org/wiki/Solubility_table).
- [17] Sgreccia, E.; Chailan, J.F.; Khadhraoui, M.; Di Vona, M.L.; Knauth, P.

- J. Power Source* **2010**, *195*, 7770.
- [18] Bai, Z.; Houtz, M.D.; Mirau, P.A.; Dang, T.D. *Polymer*, **2007**, *48*, 6598.
- [19] Nearingburg, B.; Elias, A.L. *J. Membr. Sci.* **2012**, *389*, 148.
- [20] Mabrouk, W.; Ogier, L.; Vidal, S.; Sollogoub, C.; Matoussi, F.; Fauvarque, J.F. *J. Membr. Sci.* **2014**, *452*, 263.
- [21] Zhou, G. *X-ray Diffraction of Polymers*, Press of University of Science and Technology of China, **1989**.



## Chapter 5

### Performance Analysis of Na-PBDT as Potential Proton Exchange Membrane

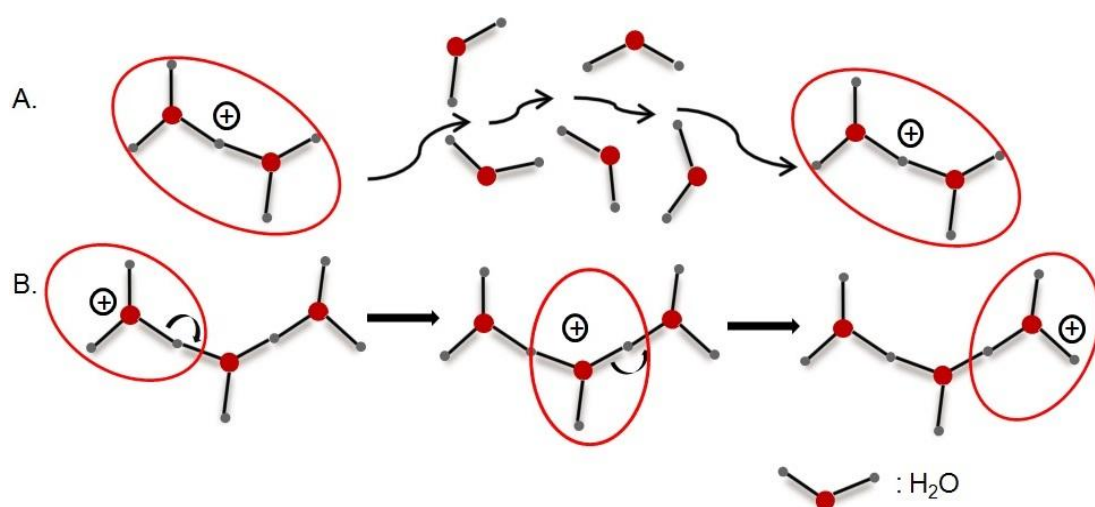
---

In this chapter, we will discuss the water diffusion, ionic conductivity and fuel cell performance of Na-PBDT and Na-PBDI. Pulsed-field-gradient NMR diffusometry reveals that the in-plane water diffusion in the nematic Na-PBDT membrane is as high as  $3.3 \times 10^{-10} \text{ m}^2/\text{s}$ , whereas the diffusion in amorphous Na-PBDI is only  $2.5 \times 10^{-10} \text{ m}^2/\text{s}$ . Whereas neat and crosslinked Na-PBDI shows isotropic diffusion, neat Na-PBDT shows a high diffusion anisotropy ( $D_{\parallel}/D_{\perp} = 3.0$ ), which increases as a function of crosslink density ( $D_{\parallel}/D_{\perp} = 4.6$  at 80% crosslinking). This diffusion anisotropy is substantially higher than that typically observed for low molecular weight liquid crystals and for oriented polymeric conductors such as Nafion<sup>®</sup> ( $D_{\parallel}/D_{\perp} \sim 2.0$ ). The nematic order in the Na-PBDT membrane also promotes directed ionic conductivity, *i.e.*  $\text{Na}^+$  conductivity in Na-PBDT is  $2.24 \times 10^{-2} \text{ S/cm}$  and  $1.67 \times 10^{-2} \text{ S/cm}$  for Na-PBDI, respectively. We propose that the rigid-rod Na-PBDT chains form nano-scale hydrophilic channels, which act as pathways for transporting water molecules and ions. In fuel cell tests, the sodium form membranes of Na-PBDT and Na-PBDI perform poorly, which is due to the lower abundance of  $\text{H}_3\text{O}^+$  ions and slower mobility of sodium ions. There is very little difference in performance between the LC Na-PBDT and isotropic Na-PBDI membranes.

*The water diffusion measurements were performed by Ms. Y. Wang and Prof. L. A. Madsen at Virginia Tech (VA, USA).*

## 5.1 Introduction

Over the last few decades, proton exchange membrane fuel cells (PEMFCs) have been intensively studied as an alternative energy supply for portable applications, such as automobiles, laptops, mobile telephones, *etc.*[1-6] The key component, the proton exchange membrane, plays a role as ion conductor and fuel separator.[7,8] A good PEM should have a high proton conductivity, which is an important parameter for evaluating PEM materials.[9,10] For a good proton conductor, transport of water molecules inside of the membrane was studied intensively, because protons usually exist in the form of hydrated ions. The mobility of water molecules reflects the mobility of protons and is another very important parameter for evaluating PEMs.[11-13] There are two main mechanisms for proton conduction: A- vehicular mechanism and B- Grotthuss mechanism[14-18], as illustrated in Figure 5.1.



**Figure 5.1.** Schematic of proton transport mechanisms: A) vehicular mechanism, and B) Grotthuss (or hopping) mechanism.

The vehicular mechanism was proposed by Kreuer and co-workers (Figure 5.1A).[14,15] In this model, the proton does not migrate as  $H^+$ , but with the assistance of some larger species ( $H_2O$ ). The water molecule plays a role as a

vehicle and diffuses together with the proton (e.g.,  $\text{H}_3\text{O}^+$ ,  $\text{H}_5\text{O}_2^+$ ). As a consequence, the conductivity of protons is related to the diffusion of the vehicle ( $\text{H}_2\text{O}$ ). In the Grotthuss mechanism, the proton is transferred via a network of hydrogen bonds formed by water molecules (Figure 5.1B). It consists of two steps. First, a proton bonds to a water molecule, and then, the hydronium ion starts a structural reorganization, which allows the proton to migrate to the adjacent water molecule, as shown in Figure 5.1B.[16-18] Both models are important for ion transport.[19] It was observed that in Nafion<sup>®</sup>117-based membranes, the Grotthuss mechanism was dominant for proton transport, while sodium ions transport via the vehicular mechanism.[21] Therefore, the water diffusion was measured for the neat and crosslinked membranes, as described in chapter 4. NMR diffusometry is often used to probe the structure and transport properties of porous materials and membranes. This method was used by us to investigate the water and  $\text{Na}^+$  diffusion in Na-PBDI- and Na-PBDT-based membranes.

As discussed above, water molecules in a membrane are essential for ion transport, which is usually quantified as ionic conductivity. Similar to electrical conductivity, ionic conductivity refers to the movement of an ion from one site to another in a membrane. Generally, the in-plane conductivity is measured for ionic conductive membranes. For our membranes, the mobile ions are sodium ions. Therefore, the ionic conductivity in this chapter means the in-plane sodium conductivity.

In addition to the tests mentioned above, fuel cell performance was investigated using a fuel cell setup. In general, sulfonated polymers of the acid-form ( $-\text{SO}_3\text{H}$ ) are used for such measurements. However, as discussed in Chapter 3, the acid-form PBDT and PBDI polymers are unstable due to hydrolysis, and no free-standing films could be prepared from the acid-form polymers, so the sodium-form membranes were used to compare the fuel cell performance of PBDT and PBDI.

## 5.2 Experimental

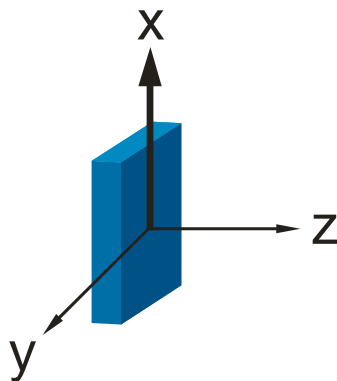
### 5.2.1 Materials

Na-PBDT ( $M_n = 7900$  g/mol) and Na-PBDI ( $M_n = 3900$  g/mol) membranes, neat and crosslinked (40%, 60%, 80%, and 100%), (all in the sodium form) were prepared using the method described in chapters 2 and 4. The electrode for fuel cell test was purchased from Quintech Company: Pt was loaded around  $0.5 \text{ mg/cm}^2$  on high surface area advanced carbon, and the electrode was used for the cathode and anode of the fuel cell. The Nafion<sup>®</sup> 117 membrane was purchased from Alfa-Aesar.

### 5.2.2 Characterization

Molecular diffusion was measured as in our previous studies of ionic polymer membranes using the simple and robust pulsed-gradient stimulated echo NMR pulse sequence (PGSTE) using a Bruker Avance III WB 400 MHz (9.4T) NMR equipped with a Micro5 triple-axis-gradient micro-imaging probe and a 8 mm double resonance ( $^1\text{H}/^{19}\text{F}$ ) rf coil.[23,26,27] As shown in Figure 5.2, the triple axis gradients (X, Y, Z) were used to measure the diffusion coefficient of  $\text{H}_2\text{O}$  with directions parallel to the membrane surface (X, Y) and perpendicular to the membrane surface (Z), respectively. The PGSTE sequence used a  $\pi/2$  pulse time of  $32.5 \mu\text{s}$ , effective gradient pulse duration  $\delta$  of 1 ms (half sinusoid pulse, 1.57 ms total duration), diffusion times  $\Delta$  of 10 - 25 ms, and the number of scans for each step was adjusted from 1 - 64 to ensure good signal-to-noise ratio (SNR). 16 gradient steps were applied for each diffusion experiment, and the maximum gradient strength was selected to achieve  $\geq 90\%$  NMR signal attenuation. All measurements resulted in clean single component fits to determine diffusion coefficients. All parameters for the gradient have been calibrated and optimized as reported earlier.[26,27]





**Figure 5.2.** Schematic representation showing the three principal axes of the membranes used for our studies. The direction of the casting (doctor blading) is along the X axis.

The sodium conductivity measurements were performed using an Autolab PGSTST 302 impedance analyzer in the frequency range of 20 Hz to 1 MHz with an amplitude of 20 mV. Two polycarbonate (PC) blocks and two copper (Cu) sheets were used to construct the in-plane conductivity cell. The two Cu electrodes were placed between the two PTFE blocks, and the distance between the electrodes was set at 10 mm. Membranes were cut into  $80\ \mu\text{m} \times 3\ \text{mm} \times 15\ \text{mm}$  pieces and placed between the electrodes. The impedance was measured in two perpendicular in-plane directions of membranes, the X and Y direction. All of the samples were measured in a 97% relative humidity atmosphere and 25 °C. In both cases, the conductivity (X and Y) was calculated using equation (1)

$$\sigma = \frac{1}{R} \frac{L}{A} \quad (1)$$

where R and A are the measured bulk membrane resistance ( $\Omega$ ) and cross-sectional area ( $\text{cm}^2$ ) of the membrane, respectively. L (cm) corresponds to the distance between two electrodes. For one data point, the conductivities of three individual membranes were measured and calculated. The average value of the three was calculated and used in the discussion.

A membrane electrode assembly (MEA) was prepared for the membrane before the fuel cell test. The electrodes from Quintech Company were cut into round discs with a diameter of 32 mm and thickness of ~270  $\mu\text{m}$ . A membrane (45  $\times$  45 mm with a thickness of ~80  $\mu\text{m}$ ) was sandwiched between two electrodes, placed in the hot pressing equipment at 135  $^{\circ}\text{C}$  without pressure for 10 min, and pressed at 50 kN for 90 s. The active surface area of the MEAs was 8  $\text{cm}^2$ .

The performance of the prepared MEAs was measured in a fuel cell station. The environment was controlled at 60  $^{\circ}\text{C}$  and 100% relative humidity. Hydrogen and air were supplied to the anode and the cathode, respectively. The cell voltage was set at 0.4 V. The open circuit voltage (OCV) was measured every 5 min. V-I curves were recorded every hour. The fuel cell test for each MEA lasted for at most 6 hours. Na-PBDT Neat, Na-PBDI Neat, Na-PBDT 40%, Na-PBDI 40%, Na-PBDT 80%, and Na-PBDI 80% (all in the sodium form) were measured in the fuel cell measurement, with Nafion<sup>®</sup> 117 as the reference.

## **5.3 Results and discussion**

### **5.3.1 Water diffusion**

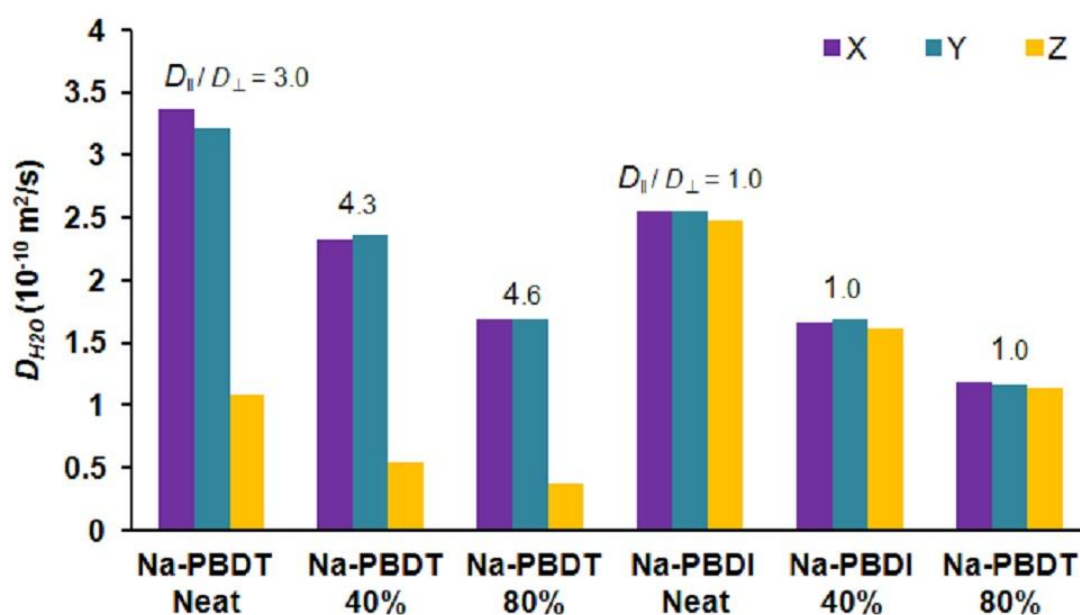
Pulsed-field-gradient NMR (PFG NMR) diffusometry is one of the most powerful and convenient techniques to probe the transport properties of small molecules absorbed in porous materials, such as ionic polymer membranes.[22-24,26-28] Here, we employed multi-axis PFG NMR to study the diffusion anisotropy of water inside the membranes for the three directions (X, Y and Z, see Figure 5.2). The results are listed in Table 5.1.

**Table 5.1.** Water diffusion and ionic conductivity results of the neat and crosslinked polymer membranes. Errors in  $D$  are  $\pm 3\%$  and errors in  $D_{\parallel}/D_{\perp}$  are  $\pm 5\%$ . Errors in  $\sigma$  are shown in Figure 5.5.

Sample	Water diffusion ( $10^{-10} \text{ m}^2/\text{s}$ )				Ionic conductivity ( $10^{-2} \text{ S/cm}$ )	
	$D_x$	$D_y$	$D_z$	$D_{\parallel}/D_{\perp}$	$\sigma_x$	$\sigma_y$
Na-PBDT Neat	3.21	3.36	1.09	3.0	2.24	1.59
Na-PBDT 40%	2.35	2.32	0.545	4.3	0.965	0.673
Na-PBDT 60%	-	-	-	-	0.496	0.426
Na-PBDT 80%	1.68	1.68	0.368	4.6	0.236	0.204
Na-PBDT 100%	-	-	-	-	0.142	0.126
Na-PBDI Neat	2.55	2.55	2.48	1.0	1.67	1.94
Na-PBDI 40%	1.68	1.66	1.61	1.0	0.47	0.482
Na-PBDI 60%	-	-	-	-	0.276	0.268
Na-PBDI 80%	1.16	1.19	1.13	1.0	0.107	0.104
Na-PBDI 100%	-	-	-	-	0.052	0.042

Figure 5.3 shows water diffusion coefficients for Na-PBDT and Na-PBDI membranes, *i.e.* neat polymers and 40 and 80% crosslinked samples, in the X, Y and Z direction. For both Na-PBDT and Na-PBDI, the diffusion coefficient  $D$  decreases with increasing crosslink density, which is attributed to the partially (barium) locked sulfonate groups, leaving hydrophilic domains with lower mobility for water transport. Here we note that the absolute  $D$  values for sodium-form Na-PBDT and Na-PBDI are only modestly lower than acid-form Nafion<sup>®</sup> 117 at similar water uptake [23,24,27], especially considering that sodium-form Nafion<sup>®</sup> will have slower water diffusion than proton-form Nafion<sup>®</sup>. Furthermore, the diffusion tensor traces (averages over X, Y, and Z directions) are equal for Na-PBDT and Na-PBDI [23,24], suggesting that the local water-polymer interactions are the same for these two polymers, while only the chain alignment influences direction-dependent diffusion in Na-PBDT.

Figure 5.3 also shows the diffusion anisotropy, defined as  $D_{\parallel}/D_{\perp}$ , for each membrane composition. For neat and crosslinked Na-PBDT membranes, the diffusion of water is a factor of three faster in the in-plane directions (X and Y) compared to the through plane Z direction for no crosslinking, and reaches a factor of 4.6 for 80% crosslinking. As expected, there is no significant diffusion anisotropy observed for the Na-PBDI membranes. Note that the high Na-PBDT diffusion anisotropies ( $D_{\parallel}/D_{\perp}$  from 3 to 4.6) are substantially higher than that observed in low molecular weight liquid crystals ( $D_{\parallel}/D_{\perp}$  typically  $\sim 2$ ) [29] as well as higher than many oriented conducting polymer membranes such as Nafion<sup>®</sup> and sulfonated polysulfone block copolymers.[23,26,28]



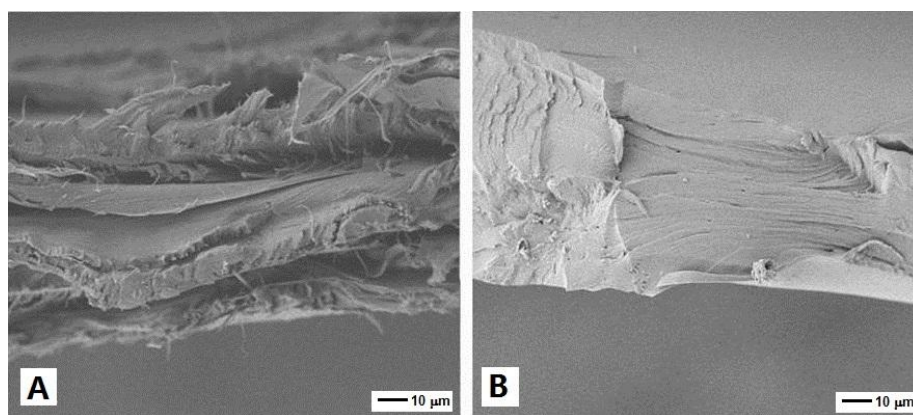
**Figure 5.3.** Water diffusion coefficient of Na-PBDT and Na-PBDI membranes.

This high anisotropy may be attributed to the formation of oriented hydrophilic pathways or channels in the X and Y in-plane directions at this relatively low water content. We can understand these channels as arising from the close proximity of the locally parallel Na-PBDT chains. At these low contents, the Na-PBDT rod-rod distance will be  $\sim 1$  nm for these membranes [25], and thus the rods form nanoscale hydrophilic channels that are

preferential pathways for water transport along the rigid rod alignment direction. Since the Na-PBDT rigid rods are arranged in a “planar” pattern, presumably with bundles of rods aligned in the plane of the membrane but where the bundles are nearly isotropically distributed within the plane, the through-plane direction of transport is highly restricted. We note that diffusion coefficients in the X and Y directions are equal to within errors for all Na-PBDT films. The introduced alignment by doctor blading ( $\overline{\langle P_2 \rangle}$  of  $\sim 0.3$  from XRD, as discussed in Chapter 2) is apparently too weak to enhance water transport in the X (casting) direction. We are working towards aligning the Na-PBDT molecules through plane (along Z), which would provide for fast and anisotropic transport in the direction desired for most membrane applications such as fuel cells and batteries. This highly aligned morphology in Na-PBDT membranes is essential for the construction of functionalized PEMs with the capability of preferential transport along predetermined directions.

For the in-plane results, *i.e.* the X and Y directions (Figure 5.3), the diffusion coefficient of Na-PBDT is at least 30% higher than that of Na-PBDI. Again, the higher  $D$  values reveal that water molecules prefer to transport along the rigid sulfonated Na-PBDT polymer chains. Bulk unidirectional transport through an amorphous (isotropic) polymer, as is the case for Na-PBDI, is clearly less favourable.

In order to investigate micron-scale organization, we conducted an SEM analysis on the Na-PBDT and Na-PBDI membranes (Figure 5.4). The fibrils apparent in the fractured Na-PBDT membranes indicate aligned bundles of polymer chains, as is typical of LC polymers, while the isotropic Na-PBDI membranes show no such fibrillar morphology.

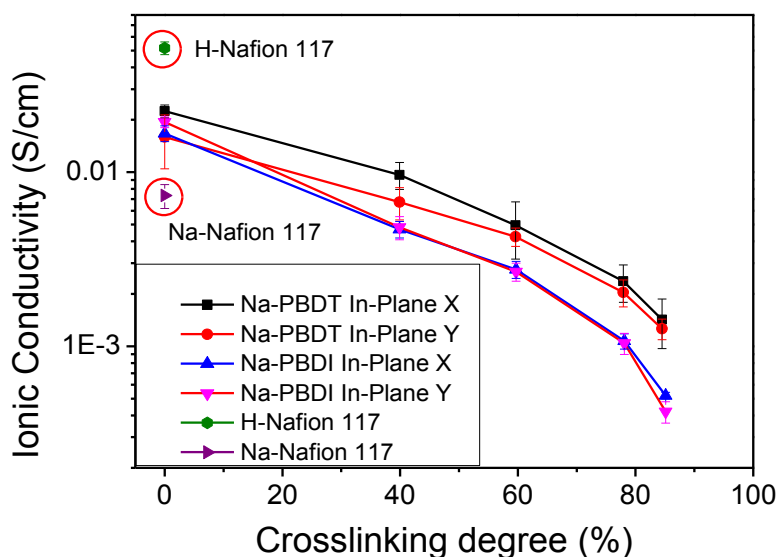


**Figure 5.4.** SEM images of A) Na-PBDT and B) Na-PBDI membranes (cross section). Samples were prepared by fracturing the films after submersing them in liquid nitrogen.

### 5.3.2 Ionic conductivity

Ionic conductivity of the two polymers was measured in the two in-plane directions, X and Y. All measurements were performed at RH = 97% and 25 °C. The results are summarized in Table 5.1.

As discussed in Chapter 4, Na-PBDT and Na-PBDI were used in their sodium-form. In general, the mobility of  $\text{Na}^+$  is much lower than that of protons. Therefore, despite the higher IEC,  $\text{Na}^+$  conductivity in our neat polymers is 0.02 S/cm, substantially lower than that of  $\text{H}^+$ -form Nafion<sup>®</sup> 117 (0.05 S/cm). However, the conductivity of our membranes compares favorably with the  $\text{Na}^+$ -form of Nafion<sup>®</sup> 117, with  $\sigma = 0.007$  S/cm (Figure 5.5).



**Figure 5.5.** Ionic conductivity results of Na-PBDT and Na-PBDI membranes in the X and Y plane direction as a function of crosslinking degree. H-Nafion<sup>®</sup> 117 and Na-Nafion<sup>®</sup> 117 are added for reference purposes.

Conductivity decreases dramatically with increasing crosslinking degree. The ionic conductivity of membranes with a degree of crosslinking of 40%, reduces by as much as 50% whereas the conductivity of membranes with a degree of crosslinking of 85% drops to 10% of that measured for the neat polymer. Considering the water uptake of the membranes, neat Na-PBDT shows a water uptake of 37%, and the water uptake of Na-PBDT 100% crosslinked is 23%. We can therefore attribute the dramatic reduction in ion conductivity to the decrease in sodium ion content combined with the decrease in water uptake.

For the same degree of crosslinking, the ion conductivities of Na-PBDT membranes are higher than those measured for Na-PBDI membranes, which is in agreement with the water diffusion results (Section 5.3.1). Since ions generally move along with water molecules, it is reasonable that the ionic conductivity of Na-PBDT is higher than that of Na-PBDI.[30]

For the two in-plane directions (X and Y) of the Na-PBDT membranes,

conductivity along X (the casting direction) appear to be marginally higher than conductivity along Y, although the error bars overlap each other. The LC polymer Na-PBDT membrane exhibits a measurable degree of order in the casting direction ( $\overline{P_2} \sim 0.3$ ), but it is not high enough to induce a large difference in ion conductivity in the X and Y direction. For Na-PBDI membranes, the conductivities in the two in-plane directions are equal as a result of the isotropic morphology.

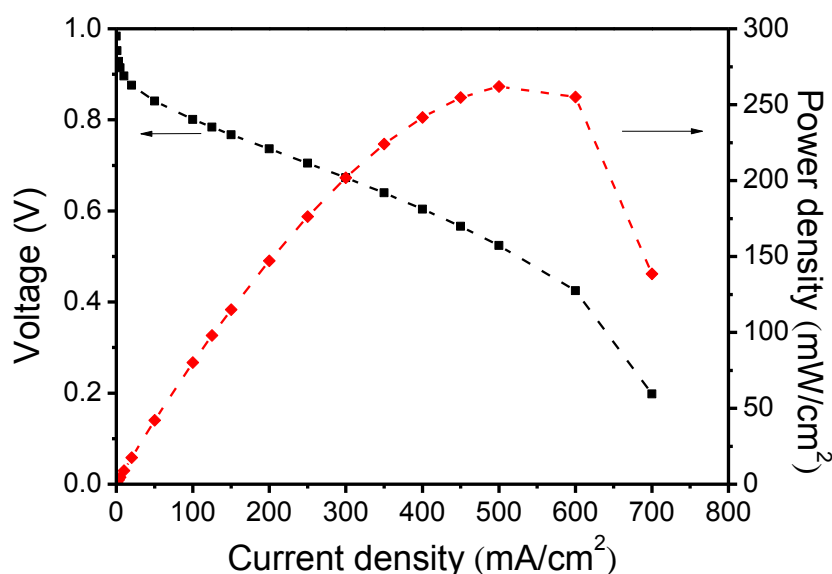
Based on XRD, water diffusion and ionic conductivity results, a molecular picture emerges on how the polymer chains are organized in the Na-PBDT and Na-PBDI membranes. The Na-PBDT polymer chains are aligned weakly along the casting direction, but with predominantly a planar arrangement of Na-PBDT chain (rigid-rod) bundles in the plane, whereas the Na-PBDI polymer chains are randomly (isotropically) oriented in the membrane.

### 5.3.3 Fuel cell performance

The fuel cell measurements were conducted at 60 °C and 100% relative humidity for 6 hours. As a reference, Nafion<sup>®</sup> 117 (acid-form) was studied under the same conditions just to check whether our set-up works properly.

Figure 5.6 shows the polarization curve and power density behaviour of Nafion<sup>®</sup> 117. The power density reached 262 mW/cm<sup>2</sup> at 500 mA/cm<sup>2</sup>, and the durability of Nafion<sup>®</sup> 117 was acceptable in this test and in line with literature values.[31] There was no visual damage on the MEA after 6 hours fuel cell test. This is not surprising, for the durability of Nafion<sup>®</sup> membranes is claimed to be more than 5000 hours.[20]



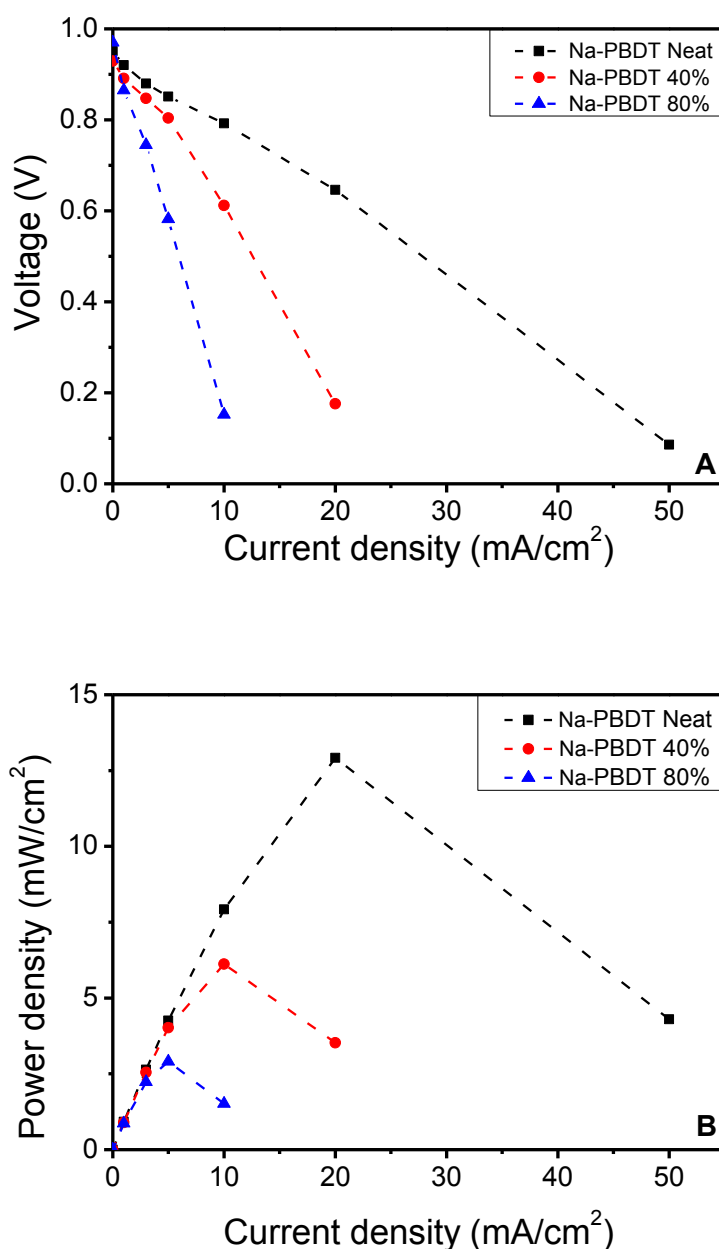


**Figure 5.6.** Polarization curve (black line) and power density (red line) of Nafion<sup>®</sup> 117.

For application in a fuel cell, apart from the power density and polarization, durability is a very important parameter for the membranes. Therefore, fuel cell experiments are often operated for extended periods of time ( $> 100$  h) to study the durability of the PEMs. However, neat Na-PBDT and Na-PBDI membranes have quite good solubility in water. In the environment of 100% relative humidity, neat Na-PBDT and Na-PBDI membranes absorb moisture and swell substantially, with damage to the compressed MEA as a result. Therefore the fuel cell experiments were only run for a maximum duration of 6 hours.

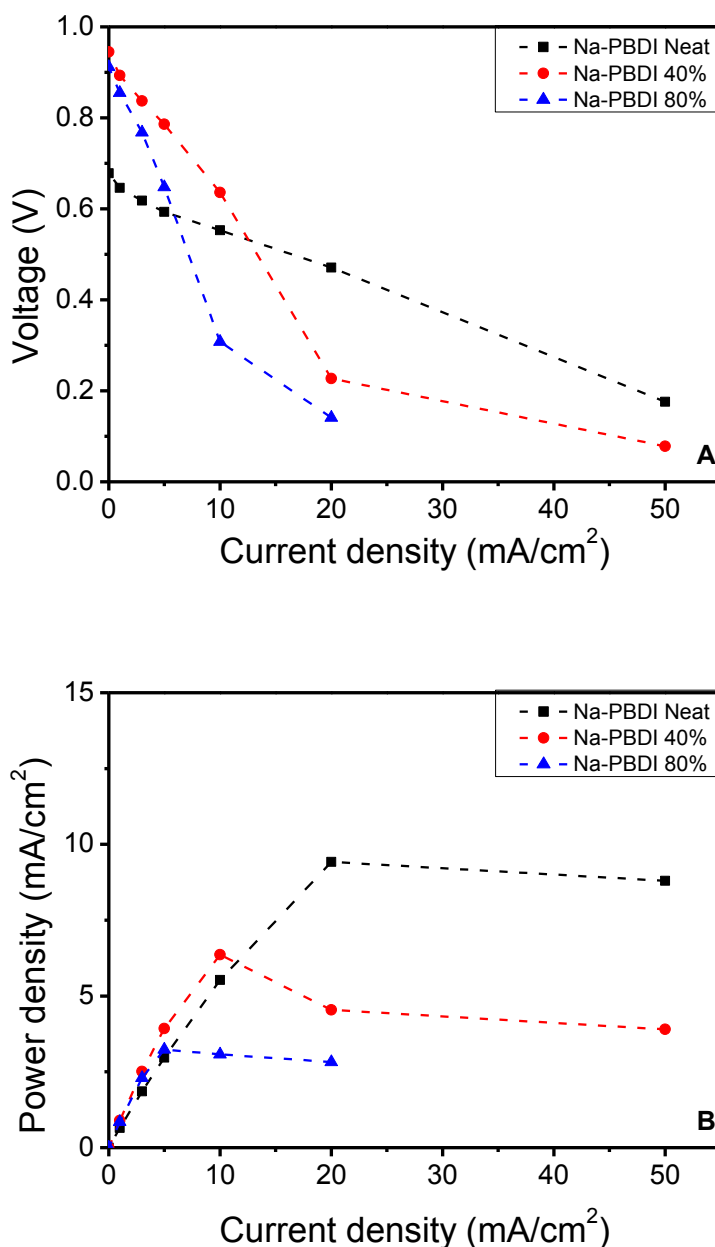
Polarization curves and power density results of Na-PBDT and Na-PBDI membranes are shown in Figure 5.7 and 5.8. The performance of Na-PBDT and Na-PBDI MEAs were inferior to Nafion<sup>®</sup> 117. The current density for neat Na-PBDT and Na-PBDI membranes reached only  $50 \text{ mA/cm}^2$ , where Nafion<sup>®</sup> 117 reached  $700 \text{ mA/cm}^2$ . The highest power density for neat Na-PBDT and Na-PBDI membranes was  $13 \text{ mW/cm}^2$  at  $20 \text{ mA/cm}^2$  and  $9 \text{ mW/cm}^2$  at  $20 \text{ mA/cm}^2$ , respectively. The performance of crosslinked polymer membranes was even worse. The most likely explanation for the inferior performance is that the sulfonic groups in Na-PBDT and Na-PBDI membranes are of the sodium-form and not the acid-form. In such membranes, there are not enough

$\text{H}_3\text{O}^+$  ions as to act as a charge carrier for proton transport, which results in the poor fuel cell performance. In addition, sodium ions can also move during the measurement, but the mobility of sodium ions is much lower than protons, which further reduces the performance of Na-PBDT and Na-PBDI membranes in the fuel cell tests.



**Figure 5.7** Fuel cell measurement results of Na-PBDT membranes: A) V-I curves, and B) power density curves.

In addition, during the measurement, protons were produced at the anode and moved through the membrane (the sodium form polymer) to the cathode. This procedure is similar to that of ion exchange column, *i.e.* the sodium ions were partially replaced by protons, and the polymer was acidified. The acidified polymers are unstable, and hydrolyze easily, especially at relative high temper-



**Figure 5.8.** Fuel cell measurement results of Na-PBDI membranes: A) V-I curves, and B) power density curves.

ature, as discussed in Chapter 3. This led to a loss in structural integrity of the membrane, and an even lower current density and power density than Nafion<sup>®</sup> 117.

The fuel cell performance decreased dramatically with the increase in crosslinking degree. That is because the barium ions block the ionic channels, which are more permeable when occupied by sodium atoms. These results agree with the water diffusion and ion conductivity results.

An overview of the durability of the different membranes is given in Table 5.2. Each membrane was tested in a MEA for 6 hours. Despite the relatively poor power performance, the Na-PBDT membranes displayed longer durability than the Na-PBDI membranes. The neat Na-PBDI membrane can only work for 1.7 hours. In contrast, the neat liquid crystal Na-PBDT membrane, continued to function in the fuel cell for 3.4 hours before failure occurred. The 40% crosslinked Na-PBDT and Na-PBDI samples could stand the conditions used in the test for 5.7 and 3.4 hours, respectively. Although these 40% crosslinked samples were not soluble in water, the swelling was significant. Therefore, the MEAs were damaged as well during the fuel cell test. Only the 80% crosslinked samples survived after the 6 hours measurement.

**Table 5.2.** Durability of Na-PBDT and Na-PBDI membranes.

Sample	Time (hour)
Na-PBDT Neat	3.4
Na-PBDT 40%	5.7
Na-PBDT 80%	>6
Na-PBDI Neat	1.7
Na-PBDI 40%	3.4
Na-PBDI 80%	>6

## 5.4 Conclusion

The water diffusion, Na<sup>+</sup> conductivity and fuel cell performance of Na-PBDT and Na-PBDI membranes was investigated. The high in-plane order resulted in a high in-plane water diffusion coefficient of  $3.3 \times 10^{-10} \text{ m}^2/\text{s}$  for Na-PBDT. Na-PBDT Neat shows a high diffusion anisotropy ( $D_{\parallel}/D_{\perp} = 3.0$ ), which increases as a function of crosslink density ( $D_{\parallel}/D_{\perp} = 4.6$  at 80% crosslinking). This diffusion anisotropy is substantially higher than what is typically observed for low molecular weight liquid crystals and for oriented polymeric ion conductors such as Nafion<sup>®</sup> ( $D_{\parallel}/D_{\perp} \sim 2.0$ ). As a consequence of the isotropic morphology, the diffusion coefficient of the Na-PBDI membranes is the same in all three directions ( $2.5 \times 10^{-10} \text{ m}^2/\text{s}$ ) and the diffusion anisotropy ( $D_{\parallel}/D_{\perp}$ ) is 1.0.

Ionic conductivity measurements show similar trends. The nematic order in the Na-PBDT membrane promotes ion conductivity, *i.e.* the Na<sup>+</sup> conductivity in Na-PBDT is  $2.24 \times 10^{-2} \text{ S/cm}$  and  $1.67 \times 10^{-2} \text{ S/cm}$  for Na-PBDI, respectively (RH = 97% and 25 °C). The conductivity drops dramatically as a function of Ba<sup>2+</sup> crosslinking density and is attributed to a decrease in Na<sup>+</sup> content and a decrease in water uptake. Although the chains in Na-PBDT membranes show a somewhat higher orientational order in the casting X direction (see Figure 5.2), the ion conductivity is only marginally higher than the conductivity in the Y direction.

In fuel cell experiments, the current density of Na-PBDT membranes (Na-PBDT Neat, Na-PBDT 40% and Na-PBDT 80%) could reach to 50, 20 and 10 mA/cm<sup>2</sup>, while the results of Na-PBDI membranes (Na-PBDI Neat, Na-PBDI 40%, Na-PBDI 80%) were 50, 50, and 20 mA/cm<sup>2</sup>, respectively. Both of the two polymers showed very poor fuel cell performance because the H<sub>3</sub>O<sup>+</sup> ions in the membranes are not abundant for proton transport and the mobility of sodium ions is much lower than protons. According to the water diffusion and conductivity results, we may conclude that LC polymers are suitable candidates for ion transport applications. The ordered structure of LC polymers

leads to a higher ionic conductivity because ions prefer to move along the molecular long axis of rigid-rod polymer chains. The main problem is that the polymer chains are usually aligned in the plane of the membrane. For fuel cell applications, the protons have to be transported in the through-plane direction. We therefore suggest to design a hydrolytically stable LC polymer and align the mesogens in the through-plane direction. This orientation will result in much higher through-plane conductivity and lead to better fuel cell performance.

## 5.5 Reference

- [1] Sharaf, O.Z.; Orhan, M.F. *Renew. Sust. Energ. Rev.* **2014**, 32, 810.
- [2] Iulianelli, A.; Basile, A. *Int. J. Hydrogen Energ.* **2012**, 37, 15241.
- [3] El-kharouf, A.; Chandan, A.; Hattenberger, M.; Pollet, B.G. *J. Energ. Inst.* **2012**, 85, 188.
- [4] Peighambardoust, S.J.; Rowshanzamir, S.; Amjadi, M. *Int. J. Hydrogen Energ.* **2010**, 35, 9349.
- [5] Kreuer, K.D. *J. Membr. Sci.* **2001**, 185, 29.
- [6] Wu, J.; Yuan, X.Z.; Martin, J.J.; Wang, H.; Zhang, J.; Shen, J.; Wu, S.; Merida, W. *J. Power Sources*, **2008**, 184, 104.
- [7] Zhao, Q.; An, Q.F.; Ji, Y.; Qian, J.; Gao, C. *J. Membr. Sci.* **2011**, 379, 19.
- [8] Lufrano, F.; Baglio, V.; Staiti, P.; Antonucci, V.; Arico, A.S. *J. Power Sources*, **2013**, 243, 519.
- [9] Jorn, R.; Savage, J.; Voth, G.A. *Accounts Chem. Res.* **2012**, 45, 2002.
- [10] Zhang, L.; Chae, S.R.; Hendren, Z.; Park, J.S.; Wiesner, M.R. *Chem. Eng. J.* **2012**, 204, 87.
- [11] Yan, Q.; Toghiani, H.; Wu, J. *J. Power sources* **2006**, 158, 316.
- [12] Guvelioglu, G.H.; Stenger, H.G. *J. Power sources* **2007**, 163, 882.
- [13] Song, M.; Pei, P.; Zha, H.; Xu, H. *J. Power sources* **2014**, 267, 655.
- [14] Kreuer, K.D. *Chem. Mater.* **1996**, 8, 610.
- [15] Kreuer, K.D.; Rabenau, A.; Weppner, W. *Angew. Chem. Int. Ed. Engl.*

- 1982**, 21, 208.
- [16] Howe, A.T.; Shilton, M.G. *J. Solid Chem.* **1979**, 28, 345.
- [17] Howe, A.T.; Shilton, M.G. *J. Solid Chem.* **1980**, 34, 149.
- [18] Bernard, L.; Fitch, A.; Wright, A.F.; Fender, B.E.F.; Howe, A.T. *Solid state ionics* **1981**, 5, 459.
- [19] Yeager, H.L.; Steck, A. *J. Electrochem. Soc.* **1981**, 128, 1880.
- [20] Asana, N.; Aoki, M.; Suzuki, S.; Miyatake, K.; Uchida, H.; Watanabe, M. *J. Am. Chem. Soc.* **2006**, 128, 1762.
- [21] Saito, M.; Hayamizu, K.; Okada, T. *J. Phys. Chem. B* **2005**, 109, 3112.
- [22] Hou, J.; Li, J.; Mountz, D.; Hull, M.; Madsen, L.A. *J. Memb. Sci.* **2013**, 448, 292.
- [23] Park, J.K.; Li, J.; Divoux, G.M.; Madsen, L.A.; Moore, R.B. *Macromolecules* **2011**, 44, 5701.
- [24] Li, J.; Park, J.K.; Moore, R.B.; Madsen, L.A. *Nat. Mater.* **2011**, 10, 507.
- [25] Wang, Y.; Gao, J.W.; Dingemans, T.J.; Madsen, L.A. *Macromolecules* **2014**, 47, 2984.
- [26] Hou, J.B.; Li, J.; Madsen, L.A. *Macromolecules* **2010**, 43, 347.
- [27] Li, J.; Wilmsmeyer, K.G.; Madsen, L.A. *Macromolecules* **2009**, 42, 255.
- [28] Shin, D.W.; Lee, S.Y.; Lee, C.H.; Lee, K.S.; Park, C.H.; McGrath, J.E.; Zhang, M.Q.; Moore, R.B.; Lingwood, M.D.; Madsen, L.A.; Kim, Y.T.; Hwang, I.; Lee, Y.M. *Macromolecules* **2013**, 46, 7797.
- [29] Burnell, E.E.; De Lange, C.A. *NMR of ordered liquids*, Springer, London, 2003.
- [30] Kreuer, K.D.; Rabenau, A.; Weppner, W. *Angew. Chem. Int. Ed. Engl.* **1982**, 21, 208.
- [31] Ticianelli, E.A.; Derouin, C.R.; Redondo, A.; Srinivasan, S. *J. Electrochem. Soc.* **1988**, 135, 2209.





---

## Summary

---

The polymer membrane of a proton exchange membrane fuel cell is designed to transport protons from the anode to the cathode. Having an aligned ordered polymer morphology, as is reported for block copolymers, is important with respect to getting high proton conductivities. Liquid crystalline (LC) polymers also have ordered structures, so they can be used for proton and ion transport applications. The main goal of this thesis is to compare the ion transport performance of a LC polymer and an isotropic polymer.

To achieve this goal, we synthesized two chemically similar highly sulfonated aromatic polyamides (note: the sulfonic groups are in the sodium-form, *i.e.*  $-\text{SO}_3\text{Na}$ ) via an interfacial polycondensation method (Chapter 2). The two polymers, poly(2,2'-disulfonylbenzidine terephthalamide) (Na-PBDT) and poly(2,2'-disulfonylbenzidine isophthalamide) (Na-PBDI), have similar molecular structures, but display totally different phase behavior. Na-PBDT in water forms a nematic LC phase at concentrations higher than 1.5 wt%, whereas PBDI in water forms isotropic solutions at all concentrations. The nematic order was maintained in Na-PBDT films after casting from a 6 wt% water solution, and the XRD results revealed an alignment along the casting direction in the films, with an orientation degree (overall order parameter) of 0.3. In contrast, films cast from a 6 wt% Na-PBDI solution were isotropic. Due to the all-aromatic backbone structure, both polymers exhibit good thermal stabilities ( $T_d^{5\%} > 427\text{ }^\circ\text{C}$ ) and high storage moduli ( $E' \sim 10\text{ GPa}$  for dry films).

Despite the excellent thermal properties and high storage moduli, the chemical stability of our protonated sulfonated polyamides turned out to be quite poor, as is discussed in Chapter 3, which based on previous experience

was a very unexpected result. Although the sodium-form polyamides (with  $-\text{SO}_3\text{Na}$  groups) are very stable, the acid-form ( $-\text{SO}_3\text{H}$ ) polymers proved to hydrolyze very quickly. After heating a  $\sim 5$  wt% H-PBDI polymer solution at  $80^\circ\text{C}$  for 6 days, the polymer decomposed into monomers, as observed via NMR experiments, indicating hydrolysis occurred in water. Since the acid-form polymers appeared to be unstable, we used the sodium-form sulfonated polyamides (Na-PBDT and Na-PBDI) for the remainder of our research.

The two sulfonated aramids, Na-PBDT and Na-PBDI, are water soluble due to the high density of sulfonic groups. To avoid the dissolution of the membranes during fuel cell operation, ionic crosslinking using barium ions was applied for the two polymers, as described in Chapter 4. Membranes with various degrees of crosslinking (40%, 60%, 80% and 100%) were prepared. With the increase in crosslinking density, the water uptake of the membranes decreases linearly. The thermal stability was found to be similar to that of the neat polymers, with  $T_d^{5\%} > 427^\circ\text{C}$ , whereas the storage modulus increased from  $\sim 4$  GPa to  $\sim 10$  GPa. Polarized optical microscopy images and XRD results confirmed that the liquid crystalline order of the Na-PBDT membrane was maintained after crosslinking, while both crosslinked and neat membranes of Na-PBDI were isotropic.

In Chapter 5, we compare the water diffusion, ionic conductivity and fuel cell performance of Na-PBDT and Na-PBDI. Due to the ordered structure; the liquid crystalline (LC) Na-PBDT membranes display anisotropic water diffusion in the in-plane and through-plane direction, where the latter is only 30% of the former. In contrast, the isotropic Na-PBDI membranes display similar water diffusion in both the in-plane and through-plane direction. The in-plane sodium conductivity results of Na-PBDT are also higher than the Na-PBDI membranes, indicating that an ordered structure is more conducive for sodium ion transport. In fuel cell tests, protons are transported in a membrane in the through-plane direction. However, the polymer membranes used in the tests were in the sodium form, so the  $\text{H}_3\text{O}^+$  ions are less available in the membranes for proton

conduction. Additionally, sodium ions also moved during the measurement, but the mobility of sodium ions is much lower than that of protons, therefore both Na-PBDT and Na-PBDI membranes displayed very poor fuel cell performance. Based on the water diffusion, and sodium conductivity results, we conclude that ions prefer to be transported along the rigid-rod polymer chains. These preliminary experiments suggest that sulfonated liquid crystal polymers should be useful as proton conducting membranes for fuel cell applications. It is advisable, however, to design and prepare a chemically more stable nematic LC polymer, in which the highly protonated polymer chains can easily be aligned in the through-plane direction.



## Samenvatting

---

Het polymeer membraan in een brandstofcel is ontworpen om protonen te transporteren van de anode naar de kathode. Om een goede protongeleiding te krijgen is het van belang dat de polymeermorfologie geordend en uitgelijnd is, zoals reeds gerapporteerd voor blokcopolymeren. Vloeibaar kristallijne polymeren hebben deze geordende structuur en kunnen gebruikt worden voor proton- en ion-transport doeleinden. Het hoofddoel van dit proefschrift is om het transport van ionen in een vloeibaar kristallijn polymeer te vergelijken met dat van een isotroop polymeer.

Om dit te realiseren hebben we twee gesulfoneerde aromatische polyamides gesynthetiseerd via een fase-gescheiden polycondensatie methode. De twee polymeren, poly(2,2'-disulfonylbenzidine terephthalamide) (Na-PBDT) en poly(2,2'-disulfonylbenzidine isophthalamide) (Na-PBDI), hebben een vergelijkbare structuur, maar vertonen een totaal verschillend fasengedrag. Na-PBDT vormt een nematisch vloeibaar kristallijne fase in water bij een concentratie van 1.5 gewichtsprocent, terwijl Na-PBDI een isotrope oplossing geeft bij elke willekeurige concentratie. De nematische orde van een 6 gewichtsprocent oplossing van Na-PBDT in water blijft behouden in de daaruit gevormde films. Röntgendiffractie metingen laten zien dat de polymeerketens oriënteren in de strijkriching waarin de film was gemaakt met een oriëntatiegraad (overall order parameter) van 0.3. Films gemaakt van een isotrope 6 gewichtsprocent Na-PBDI oplossing blijven een isotrope structuur vertonen. Vanwege de volledige aromatische structuur vertonen beide polymeren een uitstekende thermische stabiliteit ( $T_d^{5\%} > 427\text{ }^{\circ}\text{C}$ ) en hebben ze hoge opslagmoduli ( $E' \sim 10\text{ GPa}$  voor gedroogde films).

Ondanks de uitstekende thermische eigenschappen en de hoge opslagmoduli is de chemische stabiliteit van de geprotoneerde gesulfoneerde polyamides onverwacht slecht. Deze resultaten worden beschreven in hoofdstuk 3. Hoewel de natrium zouten van de polyamides (met -  $\text{SO}_3\text{Na}$  groepen) zeer stabiel zijn, blijken de zure varianten van de polymeren ( $-\text{SO}_3\text{H}$ ) gemakkelijk te hydrolyseren. Na het verwarmen van een 5 gewichtsprocent H-PBDI oplossing ( $80\text{ }^\circ\text{C}$  voor 6 dagen) blijkt het polymeer uiteen te vallen naar monomeer startmateriaal. Dit is geverifieerd met NMR en de resultaten bevestigen dat het polymeer inderdaad hydrolyseert in water. Omdat de zure polymeren instabiel bleken te zijn, zijn alleen de natrium zouten van de gesulfoneerde polymeren (Na-PBDT en Na-PBDI) gebruikt voor de rest van het onderzoek.

De twee gesulfoneerde aramides, Na-PBDT en Na-PBDI, zijn water oplosbaar vanwege de grote hoeveelheid sulfonzuurgroepen. Om te voorkomen dat de polymeren oplossen in de brandstofcel zijn barium ionen gebruikt om de polymeren te vernetten, zoals beschreven in hoofdstuk 4. Membranen met een verschillende vernettingsgraad (40%, 60%, 80% en 100%) zijn gesynthetiseerd. De opname van water door het polymeer neemt lineair af met een oplopende vernettingsgraad. De thermische stabiliteit blijkt hetzelfde te zijn als die van de lineaire polymeren ( $T_d^{5\%} > 427\text{ }^\circ\text{C}$ ) terwijl de opslagmodulus toeneemt van  $\sim 4\text{ GPa}$  tot  $\sim 10\text{ GPa}$ . Met een polarisatiemicroscoop en met Röntgendiffractie metingen is bevestigd dat de vloeibaar kristallijne orde van de Na-PBDT membranen behouden blijft na de vernettingsreactie. De Na-PBDI membranen blijven isotroop.

In hoofdstuk 5 vergelijken we de diffusie van water, de geleiding van ionen en de prestaties van de Na-PBDT- en PBDI membranen in een brandstofcel. Door de geordende structuur laten de vloeibaar kristallijne Na-PBDT membranen anisotrope waterdiffusie zien, *in* het vlak en *door* het vlak. De diffusie *door* het vlak is slechts 30% van de diffusie *in* het vlak. Dit is in tegenstelling tot de waterdiffusie in Na-PBDI membranen waar de

waterdiffusie in alle richtingen gelijk blijkt te zijn. De geleiding van natrium *in* het vlak is voor Na-PBDT ook hoger dan voor Na-PBDI membranen, wat er op wijst dat de geleiding van natrium ionen plaats vindt via een geordende structuur. In brandstofcellen vindt protonen transport doorgaans plaats *door* het vlak. De door ons onderzochte polymeren zijn echter in de natrium vorm. Aangezien de mobiliteit van natrium ionen veel lager is dan voor protonen, presteren beide membranen slecht in een brandstofcel. Concluderend mogen we vaststellen dat water- en ion-diffusie gemakkelijker plaats vindt langs zogeheten starre polymeerketens. Deze eerste resultaten bevestigen dat gesulfoneerde vloeibaar kristallijne polymeren zeer nuttig kunnen zijn als proton-geleidende membranen voor brandstofcel toepassingen. Het is daarbij echter wenselijk dat er een meer chemisch stabiel nematisch vloeibaar kristallijn polymeer wordt ontworpen, waarin de geprotoneerde polymeerketens kunnen worden uitgelijnd in de richting *door* het vlak.





---

## Curriculum vitae

---

### **Jianwei Gao**

Born on 08<sup>th</sup> October, 1984,  
in Hebei, China

#### **Nov. 2010 – Sep. 2015**

PhD candidate in Novel Aerospace Materials group, Faculty of Aerospace Engineering, Delft University of Technology, Delft, The Netherlands

#### **Sep. 2007 – Jun. 2010**

Master of Science, Department of Chemical Physics, University of Science and Technology of China, Hefei, China

#### **Sep. 2003 – Jun. 2007**

Bachelor of Science, Department of Polymer Science and Engineering, University of Science and Technology of China, Hefei, China

---

## Acknowledgements

---

I would like to sincerely thank my promoter and supervisor Theo J. Dingemans. It is impossible for me to finish my PhD study without your continuous support and motivation. You not only gave me many valuable suggestions on my study, but encouraged me a lot when I was in the lowest point of my PhD period as well. I know it took you too much energy on my project. I really appreciate for your endless help, patient and tolerance.

I warmly thank my copromoter Stephen J. Picken. It was you and Theo giving me the opportunity to work in TU Delft. You are always kind and helpful for me. I learned a lot of new knowledge from you in the many times of discussion.

I am heartily thankful to Johan. You gave me great help on my thesis as well as my experiment. During writing my thesis, you spent a lot of time on the structure and language modification, which made the thesis much better and more logical. Thank you so much for your selfless help.

I do not want to forget prof. dr. Louis Madsen and ms. Ying Wang. Without your help, I would not finish the water diffusion measurement. You also provided valuable insights of data analysis, which made me much easier to understand and explain the experiment results.

I am grateful to Santiago for helping me for the conductivity measurement. With your kind guidance, I could operate the test easily. I also want to thank Ben Norder to help me do the XRD tests several times. You always replied my request in time. It is my pleasure to work with you. My special thanks to Kristina. You help me a lot to get good NMR data for my liquid crystalline polymers. After several times of attempts, we finally succeeded to obtain the best NMR results.

I would further more thank prof. Sybrand van der Zwaag, prof. Guangzhao Zhang and prof. Liangbin Li for giving me encouragement on my PhD study.

I wish to thank all my colleagues in NovAM group and Aerospace Engineering Faculty. Maruti, thanks for teaching me how to use the TGA, DMA, DSC and other equipment in our lab. Lijing and Frans, thank you for helping me on my experiment operating. Shanta, thanks for your kind help in every aspect during my study. Miranda, thank you for helping to improve my English. Thank Wei, Qingbao, Hari, Jimmy, Martino, Daniella, Nijesh, Arijana, Nan, Wouter (Post), Xiaojun, Hao, Wei, Pim, Jesus, Emman, Mina, Qi, Hongli, Michiel, Zeljka, Jie, Hamideh, Ranjita, Wouter (Vogel), Renee, Jason, Mladen and all NovAM members. You guys made my study much easier and more familiar with Holland life.

I also want to thank the guys in ASM groups for helping me for the fuel cell test. Emma, thank you to do the fuel cell tests together with me for several times. Roman, thanks for teaching me how to prepare an MEA. Krishna, thank you for giving me a lot of help for using the small fuel cell setup. I learned a lot of knowledge on ionic conductivity from Miguel, and many thanks for Miguel and Daniël's help for the fuel cell test. I am grateful to thank Haining, Guanglin, Serhii, Kai, Karolis, Zhen and Anping. You gave me a lot help on the experiment.

I offer my regards and blessings to my friends: Cong, Hui, Jitang, Xiaojia, Xuliang, Yue, Yunlong, Zhutian... You made my life in Delft much more colorful and easy.

I would like to thank the China Scholarship Council (CSC) to give me financial support to study in TU Delft.

Last, but not least I sincerely thank my family – my parents, my parents-in-law, my wife and my son. You are giving me the strongest support all the time. You are very important in my life.

*Jianwei*